Title
Transportation Modeling For The Environment: Final Report

Authors
Barth, Matthew
Norbeck, Joseph

Publication Date
1996

CALIFORNIA PATH PROGRAM
INSTITUTE OF TRANSPORTATION STUDIES
UNIVERSITY OF CALIFORNIA, BERKELEY

Transportation Modeling for the Environment: Final Report

Matthew J. Barth
Joseph M. Norbeck

University of California, Riverside

California PATH Research Report
UCB-ITS-PRR-96-6

This work was performed as part of the California PATH Program of the University of California, in cooperation with the State of California Business, Transportation, and Housing Agency, Department of Transportation; and the United States Department of Transportation, Federal Highway Administration.

February 1996

ISSN 1055-1425

Transportation Modeling for the Environment

Research Report for the California PATH Program, MOU #105

July, 1995

College of Engineering - Center for Environmental Research and Technology
University of California, Riverside, CA 92521

Matthew J. Barth
Joseph M. Norbeck

CE-CERT Technical Document #95:TS:053:F

This work was performed as part of the California PATH Program of the University of California, in cooperation with the State of California Business, Transportation, and Housing Agency, Department of Transportation; and the United States Department of Transportation, Federal Highway Administration.

Preface

This research report has been prepared for the California PATH Program, MOU #105, entitled "Transportation Modeling for the Environment". This report covers the work that has been performed during a two year research project, with emphasis on the second year of work. Greater detail of the first year's work can be found in this project's interim research report, PATH document #UCB-ITS-PRR-94-27. Contributions to this report have been made by Joseph Norbeck, Ramakrishna Tadi, Gary Zheng, Eric Johnston, and Theodore Younglove. Parts of this report are based on other research reports written at the Center for Environmental Research and Technology.

Abstract

Transportation Modeling for the Environment

Matthew J. Barth and Joseph M. Norbeck

College of Engineering
Center for Environmental Research and Technology
University of California, Riverside, CA 92521

July, 1995

Intelligent Transportation Systems (ITS) offer the potential to improve highway safety, reduce highway congestion, and increase economic productivity. However, it is not clear what the effect ITS will have on air quality, specifically, vehicle emissions. As a result of various ITS technological bundles, average vehicle emissions should decrease due to smoother traffic flow and less congestion. In contrast, the transportation system may become more attractive, inducing greater travel demand and higher VMT (vehicle-miles traveled), resulting in an increase of emissions. In this research report, we describe preliminary research dealing with vehicle emissions associated directly with 1) Automated Highway Systems (AHS) and 2) ramp metering. In performing this analysis, a power-demand modal emissions model has been integrated with several transportation simulation models in order to quantitatively determine the effects of ITS technology on vehicle emissions. For AHS, a steady-state speed/emissions comparison has been conducted between vehicles that are platooned and non-platooned. Due to the reduction of aerodynamic drag while platooning (the "drafting" effect), the emissions for the platoon are significantly lower at higher steady-state speeds. Further, AHS platoon maneuvers (e.g., splitting, merging, etc.) can have a significant impact on vehicle emissions, since the vehicles involved will incur a number of acceleration and deceleration events. For ramp metering, a general evaluation has been conducted concentrating on the effect of vehicle emissions. Three components of ramp metering were evaluated: 1) the effect of freeway traffic smoothing; 2) ramp and surface street congestion; and 3) hard accelerations from the ramp meters. The impact of each of these components on vehicle emissions was analyzed separately and then integrated together for an overall emissions evaluation.

KEY WORDS: environmental impacts, emissions, transportation simulation modeling, Automated Highway Systems (AHS), platooning, ramp metering

Executive Summary

Intelligent Transportation Systems (ITS) have generated considerable enthusiasm in the transportation community as potential methods to improve highway safety, reduce highway congestion, enhance the mobility of people and goods, and to promote the economic productivity in the country's transportation system. However, it is uncertain what effect ITS will have on air quality, specifically, vehicle emissions. There are primarily two influential factors: 1) Potentially, vehicle emissions can be reduced through the implementation of several ITS user service bundles. For example, Advanced Vehicle Control Systems (AVCS) implemented at the vehicle level will safely smooth the traffic flow, minimizing the stop-and-go effect that leads to higher emissions. Further, Advanced Traffic Management/Information Systems (ATMIS) will minimize congestion and subsequently emissions by allowing dynamic re-routing to take place on the roadway network, and aiding in trip-chaining practices. 2) In contrast, the implementation of ITS technologies may induce traffic demand that leads to an increase of total vehicle miles traveled (VMT) by making the transportation system more desirable. For example, if ITS allows smoother flow and higher speeds on the roadways, people may choose to live farther away from work while still commuting in the same amount of time. In this research, we have begun to evaluate the direct impact of ITS traffic operation on vehicle emissions. We concentrate on the actual implementations of proposed strategies, and do not consider the effect of potential induced traffic demand as outlined above.

In order to estimate the direct impact of ITS technologies on air quality, significant improvements must be made in traffic simulation and travel demand models by closely integrating vehicle emission models. Existing traffic, emissions, and planning models have been developed independently of each other and are difficult to integrate together when determining accurate air quality impacts. Current emission models (i.e., MOBILE, developed by the US Environmental Protection Agency (EPA) and EMFAC, developed by the California Air Resources Board (CARB)) functionally relate emissions to average vehicle speed and density, and are not appropriate for analyzing ITS scenarios. Under ITS conditions, the dynamic behavior of vehicles will be very different compared to today's traffic conditions, upon which the current emission models are based. As a result, *modal* emissions models (i.e., models that relate emissions to vehicle operating modes such as idle, cruise, various levels of acceleration/deceleration, etc.) can be used with microscale traffic simulations to obtain more realistic results.

We have integrated a power-demand modal emissions model with several traffic simulation models in order to quantitatively determine the effects of ITS technology on vehicle emissions. The vehicle dynamics equations and load-based emissions used in this study have been calibrated to a modern, closed-loop emission controlled vehicle (1991 Ford Taurus). As further modal emission data become available and modal emission models become more comprehensive, better emission estimates can be made. Even though the preliminary results in this report are based on a single vehicle type, trends are seen and important conclusions can be made regarding the importance of linking modal emissions with dynamic vehicle activity.

In this research report, we have applied the unique traffic/emission models to study vehicle emissions associated with an Automated Highway System (AHS) and ramp metering.

For AHS, a steady-state speed/emissions comparison has been conducted between vehicles that are platooned and non-platooned. Due to the reduction of aerodynamic drag while platooning (the "drafting" effect), the emissions for the platoon are significantly lower at higher steady-state speeds. Preliminary results indicate that with AHS's approximate four-fold increase of capacity, emission rates will increase over current manual conditions by a factor of two if the system is used at full capacity (~8000 vehicles/hour-lane), stay the same at half capacity (~4000 vehicles/hour-lane), and will decrease by half at current traffic volumes (~2000 vehicles/hour-lane). Further, preliminary analysis has been carried out to evaluate vehicle emissions associated directly with the AHS maneuvers of free-speed accelerations, platoon merging, and platoon splits. The current version of PATH's AHS simulator SmartPath uses a constant acceleration strategy in these maneuvers. This can be problematic at high speeds since a constant acceleration constraint can cause a modern emission-controlled vehicle to enter a power enrichment state, in which very high emissions are produced. We have devised a constant-power approach which limits the accelerations of automated vehicles, eliminating power enrichment states, and greatly reducing emissions. Emissions can also be reduced by developing "emission-friendly" protocols, that do not require high power episodes while still maintaining system safety. Also, by keeping the size of platoons as large as possible, traffic density and highway capacity will both increase, and the number of vehicles benefiting from the aerodynamic drafting effect increases.

For ramp metering, an evaluation has been conducted concentrating on the effect of vehicle emissions. Three components of ramp metering were evaluated independently: 1) the effect of freeway traffic smoothing; 2) ramp and surface street congestion; and 3) hard accelerations from the ramp meters. In this research, simulation experiments have been carried out for generalized ramp metering scenarios using the FRESIM traffic model coupled with the developed modal emissions model. It was found that the overall effect of ramp metering on vehicle emissions is

highly dependent on a number of localized factors such as the *topology of the road network* (e.g., spacing of ramps, surface street to highway interface, etc.), the *road geometry* (e.g., number and types of lanes, road grade of the highway and ramps, etc.), the *type of ramp metering used* (e.g., fixed cycle vs. traffic responsive), the *vehicle mix* (e.g., proportion of trucks and cars, etc.), and the *overall VMT*. As expected, simulation experiments have shown that the use of ramp metering increases the overall traffic speed on the mainline by restricting the ramp volume and by minimizing the disturbances caused by merging vehicles. As the ramp meter cycle time increases, the traffic volume from the ramp decreases and the freeway speeds increase, resulting in a total emissions decrease due to lower traffic density and smoother flow. Queues of vehicles on the on-ramps and their emissions have also been studied using a simulation model. It is shown that the density of vehicles increases for longer ramp cycle times, and the average vehicle speed on the ramps decreases. However, it was shown that emissions tend to be higher for shorter ramp meter cycle times, primarily due to an increased stop-and-go effect. We have also developed a simulation model that predicts velocity and acceleration profiles for vehicles accelerating under constrained speeds and distances, using constant engine power. This was applied to freeway on-ramps, in particular, accelerating from a ramp meter to the merge point on the freeway. If the distance is short (and if the grade is steep), the engine power required may cause the vehicle to go into a power enrichment mode, causing high emissions.

When all three sources of ramp metering emissions (i.e., freeway mainline, ramp queuing, and hard accelerations) are integrated together (for the generic scenarios in the experimentation), the freeway mainline is the dominant emissions source, simply because of the larger number of vehicles associated with it. The amount of emissions caused by ramp queuing is small in comparison, and only when the distance to get up to speed from the meter to the merge point is short and steep, is the effect of hard accelerations an emissions factor. When developed as a function of ramp meter cycle time, the net change of emissions is small. For the case of no metering, the mainline traffic moves slower with moderately high emissions, and the acceleration required to get up to speed is small (as are the corresponding emissions) since there is a longer distance to accelerate and the final traffic speed is relatively low. For the case of metering with long cycle times, the mainline moves faster and has relatively lower emissions (due to smoother traffic flow), but the accelerations to get from the meter to the higher mainline speeds are often hard enough to drive vehicles into a power enrichment state. These hard acceleration emissions offset the benefits achieved from smoother traffic flow.

Table of Contents

List of Tables and Figures

TABLES

1 Introduction

1.1 INTELLIGENT TRANSPORTATION SYSTEMS

It has been estimated that surface transportation congestion is costing the nation approximately $100 billion each year, and traffic accidents represent another $70 billion in costs (Arnott et al. 1994; US DOT 1995). The inefficient flow of vehicles reduces overall productivity, wastes energy, and increases emissions. In order to address these problems, Intelligent Transportation Systems (ITS) can apply advanced and emerging technologies from the fields of electronics, communications, control, and information processing to improve surface transportation. With the application of these technologies, it is expected that significant improvements in safety, mobility, accessibility, and productivity will occur and our infrastructure and energy resources will be used more efficiently.

In March 1995, the US Department of Transportation (US DOT) published a National ITS Program Plan (NPP) to provide a comprehensive planning reference for the application of ITS (US DOT 1995). It states that the key goals of the national ITS program are to:

- Improve the safety of the nation's surface transportation system;
- Increase the operational efficiency and capacity of the surface transportation system;
- Reduce energy and environmental costs associated with traffic congestion;
- Enhance present and future productivity;
- Enhance the personal mobility, convenience, and comfort of the surface transportation system;
- Create an environment in which the development and deployment of ITS can flourish.

The NPP has identified 29 individual "user services" that will serve as the building blocks for the deployment of ITS. These user services have then been grouped into "bundles" and are listed in Table 1.1.

BUNDLE	USER SERVICES
Travel and Transportation Management	En-Route Driver Information Route Guidance Traveler Services Information Traffic Control Incident Management Emissions Testing and Mitigation
Travel Demand Management	Demand Management and Operations Pre-Trip Travel Information Ride Matching and Reservation
Public Transportation Operations	Public Transportation Management En-Route Transit Information Personalized Public Transit Public Travel Security
Electronic Payment	Electronic Payment Services
Commercial Vehicle Operations	Commercial Vehicle Electronic Clearance Automated Roadside Safety Inspection On-board Safety Monitoring Commercial Vehicle Administrative Processes Hazardous Materials Incident Response Freight Mobility
Emergency Management	Emergency Notification and Personal Security Emergency Vehicle Management
Advanced Vehicle Control and Safety Systems	Longitudinal Collision Avoidance Lateral Collision Avoidance Intersection Collision Avoidance Vision Enhancement for Crash Avoidance Safety Readiness Pre-Crash Restraint Deployment Automated Highway System

Table 1.1. User service bundles, from (US DOT 1995).

1.2 ITS AND THE ENVIRONMENT

There have been several recent workshops and conferences that have addressed ITS and its impact on the environment. The first workshop was held in Asilomar in April 1992 and first explored the interaction between ITS and the environment. The second workshop was held in Diamond Bar in March 1993 where it was determined that there were wide ranging policy questions associated with the subject, rather than just looking at transportation modeling and air quality. In June 1994, the *National Conference on Intelligent Transportation Systems and the Environment* was held in Arlington, Virginia. This conference highlighted the pressing environmental issues concerning the application and implementation of ITS. The key topics of the conference centered on: 1) new strategies and technologies; 2) energy and environmental implications; 3) institutional issues; and 4) societal implications (Hennessey et al. 1994). The conference produced a set of policy, research, and institutional issues that set the agenda for future action.

There have been several papers that qualitatively address each of the users services listed in Table 1.1 and the impact they will have on the environment when considered both individually and as a whole (e.g., Richardson 1994; Washington et al. 1993; Guensler et al. 1994). In addition, Little and Wooster have identified numerous existing field tests that will serve as unique opportunities to assess the operational, behavioral, and environmental impacts of various ITS configurations (Little et al. 1994). This paper also discussed the capabilities and limitations of current transportation/emissions modeling tools and their application to ITS evaluation. This is addressed in more detail in Chapter 2 of this report.

One of the more important results that came out of these workshops and conferences is that in order to truly assess the environmental impacts of ITS, the full environmental costs of ITS application and implementation must be considered. This includes evaluating the *direct* effects as well as the *indirect* effects:

Direct Effects—By improving the efficiency and capacity of the existing roadway system, congestion will decrease, safety will increase, and vehicle emissions are expected to decrease. By smoothing the traffic flow on the roadways, the heavy acceleration and deceleration components of vehicle trips can be eliminated, minimizing energy consumption and associated emissions of these vehicle operating modes. Further, Advanced Traffic Management / Information Systems (ATMIS) will allow dynamic re-routing to take place on the roadway network, minimizing congestion and subsequently emissions. In addition, navigational systems will allow users to reduce unnecessary driving and avoid congestion. Several studies have addressed specific

examples of these direct effects of ITS on vehicle emissions (see, e.g., Washington 1995; Barth 1995).

Indirect Effects—The application and implementation of ITS may lead to potential induced traffic demand. If ITS allows smoother flow and higher speeds on the roadways, people may choose to live farther away from work while still commuting in the same amount of time—thereby increasing total vehicle miles traveled (VMT). Farther, attractive trip-ends will become reachable, again increasing VMT. Further, advanced navigational technology may divert travelers from higher-occupancy modes such as buses and carpools to single-occupant vehicles. In general, if travel becomes easier due to advanced technology, VMT will likely increase. For a complete environmental analysis, driver behavior and transportation supply must also be taken into account. There are several recent papers that address these indirect effects of ITS (see, e.g., Ostria et al. 1994; Vaughn et al. 1995; Ostria 1995).

1.3 RESEARCH SCOPE

In this research project, we address only the direct relationship between vehicle emissions and ITS traffic operations. Specifically, we analyze vehicle emissions associated with two services: Automated Highway Systems (AHS, see user service in Table 1.1) and ramp metering. In order to perform this analysis, we have developed and integrated a unique modal emissions model with state-of-the-art transportation simulation models. A modal emissions model predicts emissions based on vehicle operational modes, such as idle, cruise, and various levels of acceleration/deceleration. The application of a modal emissions model is far better suited for ITS evaluation, as is outlined in Chapter 2. For this research, the modal emissions model was calibrated to a single vehicle, a 1991 Ford Taurus, and the results of the analysis should be considered preliminary until a more comprehensive modal model is used. Even with a single vehicle model however, various traffic scenarios can be compared and useful conclusions can be made.

This research project was carried out over two years, and the first year's interim results are described in PATH Research Report #UCB-ITS-PRR-94-27 (Barth et al. 1994). This final report incorporates some of the material from the interim report for completeness. The research from Year 1 is summarized below, followed by a brief outline of the work carried out during Year 2.

1.3.1 Year 1 Summary

In the first year's work, specific traffic modeling components and the modal emissions modeling component of CE-CERT's Integrated Transportation/Emission Modeling (ITEM, see (Barth et

al. 1993; Barth et al. 1995)) set were adapted and modified so that several ITS scenarios could be evaluated. With these modeling tools, initial studies of Advanced Vehicle Control System (AVCS) and Advanced Traffic Management and Information System (ATMIS) strategies were performed. Specifically for AVCS, vehicle emissions associated with platooning in an AHS were investigated. For ATMIS, the impact of ramp metering effects on vehicle emissions was investigated.

Vehicle Platooning

In order to achieve high traffic flow rates, automated highway systems will most likely have vehicles travel in platoons, where a platoon consists of a number of vehicles (approximately 5 to 30), separated by very short distances (on the order of a meter), traveling at high speeds (100 km/hr +). In the first year's work, we have taken a microscopic traffic/emissions simulator used for studying uninterrupted flow (freeway) and have modified it by eliminating the human driving behavior components corresponding to car-following and lane-changing logic. These components have been replaced with control laws for automated driving. Two types of car-following logic within a platoon have been investigated: 1) Coordinated Intelligent Cruise Control (CICC) where a platoon leader has a rearward-looking transponder or other means of transmitting information on vehicle dynamics to the following vehicles, and 2) Autonomous Intelligent Cruise Control (AICC) where a following vehicle can only measure a preceding vehicle's position and velocity. These control laws are being adapted from the PATH literature, specifically (Sheikholeslam 1991) for CICC and (Ioannou et al. 1992) for AICC.

As an initial study of AVCS strategies, total emissions from platoons have been evaluated. Specifically, the following evaluations were conducted:

Steady-state speed/emissions comparison—The emissions for a 20-vehicle platoon were calculated at different steady state speeds. These emissions are then compared to 20 vehicles driven manually (i.e., no platooning), with no intervehicle interaction for the same set of velocities. Due to the reduction of aerodynamic drag while platooning (the "drafting" effect), the emissions for the platoon are significantly lower at higher steady-state speeds.

Optimized vs. non-optimized CICC comparison—A comparison was made between a platoon under optimized and non-optimized CICC control laws. In the optimized case, control constants were set at their optimized values for best maintaining intraplatoon spacing. For the non-optimized case, these control constants were perturbed and the

resulting emissions were compared to the optimized case. At high speeds under high load conditions, the non-optimized case tends to produce higher emissions.

CICC vs. AICC comparison—Various driving cycles (velocity profiles of on-road vehicle motion) have been simulated for both CICC and AICC platoon operation. Although platoons will be operated smoothly in a typical AHS, more aggressive driving cycles were used in simulation in order to identify potential emission producing events. For specific velocity transients, hard accelerations and decelerations were often required of follower vehicles to maintain proper platoon formation. These accelerations often lead to short bursts of high emissions during the driving cycles, depending on the control laws governing intraplatoon spacing. A comparison of total emissions were carried out using CICC and AICC control laws.

Ramp Metering

In addition to evaluating vehicle platooning emissions in Year 1, a preliminary analysis of the effect of ramp metering on vehicle emissions was carried out. Three basic effects of ramp metering on vehicle emissions were analyzed: 1) smoothing of mainline traffic flow, leading to lower emissions; 2) increased ramp and surface street congestion, possibly leading to higher emissions; and 3) induced hard accelerations from the meters on the ramps, leading to higher emissions. These three effects are interrelated and vary as a function of traffic demand, ramp meter cycle time, and ramp meter placement. In the first year of work, a preliminary evaluation of these three effects was done separately with no interaction between them. A large concentration of work took place on the induced hard accelerations. A ramp-acceleration simulation model was used to predict the amount of vehicle emissions during hard accelerations on freeway on-ramps. These ramp accelerations were also compared to data measured in the 1993 Caltrans project “Vehicle Speeds and Accelerations Along On-Ramps: Inputs to Determine the Emissions Effects of Ramp Metering” performed by Cal Poly San Luis Obispo (Sullivan et al. 1993).

1.3.2 Year 2 Research Outline

AHS Emissions Evaluation

In the first year of work, vehicle emissions associated with platooning were evaluated. In order to evaluate the total emissions from an automated highway system, further AHS modeling was performed in the second year of research. As an initial step, multiple platoons on multiple lanes were modeled with no interlane interaction. The initial platooning emissions results from the first

year were extended to the multilane, multiplatoon case. This was accomplished by enhancing the platoon simulator developed in the first year.

However, vehicles in a complete AHS scenario will also undergo maneuvers such as platoon merging, platoon splitting, and free-speed accelerations (see, e.g., (Hsu et al. 1991)). Therefore, the modal emission model was integrated with the PATH-developed AHS simulator SmartPath (Eskafi et al. 1992; Hongola et al. 1993). SmartPath is capable of simulating multiple platoons and the above mentioned maneuvers. The modal emission modeling component was implemented as a post-processing module to the SmartPath simulator. It was found that modifications were necessary to some of SmartPath's routines in order to correctly estimate vehicle emissions. In particular, the mathematical formation characterizing the physics of speed and acceleration were modified so that the overall vehicle dynamics operated in a more realistic fashion, with respect to acceleration motion.

With the SmartPath/emissions modeling tool, vehicle emissions associated with various AHS scenarios were analyzed. Specifically, a steady-state velocity analysis was made of vehicle emissions specified as a function of traffic flow, both for an AHS case and a manual-driving case. Within this analysis, we compared total emissions between AHS and non-AHS scenarios at different levels of throughput. Further, we compared the throughput of AHS and non-AHS scenarios at equivalent emission rates. This analysis is described in more detail in Chapter 3.

Ramp Meter Emissions

In the first year of work, three sources of emissions related to ramp metering were identified. Each emissions source was then evaluated independently. Emissions reduction from freeway smoothing was determined from analytical formulas acquired from empirical data in the literature. An emissions increase due to ramp queuing was determined using a simplified lane queuing simulation. Finally, emissions due to hard accelerations from the meters were determined based on a constant engine power assumption under constraints of start and end velocities, ramp grade, and ramp length.

In the second year of work, the model FRESIM (Halati et al. 1991; FHWA 1993) was used to *integrate* all of these sources of emissions together, under varying conditions of ramp metering. The developed modal emission model was integrated with FRESIM to provide the total vehicle emission results. This analysis and results are described in further detail in Chapter 4.

1.4 REPORT ORGANIZATION

Chapter 2 provides background information on the modal emissions modeling approach that was taken and applied to the various transportation simulation models for this analysis. Chapter 3 then describes the details of the AHS emissions analysis that was carried out with the developed tools. Chapter 4 then describes the ramp metering emissions analysis, followed by conclusions in Chapter 5.

2 Emissions and Transportation Modeling

Prior to describing the project's experimental setup and results, it is necessary to give background information on emissions and transportation modeling techniques. Further information is given on the modal emissions modeling approach used throughout the experiments.

2.1 CURRENT EMISSIONS MODELING TECHNIQUES

The common modeling approach (specifically the MOBILE model, developed by the US Environmental Protection Agency (EPA) (Eisinger 1993) and EMFAC, developed by the California Air Resources Board (CARB) (Maldonado 1991; Maldonado 1992)) used to produce a mobile source emission inventory is based on two processing steps, as shown in Figure 2.1. The first step consists of determining a set of *emission factors* which specifies the rate at which emissions are generated, and the second step is to produce an *estimate of vehicle activity*. The emission inventory is then calculated by multiplying the results of these two steps together.

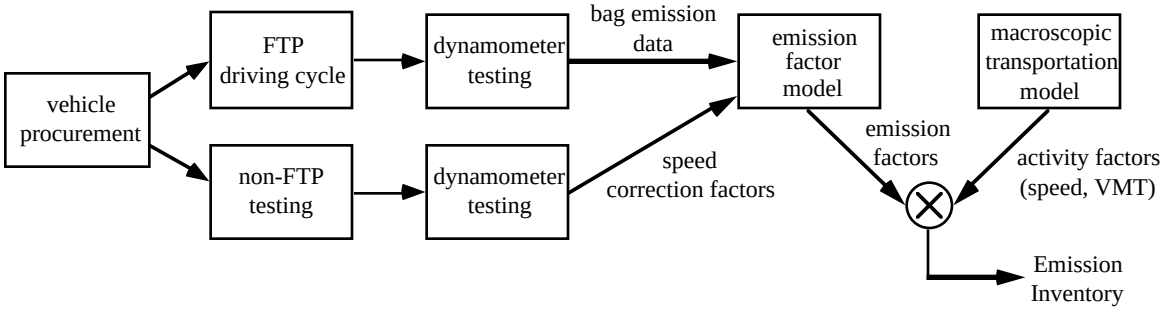

Figure 2.1. Current Emission Inventory Process

The current methods used for determining emission factors are based on laboratory-established emission profiles for a wide range of vehicles with different types of emission control technologies. The emission factors are produced based on average driving characteristics embodied in a pre-determined driving cycle, known as the Federal Test Procedure (FTP 1989). This test cycle was originally developed in 1972 as a certification test and has a specified driving trace of speed versus time, which is intended to reflect actual driving conditions both on arterial roads and freeways. Emissions of carbon monoxide (CO), oxides of nitrogen (NO_x), and hydrocarbons (HC) are integrated and collected for three sections of the cycle (called bags) and are used as base emission rates.

Adjustments are then made to the base emission rates through a set of correction factors. There are correction factors for each bag, which are used to adjust the basic emission rates to reflect the observed differences between the different modes of operation. There are also temperature correction factors and speed correction factors, used to adjust the emission rates for non-FTP speeds. These speed correction factors are derived from limited off-cycle testing (speeds greater than 57 mi/h (92 km/hr), accelerations greater than 3.3 mi/h-s (5.3 km/hr-s)) performed on laboratory dynamometers.

Vehicle activity data used for the emission inventory can come from a number of sources, although it is typically produced from a macroscopic transportation model. Traffic activity data is generated regarding vehicle miles traveled (VMT), number of vehicles, number of trips, and speed distribution on a region specific basis. Along with using an estimate of vehicle mix, the key variables of VMT and associated speed distribution are then multiplied with the emissions factors, producing a final emissions inventory. This methodology for calculating an emission inventory has several shortcomings, outlined below:

1) **Inaccurate characterization of actual driving behavior**—One of the underlying problems is that the standardized driving cycle of the Federal Test Procedure, which is used to certify vehicles for compliance of emission standards and from which most of the emissions data are based, was established over two decades ago (FTP 1989). At the time, the FTP was intended to exercise a vehicle in a manner similar to how a typical in-use urban vehicle would operate, however it did not include “off-cycle” vehicle operation which consist of speeds in excess of 57 mi/h and acceleration rates above 3.3 mi/h-s, common events in today’s traffic operation. It has been shown in a number of studies that the FTP does not accurately characterize today’s actual driving behavior (Markey 1993; Carlock 1993; Winer et al. 1993). Efforts are currently underway to revise the FTP (Markey 1993; US EPA 1993; US EPA 1995A; US EPA 1995B; US EPA 1995C).

2) **The emissions factor approach is limited**—The non-representative nature of the FTP driving cycle tests is exacerbated by the procedure used for collecting and analyzing emissions. As mentioned before, the FTP is divided into three segments in which emissions are collected into separate bags. The emissions from these three segments are then used by the emission models to statistically reconstruct the relationship between emission rates and average vehicle speeds. Thus the models statistically smooth the effect of accelerations and decelerations. In simple terms, two vehicle trips can have the same average speed, but may have different speed profiles that consist of drastically different modal characteristics (acceleration, deceleration, idle, etc.) and thus drastically different emissions output. This is

particularly true for current closed-loop emission control systems where it has been shown that dynamic operations of the vehicle are an important variable in predicting vehicle emissions (CRC-APRAC-91 1991; CRC-APRAC-92 1992; CRC-APRAC-94 1994; CRC-APRAC-95 1995; St. Denis et al. 1993).

Further, the speed correction factors used as the model input are derived from transient tests (not steady-speed tests) including the light-duty-vehicle FTP. The tests span a series of average speeds up to 65 mi/h. Running the nine cycles and scaling them to construct the speed correction curves may not accurately mimic real-world driving conditions. Inherent in this derivation of the speed correction curves is the assumption that averages in the skewed distributions representing the range of emissions at measured speeds can be validly combined to yield emissions factors for other (non-measured) speeds. On cycles other than the FTP, emissions are less well known since far fewer vehicles are tested on the other cycles. Actual emissions at a given speed depend on engine load (e.g., acceleration); hence, for example, the fluctuations about a given average speed—their amplitudes, time constants, and frequency of occurrence—will greatly affect the emissions accompanying that average speed. Real-world conditions may, in some cases, exceed the valid range of the test cycles; for example, real-world speeds often exceed the test cycle maximum of 65 mi/h (105 km/hr), and real-world accelerations commonly exceed the 3.3 mi/h-s (5.3 km/hr-s) maximum in the FTP cycle.

The importance of accelerations/decelerations is also underestimated by the models. Studies have shown that a single power acceleration can produce more CO than is emitted in the balance of a typical short (< 5 mi) trip (Kelly et al. 1993). Other events leading to high engine load can also produce high emissions. For example, vehicles traveling on significant road grades can dramatically increase emissions, and because of the nature of the current model inputs, grades are not taken into account. This raises doubts over the validity of the FTP for use in assessing the true impact of accelerations/decelerations and grades on tailpipe emissions and it is apparent that both the effect of high engine loads and the impact of gross-emitters are underestimated by the current methods used to estimate emissions.

Because of the inherent emissions and vehicle operation “averaging” that takes place in the conventional emission models, they offer little help for evaluating traffic operational improvements that are more microscale in nature. State and federal air quality management plans consist of numerous traffic control measures and more sophisticated inspection/maintenance programs. Further, traffic flow improvements can be accomplished through the advent of intelligent transportation systems. Operational improvements that improve traffic flow (e.g., ramp metering, signal coordination, automated highway systems, etc.) cannot be evaluated

accurately with the conventional emissions models, and thus a new modal emissions approach is necessary.

In recent years, a number of research projects have started to collect highly time resolved (e.g., second-by-second) emissions data and associated vehicle operating parameters (see, e.g., (Markey 1993)). With these data, it is possible to improve our understanding of what types and what amounts of emissions are resulting in relation to the measured vehicle parameters, and develop *modal* emission models, which can predict emissions as a function of vehicle operating modes, such as idle, various levels of acceleration/deceleration, steady-state cruise, etc. This is particularly important for the evaluation of various ITS scenarios, where driving conditions will not be similar to the conditions of the FTP, but rather be composed of diverse operating conditions that can only be evaluated using such a modal emissions modeling approach.

2.2 MODAL EMISSIONS MODELING APPROACH

For this project, we have taken a physical, power-demand modal modeling approach based on a parameterized analytical representation of emissions production. In such a physical model, the entire emissions process is broken down into different components that correspond to physical phenomena associated with vehicle operation and emissions production. Each component is then modeled as an analytical representation consisting of various parameters that are characteristic of the process. These parameters vary according to the vehicle type, engine, and emission technology. The majority of these parameters are stated as specifications by the vehicle manufacturers, and are readily available (e.g., vehicle mass, engine size, aerodynamic drag coefficient, etc.). Other key parameters relating to vehicle operation and emissions production must be deduced from a comprehensive testing program.

This type of modeling is more deterministic rather than descriptive. Such a deterministic model is based on *causal* parameters or variables, rather than based on simply observing the effects (i.e., emissions) and assigning them to statistical bins (i.e., a descriptive model). Further, the essence of this modeling approach is that the major effort is up front, in the model-development phase, rather than in application. Once the model forms are established, data requirements for applications and for updating to include new vehicles are modest. This limited requirement for data in future applications is perhaps the main advantage of this modeling approach. Of comparable importance, this approach provides understanding, or explanation, for the variations in emissions among vehicles, types of driving, and other conditions. Analysts will be able to discuss “whys” in addition to providing numbers.

There are several other key features that make the physical, deterministic model approach more appropriate:

- It inherently handles all of the factors in the vehicle operating environment that affect emissions, such as vehicle technology, fuel type, operating modes, maintenance, accessory use, and road grade. Various components model the different processes in the vehicle related to emissions.

- It is applicable to all vehicle and technology types. When modeling a heterogeneous vehicle population, separate sets of parameters can be used within the model to represent all vehicle/technology types. The total emission outputs of the different classes can then be integrated with their correctly weighted proportions to create an entire emission inventory.

- It can be used with both microscale and macroscale vehicle activity characteristics. For example, if a second-by-second velocity profile is given, the physical model can predict highly time resolved emissions. If average vehicle activity characteristics such as average speed, peak average speed, idle time, positive kinetic energy (PKE, a measure of acceleration) are given, the physical model can still be used based on average power requirements calculated from the activity parameters.

- It is easily validated and calibrated. Any second-by-second driving profile can be applied to the model, while simultaneously measuring emissions. The two results can be compared and the parameters of the model can be calibrated accordingly.

- It does not require extensive testing. As previously mentioned, the majority of key parameters affecting emissions production are already available from the vehicle manufacturers, such as vehicle weight, engine displacement, aerodynamic drag coefficient, etc. Other required parameters may be determined through abbreviated tests on a dynamometer.

- It is not restricted to pure steady-state emission events, as is an emissions map approach, or a speed/acceleration matrix approach. Therefore, emission events that are related to the transient operation of the vehicle are more appropriately modeled.

- It identifies explicitly the sources of errors. The majority of these errors are related directly to the inaccuracy or uncertainty of key parameters. In other words, the accuracy level of the model is largely dependent on how accurately these parameters can be determined. These key parameters could be some engine parameters such as enrichment power threshold and air-fuel

ratio at wide-open-throttle, or some driving cycle characteristics. One of the major advantages of this approach is that it tells us where and how to improve the model's accuracy.

- Functional relationships within the model are well defined. In contrast to a model which operates by sampling numerical data, this analytical approach avoids extrapolation and interpolation. Moreover, it will be possible to simply describe delay effects, such as with the introduction of times for command enrichment.

- The model is transparent. Results are easily dissected for evaluation. It is based on physical science, so that data are tested against physical laws and measurement errors can be identified in the model establishment phase.

- The computations performed in the model consist primarily of evaluating analytical expressions, which can be done quickly with only modest memory requirements.

Establishment of this type of model is data intensive. The modeling approach is based on the study of extensive emissions measurements in the context of physical laws. This involves systematic inductive study of physical mechanisms such as energy loss and chemical equilibrium, making extensive use of measurements. Models of this kind have been developed to predict fuel use, with data from the 1970s (e.g. (An et al. 1993; Ross et al. 1993)). Through this process one finds that the variations in fuel use and emissions among vehicles and in different driving modes are sensitive to only a few critical parameters. Satisfactory accuracy will be achievable with publicly available parameters, and with parameters which can be obtained from brief dynamometer tests.

The statement about the degree of parameterization *which is adequate* assumes that accuracy is interpreted in absolute terms on the basis of regulatory needs. For example, analytic modeling of extremely low emissions (that can occur for short periods during moderate-power driving) with high relative accuracy might complicate the model to no purpose. We are not concerned with relative accuracy where the emissions are below those of interest for regulatory purposes. Similarly, in current second-by-second data there is some temporal variability to emissions (which may not be real) whose study may not justify more detailed measurements and model making. For regulatory purposes, accurate prediction of emissions over modes on the order of ten seconds and more may be adequate.

Another critical component of the approach is that malfunctions and tampering have to be explicitly modeled. There is evidence that the emissions control devices of a high percentage of

in-use vehicles have been tampered with (Tierney 1991). Further, problems of high deterioration rates of catalyst efficiency, mis-fueled vehicles, etc., must be accounted for. Modeling components that estimate the emissions of gross-emitters are also an important part of this approach.

An outline of an example physical model (that used in this ITS analysis) and its components is first described, followed by a brief discussion of the modeling methodology.

2.2.1 Physical Model

A block diagram of this physical model is shown in Figure 2.2 and each component is described in detail below.

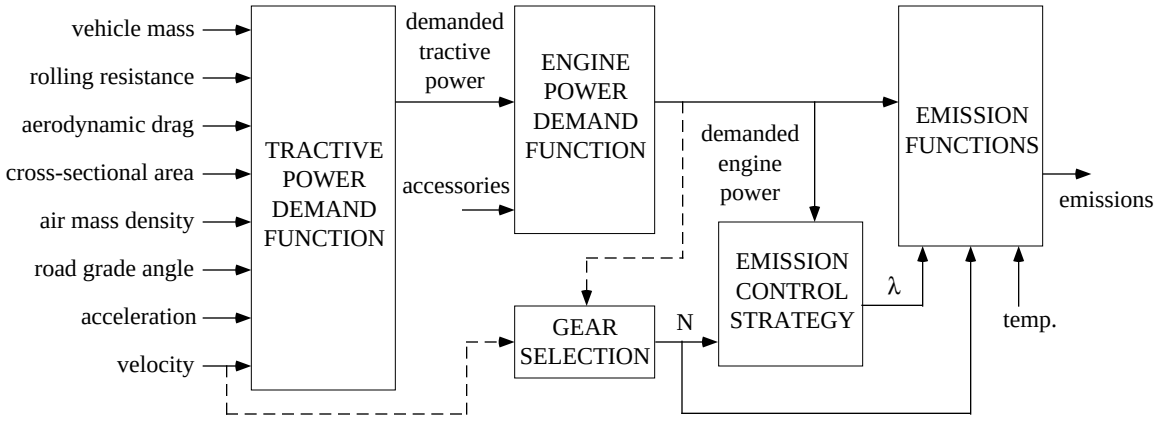

Figure 2.2. Power-demand emissions modeling methodology.

Tractive Power Demand Function

The instantaneous power requirements placed on a vehicle (at the wheels) for it to move depend on three types of parameters:

1) *Environmental factors:* e.g., mass density of air, road grade;

2) *Static vehicle parameters:* e.g., vehicle mass, rolling resistance coefficient, aerodynamic drag coefficient, cross sectional area;

3) *Dynamic vehicle parameters:* e.g., commanded acceleration, and velocity.

Given these parameters, the inertial power requirements (in kilowatts) are given in simplest form as:

$$P_{inertial} = \frac{M}{1000} \cdot V \cdot \left(a + g \cdot \sin\theta\right) \tag{2-1}$$

where M is the vehicle mass (kg), V is the vehicle velocity (meters/second), a is the vehicle acceleration (meters/s^2), g is the gravitational constant (9.81 meters/s^2), and θ is the road grade angle. The power requirements due to the drag components are given in simplest form as:

$$P_{drag} = \left(M \cdot g \cdot C_r + \frac{\rho}{2} \cdot V^2 \cdot A \cdot C_a \right) \cdot \frac{V}{1000} \tag{2-2}$$

where C_r is the rolling resistance coefficient, ρ is the mass density of air (1.225 kg/meter^3, depending on temperature and altitude), A is the cross sectional area (meter^2), and C_a is the aerodynamic drag coefficient. Thus the total tractive power requirements placed on the vehicle (at the wheels) is given as:

$$P_{tract.} = P_{inertia} + P_{drag} \tag{2-3}$$

Engine Power Demand Function

To translate this tractive power requirement to demanded engine power requirements, the following simple relationship can be used as a first approximation:

$$P_{engine} = \frac{P_{tract.}}{\eta_{tf}} + P_{acc.} \tag{2-4}$$

where η_{tf} is the combined efficiency of the transmission and final drive, and $P_{acc.}$ is the engine power demand associated with the operation of accessories, such as air conditioning, power steering and brakes, and electrical loads. In the final model, P_{acc} may be modeled as a function of engine speed, and η_{tf} can be modeled in terms of engine speed and P_{tract}.

Gear Selection and Engine Speed

The speed of the engine in relation to the speed of the vehicle is determined by the driver (manual transmission) or, in the case of automatic transmissions, by an internal gear selection strategy (or shift schedule) that depends on inputs such as engine and vehicle speeds, and possibly other related inputs such as demanded engine power. Engine speed N (rps) plays a role in fuel use and the emission control function.

Gear selection and engine speed are complicated by the wide variety of automatic transmissions and their management. It is not necessary, however, for the model to accurately specify engine speed every second. Rather, accuracy is required for longer intervals. For these purposes, simple statistical specification of shift scheduling/engine speed will be adequate. It should prove satisfactory to determine engine speed in terms of immediate prehistory and vehicle speed in combination with the power requirement.

Emission Control Strategy and Equivalence Ratio

One of the most important components of this physical model is approximating the emission control mechanisms of the vehicle. For older vehicles, engine control was accomplished through some combination of mechanical, pneumatic, or hydraulic systems. The engine control regulates fuel and air intake as well as spark timing and EGR (Exhaust Gas Recirculation) to achieve the desired performance in fuel economy, emissions, and power output. Due to the advent of automotive electronics, modern vehicles have complex emission control systems that closely regulate fuel injectors.

For a hot-stabilized engine operating under normal conditions, it is desired to maintain the fuel mixture at the stoichiometric ratio, where the performance of the catalytic converter is maximized. However, there are several other vehicle operating modes that can affect the commanded air/fuel ratio. During engine start and warm up, the air/fuel ratio is typically commanded rich so that there is improved combustion stability (older, carbureted vehicles use a choke). Another important operating mode is during high power episodes, such as those induced by hard accelerations and/or steep grades. During such an episode, the air/fuel ratio is again commanded rich for peak demand power and protection of engine and catalyst components.

When modeling the emission control function, we consider λ as the regulated output variable, where λ is the "equivalence ratio" and is defined as:

$$\lambda = \frac{(A/F)_0}{(A/F)} \tag{2-5}$$

where $(A/F)_0$ is the air/fuel ratio at stoichiometry (≈ 14.7), and (A/F) is the commanded air/fuel ratio. Like engine speed, the equivalence ratio must be modeled in terms of the driving characteristics (especially the engine power required, and engine warm-up history) and parameters which describe the vehicle's command enrichment strategies. As with engine speed, it is not necessary to accurately specify equivalence ratio every second; but, since λ is a sensitive

parameter for emissions control in short, high-powered driving episodes, it must be accurately specified for relatively short periods.

Emission Functions

The final component of the physical model is a set of analytical functions that describe the emissions rates of the vehicle, with inputs such as engine power demand, engine speed, equivalence ratio, and temperature. As part of these functions, it may be useful to model fuel use which focuses on energy loss modes in the engine and transmission. Given engine power, engine speed, and equivalence ratio, good results may be obtained with just one additional parameter, engine displacement. In addition, average engine and transmission loss parameters can vary with type of transmission, but do not otherwise vary from vehicle to vehicle. Good accuracy can be obtained using a few additional parameters which require measurement.

The authors are currently conducting research using second-by-second data for 28 modern vehicles from the FTP Revision Project. The variations with high power and enrichment of engine-out emissions and catalyst pass fraction are being studied. Preliminary results suggest that an accurate representation can be achieved with a few parameters. It may prove that the necessary parameters can be determined from the expected supplement to the FTP on emissions at high power. The emissions at low power and stoichiometric conditions require parameterization, for which the FTP bag measurements may prove adequate.

2.2.2 Methodology

Using this physical model approach, it is necessary to establish models for different engine/emissions technologies that are represented in the national vehicle fleet. This includes the appropriate combinations of engine type (spark ignition, diesel), fuel delivery system (carbureted, fuel injection), emission control system (open-loop, closed-loop technology), and catalyst usage (no catalyst, oxidation catalyst, three-way catalyst). The physical model outlined above only considers the different components for a modern, closed-loop emission controlled vehicle having a spark ignition engine. There are several other vehicle/technology/year combinations that will require variations of the physical model.

After the models corresponding to the different technologies have been approximately established, the key parameters in each component of the models must be identified that characterize vehicle operation and emissions production. These parameters can be classified into several categories: 1) readily available (i.e., public domain) static vehicle parameters (e.g., vehicle mass, rolling resistance coefficient, engine size, etc.); 2) measurable static vehicle

parameters (e.g., vehicle accessory power demand, enrichment power threshold, etc.); 3) deterioration parameters (e.g., catalyst aging, etc.); 4) fuel type parameters; and 5) vehicle operating parameters.

When the physical models and associated parameters are established for all vehicle/technology/year combinations, they must be combined with vehicle operating parameters that are characteristic of real-world driving. These vehicle operating parameters consist of static environmental factors such as ambient temperature and air density, as well as dynamic factors such as commanded acceleration (and resultant velocity), road loads such as road grade, and use of vehicle accessories (e.g., air conditioning, electric loads, etc.).

Combining the physical models with vehicle operating parameters results in highly time resolved emission rates. These predicted rates can then be compared directly to measured emissions data, and the parameters of the modeling components—or the modeling components themselves—can be adjusted to establish an optimal fit. This calibration/validation process can occur iteratively until the models are well developed. The physical models and associated parameters can also be combined with average trip vehicle operating parameters to provide a more generalized description of emissions.

2.3 MODAL MODEL IMPLEMENTATION

For the emissions evaluation conducted in this project, we have used a preliminary model that is based on a single passenger vehicle. The equations corresponding to vehicle dynamics and power-demand based emissions are calibrated to a 1991 Ford Taurus, using data received from Ford Motor Company. This electronic fuel injection vehicle has state-of-the-art emission control equipment. The results of the simulation models with these preliminary data are given in this report. It is important to point out that the emissions for this single vehicle do not represent the emissions behavior for an entire fleet of automobiles. It has been noted that there is high variability in the emissions output of different vehicles on identical tests, and even identical vehicles on different tests. Even though the preliminary results in this report are based on a single vehicle, trends can be seen and important conclusions can be made regarding the importance of linking modal emissions with dynamic vehicle activity. As further modal emission data becomes available for other vehicles from Ford and other sources, they can easily be incorporated into the models when determining a more complete, comprehensive emissions estimate.

2.4 TRANSPORTATION MODELING

In general, transportation modeling consists of several integrated models that are used together to define the transportation planning process. These components are described in detail in the literature (e.g., Warner 1985), and are briefly outlined below:

Trip Generation Models: This initial component is concerned with the causes of trips, i.e., what environmental circumstances lead to the production or attraction of traffic. This is usually based on demographic variables such as household size, income, and number of vehicles per household. Trip generation models estimate the number of total trips based on trip purpose on an area-by-area basis.

Trip Distribution Models: After estimating the traffic demand generated in each area, trip distribution models determine the destinations of the outflows and the origins of the inflows for the different areas.

Modal Choice Models: This component deals with the transportation modes that the anticipated flows will use: private car, bus, train, etc. These models estimate the distribution of the transportation flows over the various transportation modes.

Trip Assignment Models: This final component is concerned with what route the transportation flows will take. With a network of different transportation routes, trip assignment models predict the paths of travel for the distribution of transportation flows. These network loading models usually are based on the assumption that users will always use the quickest route.

Once all of these components are in place, traffic can be simulated on a transportation network, usually composed of links and nodes. The links represent road segments and nodes represent potential turning points. Based on the demand database consisting of sources, destinations, volumes, and types of vehicles determined by the first three components described above, the traffic simulation predicts the traffic operation over the network as a function of time using the trip assignment component. The traffic simulation can illustrate such things as congestion due to inadequate road systems, construction, accidents, or similar factors.

2.4.1 Microscale and Macroscale Models

Transportation simulation models typically fall into one of two categories, microscale and macroscale. Microscale models typically model at the vehicle level and have high accuracy, but require extensive data on the system under study and require more computing power than

macroscale models for problems of the same scope. Macroscale models often require less detailed data, but they sacrifice detail in order to enable the modeling of larger areas using computers with modest power. Transportation simulation models are used for analyzing various operating environments of the road system. These operating environments include signalized intersections, arterial networks, freeway corridors, and rural highways.

Some examples of microscale performance models are TRAF-NETSIM (FHWA 1989, for arterial networks) and FRESIM (Halati et al. 1991, for the freeways). Macroscale models that are based on analytic flow models include FREFLO (May 1990), TRANSYT-7F (FHWA 1986) and HCS (TRB 1985). Many of these models were developed before the introduction of efficient and cost-effective mini- and micro-computers. The models have been enhanced over the years, and many are powerful and effective. However, most are difficult to maintain and modify, contain bugs even after over a decade of development, and have rigid input/output routines structured around the punched card concept.

Therefore, newer traffic models have been developed in recent years that take advantage of the many developments of modeling, software engineering, and hardware platforms which have occurred over the past decade. For example, the THOREAU model (McGurrin et al. 1991) makes use of object-oriented programming for greater flexibility, and is based on event-stepped simulation rather than time-stepped, resulting in greater speed performance. Another recently developed transportation model is the model INTEGRATION (Van Aerde 1992). These more recent models are better suited for simulating various ITS scenarios, since they have greater flexibility and greater level of detail that are required for simulating new transportation technologies. Other specific transportation simulation models have been developed in particular for the evaluation of ITS, such as the simulators SmartPath (Eskafi et al. 1992; Hongola et al. 1993; Eskafi et al. 1993) and SmartLink (Rao et al. 1994) developed within the PATH program.

Few of these transportation models have been combined with vehicle emission models, and those that do simply predict vehicle density and speed as a function of link and time to be integrated with current speed-emissions data. Although this is a step in the right direction, much better emission estimates can be achieved using transportation models that can predict dynamic vehicle operating characteristics such as acceleration and deceleration, by combining these with a modal-based emissions model.

2.4.2 Transportation/Emissions Modeling Interface

The particular method for combining a modal type of emissions model with transportation activity information is an important issue when determining an emissions inventory for either a

specific facility (e.g., an intersection) or a large roadway network (i.e., regional inventory). Transportation activity information can come either from traffic data measured in the field, or from data generated by various kinds of transportation models.

As mentioned previously, the current method of estimating regional emissions is based on averaged, FTP-based emission estimates of in-use vehicles, indexed by the vehicle activity factor of speed. Since average vehicle speed is a readily usable parameter from macroscale transportation models, they can be effectively combined with regional emission models (e.g., EMFAC and MOBILE). However, in order to evaluate microscale traffic scenarios (i.e., ramp metering, signal coordination, ITS scenarios, etc.), a modal emissions model is better suited.

The physical, power-demand modal emissions model described earlier is microscale in nature. It is able to simulate highly time resolved vehicle tailpipe emissions (for a specific vehicles) under any given driving activity. Driving activity is typically represented as a velocity-vs.-time profile, sometimes referred to as a driving cycle. Given a velocity-vs.-time profile, commanded acceleration can be determined, and inertial power requirements for the vehicle can be computed. In addition, the velocity information can be used in determining the power requirements due to the drag components, such as rolling and aerodynamic resistance. In addition to this velocity-vs.-time profile, the driving activity data should also contain information pertaining to dynamic road changes, in particular road grade information. A grade-vs.-time profile can be matched with the velocity-vs.-time profile to provide a complete representation of driving activity. The other parameters used in the power demand equations are usually considered to be constant. However, if there are some parameters that are not constant for a specific driving activity, they too can be represented as a dynamic time profile (e.g., if the air conditioner usage varies during the driving profile). Once the demand power is determined as a function of time, tailpipe emissions can be calculated primarily as a function of demand power.

Therefore, driving activity information in the form of velocity-vs.-time and grade-vs.-time profiles are all that is required for the modal emissions model to estimate emissions at this microscale level. If grade is assumed to be constant or zero, then the velocity-vs.-time profile alone is sufficient. In microscale traffic simulations, vehicle trajectories (position indexed by time) are often provided as output. Most microscale traffic simulations provide access to highly time resolved vehicle trajectory data, from which emissions can be predicted with the modal emissions model (e.g., TRAF-NETSIM, FRESIM, SmartPath, etc.).

It is important to point out that a modal emissions model can also be integrated directly with velocity (and grade) data measured on the road. A large database of driving patterns exist from

various sources (e.g., EPA driving pattern studies in Spokane, Atlanta, and Baltimore (Markey 1993)). Thus, given any set of driving pattern data (that contains velocity and possibly grade profile information), estimates of total emissions can be made using the modal emissions model.

2.4.3 TRANSITION FROM MICROSCALE TO MACROSCALE EMISSIONS

The application of a modal emissions model to detailed traffic simulation models is relatively straightforward, but the estimation of larger, regional emissions is somewhat more complicated. Again, because microscale models typically model at the vehicle level and have high accuracy, they require extensive data on the system under study and are typically restricted in size due to the non-linear complexity gain incurred with larger networks. In order to produce emission inventories of greater scope, researchers at CE-CERT have developed an Integrated Transportation/Emissions Model (ITEM) that can produce regional emission inventories as well as facility-specific inventories (e.g., an intersection). The general architecture of ITEM is based on a hybrid macroscale/microscale approach which is illustrated in Figure 2.3. Various microscale simulation sub-models are used, organized by roadway facility type (e.g., freeway section, arterials, intersections, rural highways, freeway on-ramps, etc.). At this microscale level, emissions are estimated as a function of vehicle congestion on each facility type, with different degrees of geometrical variation. Statistical emission rates are derived from the microscale components as a function of roadway facility type and congestion level. These rates are then applied to individual links of a macroscale traffic assignment model. A travel demand model drives the traffic assignment for the macroscale traffic model, which can dynamically re-route traffic as network capacities change. The microscale simulation components are tightly coupled with the macroscale traffic assignment model and can operate in parallel. Thus, users of the model can simulate real-time events (such as a traffic accident) and see the effect on traffic dynamics and emissions at both macro- and microscale levels.

The macroscale traffic assignment simulation model in ITEM is event-driven and can dynamically determine link densities and speeds for a large, regional road network. It uses queuing theory which features single vehicle level of detail, but is event-stepped rather than time-stepped. This allows for an accurate treatment of high traffic volumes without loss of detail. The macroscale model provides input into the microscale simulation components that can handle numerous transportation events with a high level of detail. Each microscale component incorporates the detailed modular emissions data for its particular case. It is important to point out that there is a high level of interaction between the macroscale and the microscale components, indicated by two-way arrows in Figure 2.3. When the various components operate simultaneously, transportation parameters determined by the macroscale model are used to drive

the input parameters of the microscale components. Further, control information sent back from the microscale components can be used as feedback to the macro model, thus dynamically altering the global traffic assignment.

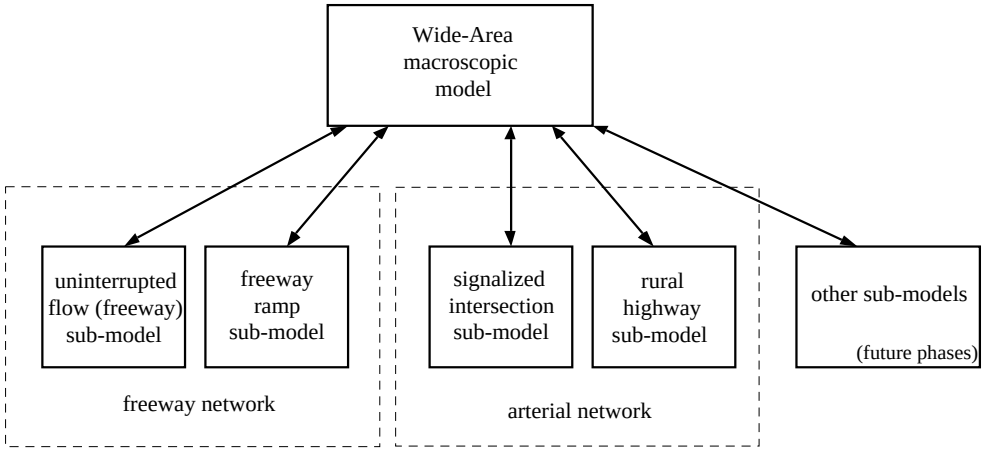

Figure 2..3 Integrated Transportation/Emissions Model Set

In order to implement a model like ITEM for a specific region, several sources of input are required:

- **Roadway Network Data—**The roadway network to be evaluated needs to be specified in terms of topology. Regional network data generally exist for almost every city or metropolitan area. Different roadway facility types are typically identified as different links within the network.

- **Grade Information—**If the roadway network data exists as part of a Geographical Information System (GIS), then it is likely that grade information can also be incorporated into the network.

- **Travel Demand Data—**Once a roadway network has been established, a travel demand model must be used to estimate trip generations and distributions, while specifying the travel mode. Travel demand data is typically represented as a time-indexed origin/destination matrix by mode. City and metropolitan planning organizations generally use travel demand models which can be readily used with a model like ITEM.

3 Automated Highway System Emissions

As a key culmination of ITS technology, an Automated Highway System (AHS) will substantially improve the safety and efficiency of highway travel. An AHS is a fully automated system in which instrumented vehicles will operate on instrumented roadways without operator intervention (US DOT 1995). Various sensors and communication devices will link the vehicles and roadway, virtually eliminating driver error and maximizing traffic performance. Drivers equipped with a vehicle instrumented for AHS operation will be able to enter an AHS through a check-in area and proceed onto a transition lane, where control of the vehicle will be assumed by the AHS. The system will then move the vehicle onto one of the automated lanes where it then merges with other traffic. When the driver's destination is reached, the system will move the vehicle back to the transition lane where the driver will be able to resume control of the vehicle (US DOT 1995).

Some of the key benefits of an AHS are (Saxton 1993; Congress 1994):

- Improved safety, since the human error factor will be eliminated;
- Increased roadway flow rates, since vehicle spacings can be safely reduced, resulting in higher traffic densities traveling at higher speeds;
- Reduced congestion, since traffic flow variances due to slow human reactions will be eliminated;
- Increased user comfort, since there will be less strain on the drivers;
- Reduced fuel consumption and vehicle emissions, since there will be little or no stop-and-go driving.

There is concern, however, that a reduction in congestion due to an AHS implementation will lead to an increase in travel demand, resulting in an increase of total vehicle miles traveled (VMT) and a concomitant increase of vehicle emissions. If an AHS allows smoother flow and higher speeds on the roadways, people may choose to live farther away from work while still commuting in the same amount of time—thereby increasing the VMT. Farther, attractive trip-ends will become reachable, again increasing VMT. This induced traffic demand issue is important and is the subject of several studies (e.g., (Ostria 1995; Washington et al. 1993; Meyer et al. 1994; Vaughn et al. 1995)). In this research, however, we address only the *direct* relationship between vehicle emissions and the operation of an AHS. Specifically, we are

interested in quantifying the emissions benefit an AHS may have over today's manually driven highways due to smoother traffic flow (i.e., less stop-and-go traffic in congestion) and increased overall throughput.

The National Automated Highway System program was given high priority in response to the mandate of the Intermodal Surface Transportation Efficiency Act of 1991 (ISTEA) to "develop an automated highway and vehicle prototype from which future fully automated intelligent vehicle-highway systems can be developed." In the summer of 1993, 15 precursor systems analysis projects were started to investigate the issues and risks related to AHS design, development, and implementation (AHS Precursor Workshop 1994). The completion of these precursor projects has led to the development of a National AHS Consortium (NAHSC) that will provide leadership and focus to the nation's AHS effort. The NAHSC will lead the development of a prototype AHS to be demonstrated in 1997. The California PATH program is a core participant of NAHSC.

Research conducted at PATH has shown conceptually that an AHS can provide safe, efficient movement of vehicles on the highway (e.g., (Karaaslan et al. 1990; Varaiya et al. 1991; Rockwell 1992; Zhang et al. 1994)). However, an AHS is a complex system and must be capable of performing a wide range of operations, such as network traffic management, route planning and guidance, coordination of vehicle movements, and automated vehicle maneuver control. Each of these operations will have an effect on vehicle emissions.

In this research project, we have begun to evaluate the impact of AHS on vehicle emissions using simulation modeling. Initially, we have concentrated on automated vehicle control, specifically on the operation of "platooning" implemented using longitudinal control. A fully automated highway system will consist of automated traffic in several lanes using both longitudinal and lateral control, with numerous platoon maneuvers such as platoon splitting, merging, etc. (see, e.g., (Hsu et al. 1991; Varaiya et al. 1991)). The impact of these maneuvers on vehicle emissions has also been investigated.

Principles of uninterrupted traffic flow are first reviewed, followed by a brief description of platooning concepts. A platoon simulation model developed for emissions analysis is then described. The use of PATH's SmartPath AHS simulator for emissions prediction is then discussed. Using the simulation models, steady-state emissions are evaluated and compared to manual traffic emissions. An analysis of emissions related to AHS maneuvers is then presented.

3.1 UNINTERRUPTED TRAFFIC FLOW

Current highway traffic (i.e., uninterrupted traffic flow) can be characterized by the traffic volume (v), average vehicle speed (S), and vehicle density (D). These terms are generally related by the product $v = S \times D$ (TRB 1985). Further constraints operate on these parameters which restrict the type of flow conditions on a highway link. The general form of these constraints is shown in Figure 3.1, which illustrates some key points of uninterrupted traffic flow:

- Zero rate of flow occurs in two distinct cases: 1) when there are no vehicles on the roadway, and 2) when the density is so high that all vehicles are stopped and cannot move. In the first case, the density is zero, thus the flow rate is zero, and the speed in this case is assumed to be the driver's desired speed (i.e., vehicle free speed). In the second case the density is at its maximum and the vehicle speed is zero. The density at which this occurs is called the jam density.

- As density increases from zero, the traffic flow increases due to the increased number of vehicles. The average vehicle speed is reduced to maintain safety during higher density conditions.

- Traffic flow is maximized at a specific critical density. As density increases above the critical density point, speed drops off at a faster rate. Traffic flow tends to become unstable in this region due to perturbations from lane change maneuvers, merging, or any external variables (e.g., debris in roadway, accident in adjoining roadway, etc.). These perturbations can create disturbances that are not damped or dissipated in the flow. These unstable, forced flow regions in the curves are characterized by stop-and-go congestion.

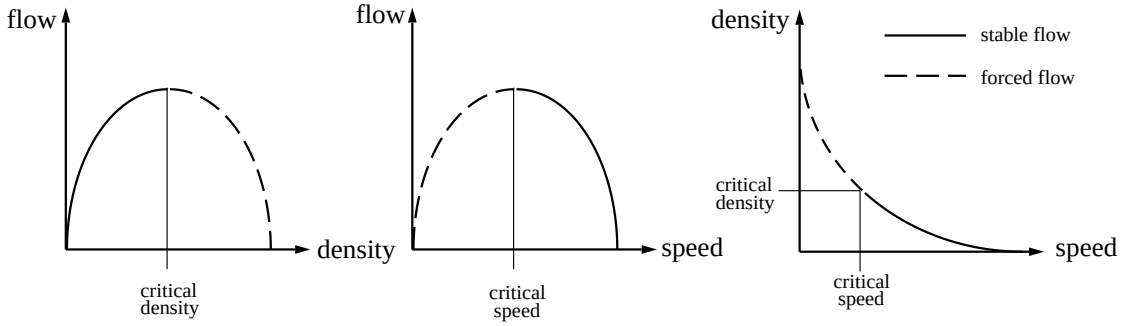

Figure 3.1. Flow, density, and speed relationship of uninterrupted traffic flow.

Human driver flow-density-speed relationships can be approximated mathematically by specifying the spacing, or gap, between vehicles required for safe stopping if one car suddenly brakes, and after a time lag, the second car also brakes without collision. The flow-density curve in Figure 3.2 was produced for the case when the first car brakes at 0.9 g (8.82 meters/second^2) and the second car brakes at 0.6 g (5.88 meters/second^2) after a one second time lag. This curve (after (Rockwell 1992)) is for a single lane and is similar to curves predicted by the Highway Capacity Manual (TRB 1985).

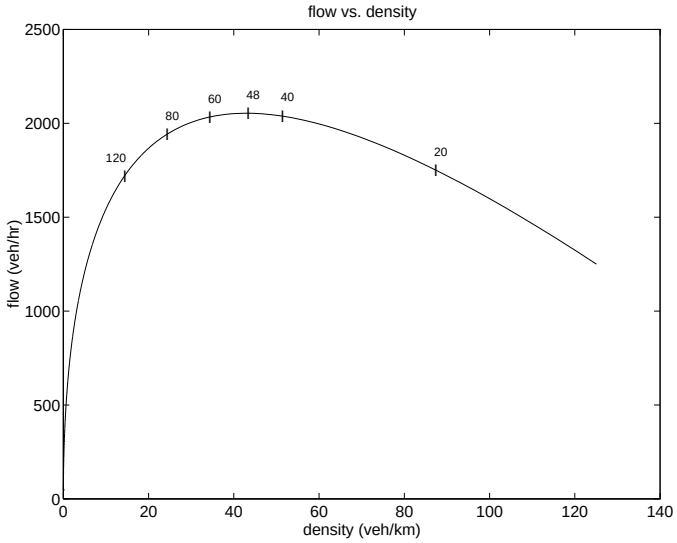

Figure 3.2. Flow-density relationship for manual traffic. Velocity values (km/hr) are annotated on the curve.

3.2 PLATOONING

In order to improve the flow rate on the highway, ITS technology in the form of AVCS can be applied to control vehicle motion so that vehicles can operate in platoons, i.e., follow each other very closely at high speeds, while still maintaining a high safety margin. This has several implications: 1) traffic flow will increase dramatically over current highway conditions due to denser traffic traveling at higher speeds; 2) congestion should decrease since the stop-and-go effect caused by relatively long human reaction delays will be eliminated and accidents will be minimized.

A similar mathematical formulation to that above can be developed for the flow-density-speed characteristics of an automated highway system. Within a platoon of vehicles, the spacings are much smaller and closely regulated by automated controls. Therefore, platooned vehicles can travel faster at higher densities, thus improving the traffic throughput. If we consider a single lane of platooned traffic as shown in Figure 3.3, we can mathematically approximate the flow-

density-speed characteristics. Using the notation given in Figure 3.3, the vehicle density for an automated lane is given as:

$$D = \frac{n}{\Delta + n(L+\delta) - \delta} \tag{3-1}$$

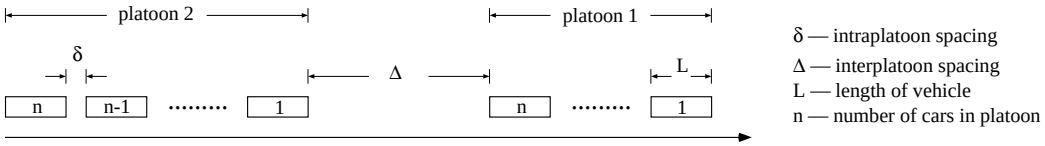

Figure 3.3. Platoons of vehicles on a highway.

The interplatoon spacing is determined as described before, i.e., requiring safe stops if one platoon suddenly brakes, and after a time lag, the second platoon (leader) also brakes. In the automated scenario, the time lag is much shorter than that for human drivers. The resulting flow-density curve in Figure 2.4 was produced for the more restrictive case when the first platoon brakes at 2 g (19.6 meters/second^2), and after a 0.3 second time lag, the second platoon (leader) brakes at 0.3 g (2.94 meters/second^2). It is assumed that the intraplatoon spacing is precisely controlled and can also perform safe stops under these specified stopping conditions. In the mathematical formulation, the intraplatoon spacing is set to one meter, the car length is five meters, the number of vehicles in each platoon is 20 vehicles, and the vehicle free speed is 120 km/hr. The difference between the flow for manual driving and automated driving is substantial. The maximum traffic flow for this automated case is roughly four times that of the manual driving case. The maximum flow for the automated case occurs at an average speed of 103 km/hr, and for the manual case it occurs at 48 km/hr.

In the AHS architecture which serves as the basis for the SmartPath simulator (described in (Hsu et al. 1991)), a vehicle enters the AHS and announces its destination exit. The system then assigns a route for the vehicle, consisting of various path changes along the route. A path consists of a sequence of platoon maneuvers, where the three key maneuvers for a platoon are *merging, splitting*, and *lane changing.* These maneuvers are selected and implemented by the platoon leaders (and free agents, defined as one vehicle platoons), after communication takes place within the platoon. Because of these maneuvers, platoons will dynamically vary in length as vehicles travel from their specific origins to destinations. Thus the high flow rate for automated traffic shown in Figure 3.4 will be somewhat reduced, since the average platoon

length per lane will be less than the specified maximum (in this case, 20 vehicles). Figure 3.5 shows the reduction of flow with shorter platoon lengths. Further, because of the maneuvers described above, the average speed of automated traffic will be less than the assigned free speed of the platoons. This also reduces the average flow rate per lane.

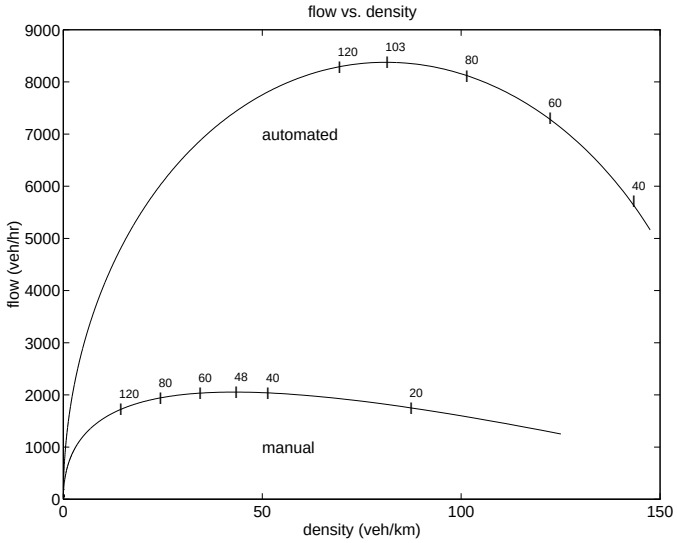

Figure 3.4. Flow-density relationship of traffic for both manual driving and automated driving. Velocity values (km/hr) are annotated on the curves.

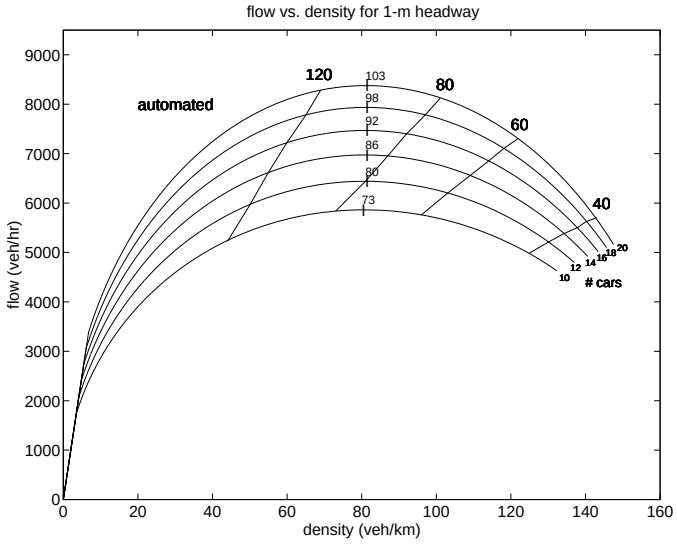

Figure 3.5. Flow-density relationship of automated traffic for different platoon lengths. Velocity values (km/hr) are annotated on the curves.

3.3 PLATOON SIMULATION MODEL

Prior to using PATH's SmartPath model, CE-CERT developed a microscale platooning simulation model in order to study platoon-related emissions. This microscale platooning model simulates individual vehicle behavior on a freeway and integrates each vehicle's calculated operating parameters to determine an emissions output, based on the modal emissions model described in Chapter 2. Although multiple lanes have been implemented in the simulation, control has been implemented only in the longitudinal direction; lateral control for lane changing, platoon merging, and platoon splitting have not been implemented.

3.3.1 Vehicle Dynamics

This simulation model considers at the fundamental level each vehicle's acceleration performance. The acceleration performance (in the longitudinal direction) is limited by the engine power and the traction limits on the drive wheels. Engine power is modeled in detail using torque curves that vary with RPM (Gillespie 1992). For a more detailed estimation of engine power transferred to the road, a powertrain model was also developed. Vehicle acceleration due to engine power is modeled as follows (from Gillespie 1992):

$$a_{ep} = 76.2 \frac{\mathrm{g} \times HP}{V \times \mathrm{W}} \tag{3-2}$$

where g is the gravitational constant (9.8 m/sec^2), HP is the engine horsepower, V is the vehicle velocity (m/sec) and W is the weight of the vehicle (kg). The constant 76.2 converts from horsepower to m-kg/sec. This is the vehicle's acceleration, given in m/sec^2, due only to engine power.

The effect of rolling resistance is based on the equation (Gillespie 1992):

$$a_{rr} = -f_r \times \mathrm{g} \tag{3-3}$$

where f_r is the rolling resistance coefficient, and again g is the gravitational constant. Note that this term is negative since the resistance results in negative acceleration. This rolling resistance coefficient takes into account energy due to deflection of the tire sidewall near the contact area, energy loss due to deflection of the road elements, scrubbing in the contact patch, tire slip in the longitudinal and lateral directions, deflection of the road surface, air drag on the inside and outside of the tire, and energy loss on bumps (after Gillespie 1992). Changes in vehicle weight alter this relationship, but not significantly and therefore will not be considered.

The effect of aerodynamic drag on acceleration is significant at high speeds. The drag depends on the dynamic pressure, and is proportional to the square of the speed. Acceleration loss due to aerodynamic drag is given as (Gillespie 1992):

$$a_{ad} = -\frac{\rho}{2} \times \frac{g\, C_D\, A\, V^2}{W} \tag{3-4}$$

where ρ is the air density, C_D is the aerodynamic drag coefficient, A is the frontal area of the vehicle, W is the vehicle weight, and V is the vehicle velocity. Again, this is a resistive force to the vehicle, and thus the acceleration is negative.

Because the follower vehicles within a platoon have very small intraplatoon spacings (e.g., on the order of one meter), the aerodynamic drag coefficient of each follower is significantly reduced due to the "drafting effect" (Zabat et al. 1994; Zabat et al. 1995). Using preliminary aerodynamic drag reduction data for vehicles in platoons (Zabat et al. 1994; Zabat et al. 1995), the calculated load on the engine is significantly smaller at higher speeds. Based on the data, even the lead vehicle of a platoon has its aerodynamic drag coefficient reduced due to the vehicle following closely behind. Therefore, when a vehicle travels in a platoon in the simulation, the aerodynamic drag coefficient is reduced by an adjustment factor derived from the results of (Zabat et al. 1994; Zabat et al. 1995).

Finally, the influence of road grade on acceleration is considered. This is a simple relationship which depends on the sine of the grade angle:

$$a_{rg} = -g \times \sin(\theta) \tag{3-5}$$

If all of these equations are now put together to get the total vehicle acceleration, the result is:

$$\begin{aligned} a_{total} &= a_{ep} + a_{rr} + a_{ad} + a_{rg} \\ &= 76.2\frac{g \times HP}{V \times W} - f_r \times g - \frac{\rho}{2} \times \frac{g\, C_{Dadj}\, A\, V^2}{W} - g \times \sin(\theta) \end{aligned} \tag{3-6}$$

where C_{Dadj} is the adjusted aerodynamic drag coefficient due to drafting within the platoon. With this equation, it is possible to determine acceleration as a function of velocity, along with several constants.

In the simulation, each vehicle was modeled as a 1991 Ford Taurus, which has the following characteristics:

maximum horsepower	140 hp
weight	2020 kg
rolling resistance coefficient	0.015
aerodynamic drag coefficient	0.42
frontal area	3.1 m^2

Table 3.1. Specifications of 1991 Ford Taurus.

These values are combined with the following constants:

gravitational constant g	9.8 m/sec^2
air density ρ	0.00236
grade θ	0°

Table 3.2. Environmental constants used in calculations.

The vehicle dynamics of coasting (little or no engine power applied) are based on the rolling resistance and aerodynamic forces applied to each vehicle. The coasting acceleration (which is negative in this case, a deceleration) is given as:

$$a_{coast} = -f_r \times g - \frac{\rho}{2} \times \frac{g\, C_D\, A\, V^2}{W} - g \times \sin(\theta) \tag{3-7}$$

The vehicle dynamics of braking are also considered, where it is assumed that a constant braking force F_b is applied to the vehicle, resulting in negative acceleration. Thus, a braking term is introduced in the acceleration equation:

$$a_{brake} = \frac{F_b \times g}{W} - f_r \times g - \frac{\rho}{2} \times \frac{g\, C_D\, A\, V^2}{W} - g \times \sin(\theta) \tag{3-8}$$

F_b is the total of all braking forces, i.e., front axle braking force, rear axle braking force, and engine braking. If F_b exceeds a certain threshold, then wheel lockup occurs, and the vehicle deceleration is dependent on the effective coefficient of friction at the tire-pavement contact surface.

3.3.2 Longitudinal Control

In an AHS, the longitudinal control for a platoon lead vehicle will likely be automated, using information based on link characteristics. For this simulation model however, the lead vehicle

longitudinal control is based on either a prescribed velocity profile, or on a simple car following equation that maintains a sufficiently safe gap between platoons. The car following equation for the later case is given as:

$$\ddot{x}_{n+1}(t+\Delta t_{n+1}) = S_{n+1}\frac{[\dot{x}_n(t)-\dot{x}_{n+1}(t)]}{[x_n(t)-x_{n+1}(t)]} \tag{3-9}$$

where Δt_{n+1} is the *reaction delay* of vehicle n+1 and S_{n+1} is the *sensitivity* of vehicle n+1. Note that this equation bases the acceleration directly proportional to relative velocity (originally from Forbes' theory (May 1990)) and inversely proportional to the distance headway (originally from Pipes' theory (Pipes 1953)). The sensitivity and reaction delay factors are stochastically assigned based on Gaussian probability densities derived from the literature.

Longitudinal control for a follower vehicle in a platoon has been implemented using control laws for Coordinated Intelligent Cruise Control (CICC) based on the work carried out by Desoer and Sheikholeslam (see, e.g., Sheikholeslam 1991) for the PATH program. The simulation model can also use an Autonomous Intelligent Cruise Control (AICC) algorithm based on the work carried out by Ioannou et al. (Ioannou et al. 1992).*

3.3.3 Platoon Generation

The microscopic platoon model simulates a highway link that has a specified length, a specified number of lanes, and a specific grade. Given these input parameters, platoons are generated independently in each lane. The simulation models the generation of platoons on each lane as a modified Markov process. In a normal Markov process (Pielou 1977), times between generations have an exponential distribution with infinite support. In order to avoid extreme behavior in the simulation, inter-generation times which are extremely high (above five standard deviations) are eliminated and the remaining sample is shifted accordingly.

The generation rate is given by:

$$T_{next} = -1.0349 \times \frac{\log(u) \times \text{mtbg}}{V_{master}} \tag{3-10}$$

* The details of these control algorithms are extensive and thus are not given here. The reader is referred to the corresponding citations for each control algorithm.

where T_{next} is the calculated generation time, u is a uniformly distributed random variable between 0 and 1, mtbg is the mean time between generations of vehicles set by the front control panel of the simulation, and V_{master} is a master volume constant for calibration (normally at 1).

3.3.4 Simulation Flow

The simulation flowchart for each lane is shown in Figure 3.6. The simulation begins with the specified parameters of number of lanes, input density and speed, output density and speed, link length, and link grade. The simulation is first initialized, checking input from the front panel. Execution is halted if the quit button is pushed. The simulation has a master clock or simulation clock which is initially compared to the simulation time, or length of the current simulation. Platoons can be generated manually or by an independent process, and if it is time to generate a platoon in any lane, the simulation processes the platoon leader generation. In the generation process, initial acceleration and velocity parameters are determined, after which the behavior parameters are set. At the end of the generation process, the next platoon generation time in the current lane is scheduled.

Beginning with the first vehicle in each lane, the simulation runs through and updates each vehicle. Each lane is considered simultaneously, i.e., vehicles are updated based on their longitudinal position on the road, not just within their lane. If the current position of a vehicle is beyond the link length, then that vehicle is deleted from the vehicle list, and the updates continue with the next vehicle. When updating a vehicle, the car-following logic described previously is assigned for platoon leaders, or if a follower vehicle, the automated control algorithm is used. This updating continues until the last vehicle is updated. The simulation clock is then incremented, and the process repeats.

This is an event-based simulation that schedules vehicle generations based on the process described above. The incrementing of the simulation is also based on events, where each update occurs at predetermined update rate. The current update rate is every 100 milliseconds.

3.4 SMARTPATH AND EMISSIONS

In addition to the platoon simulation model, an emissions post-processing program was created for PATH's AHS simulation model SmartPath. SmartPath is first briefly summarized, followed by a brief description of the post-processing emissions program.

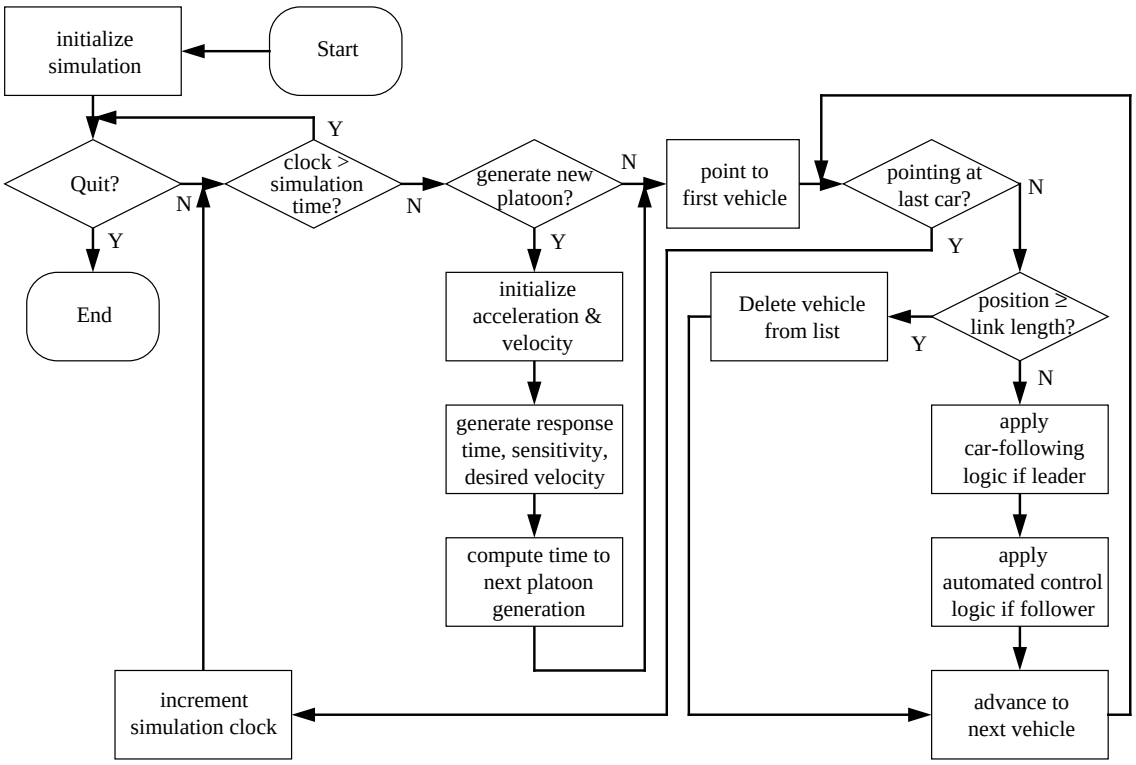

Figure 3.6. Overall flowchart of platoon simulation.

3.4.1 SmartPath Summary

The California PATH program has developed over the years an AHS simulator called SmartPath (Eskafi et al. 1992; Hongola et al. 1993; Eskafi et al. 1993). SmartPath is a microscale AHS simulator where vehicles and highways are modeled having appropriate sensors, communication devices, and actuators. SmartPath was designed around the AHS control and communication architecture described in (Shladover et al. 1991; Varaiya et al. 1991; Hsu et al. 1991). Other AHS concepts and architectures exist (see, e.g., (Stevens 1994)), however, the architecture implemented in SmartPath is believed to be the most developed at this time.

SmartPath can be used as a tool to determine AHS performance measures such as highway capacity, traffic flow, and other measures of interest to transportation system planners and users. Because SmartPath is a micro-simulator, each system element and control policy is individually modeled. These elements and control policies are parametrically specified, thus the user can alter these parameters to study the effect on AHS performance.

SmartPath is highly modular, so that users can change individual control laws in all of the layers. The user needs to set up configuration files that specify the highway network, the link layer, coordination, and regulation layer parameters. There are two types of highway lanes featured in

SmartPath: automated lanes and non-automated or transition lanes. Platoons of vehicles under full automated control occupy the automated lanes and vehicles that are manually driven occupy the transition lanes.

Communications in SmartPath are modeled as one-way or point-to-point links. Within a platoon, there are two-way links between vehicles, as well as two-way links between the platoon leader and all followers. It is also assumed that there are two way links between the leaders of neighboring platoons. Finally, there is a link between the highway link layer and every vehicle.

3.4.2 SmartPath Emissions Program

A post-processing emissions program was developed for version 1.0 of SmartPath. This version of SmartPath is only capable of running in batch mode, meaning that the actual simulator runs first, followed by a data converter, and finishing with a separate animator program (Eskafi et al. 1993). Version 2.0 of SmartPath was recently released and can run in either batch or interactive mode. The post-processing emissions program can be used with either version 1.0 or 2.0 (in batch mode).

The SmartPath simulator requires an input configuration file which specifies the roadway geometry and vehicle entry/exit information. The simulator outputs trajectory information for each vehicle for every time step in the program. In order to view the output using the animator, the trajectory data file must be converted to a specific format using a separate conversion program.

The post-processing emission program uses as input the vehicle trajectory file produced by the simulator. The program first extracts and orders the trajectories for each vehicle. For each time step, the vehicle's acceleration, velocity, and position (from which grade can be determined) are used in the power demand equations of the modal emissions model described in Chapter 2. The spacings between vehicles are also calculated in order to determine the reduced aerodynamic drag factor due to the drafting effect (see Section 3.3.1). Finally, the instantaneous emissions of CO, HC, and NOx are calculated for each time step. The program also calculates the cumulative emissions for each vehicle, and also for all of the vehicles.

The velocity, acceleration, and emissions profiles can then be plotted using standard plotting tools such as MATLAB.

3.5 STEADY-STATE SPEED EMISSIONS

Emissions produced by traffic (manual or automated) will depend on several factors. In general, large variations in velocity (i.e., numerous acceleration, deceleration events) lead to higher emissions, therefore to minimize total emissions, traffic should be kept as smooth as possible. We first consider vehicle emissions at steady-state vehicle velocities.

Using the AHS simulation models coupled with the power-demand emissions model described in Chapter 2, platoon simulations were carried out to determine average emission rates at different steady-state velocities. The motion parameters, engine power demand, and associated emission rates were calculated for each modeled vehicle in the simulation. Because the follower vehicles within a platoon have very small intraplatoon spacings (e.g., on the order of one meter), the aerodynamic drag coefficient of each follower is significantly reduced due to the "drafting effect". Using preliminary aerodynamic drag reduction data for vehicles in platoons produced by the University of Southern California (Zabat et al. 1994; Zabat et al. 1995), the calculated power demand on the engine is significantly smaller at higher speeds. Based on the data, even the lead vehicle of a platoon has its aerodynamic drag coefficient reduced due to the vehicle following closely behind.

Emission rates were calculated at constant speeds ranging from 5 km/h to 120 km/h. A 3rd-order polynomial was then used to fit the data to give continuous emission values at any prescribed speed. Comparisons between constant velocity CO, HC, and NOx emission rates for 20 vehicles that are platooned and non-platooned are shown in Figure 3.7, 3.8, and 3.9. In both cases the traffic density is low, and the vehicles are traveling near their free speeds. At lower speeds, vehicle emission rates of the two cases are roughly the same. However, at higher speeds, the platooned vehicles benefit from the drafting effect which results in less engine load, and thus less emissions output. Similar reductions for fuel consumption have been predicted in (Zabat et al. 1995). In order to illustrate the benefits of drafting, Figure 3.10 again shows the constant velocity CO emission rate for 20 vehicle platoons for two specific cases: when the platoons are spaced at one meter apart, and at three meters apart. It can be seen that if the vehicles in the platoon are closer together, lower emission rates can be achieved.

In order to determine total steady-state emissions of an automated lane within an AHS, these emission data were applied to the flow-density curves shown in Figure 3.4. It is important to note that the curves in Figure 3.4 reflect traffic density and flow associated with specified safe spacings. Thus to generate flow values at lower densities, vehicle speeds greater than the free speed (i.e., the maximum speed a driver will go on the freeway without interference from other

traffic) were used in the calculations. For purposes of generating total link emissions at lower densities, the flow values were adjusted so that the vehicle velocities at low densities were at the constant free speed.

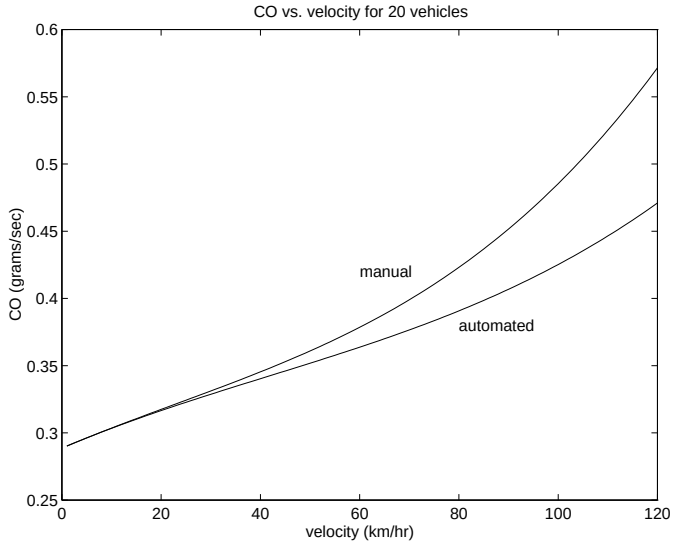

Figure 3.7. Constant velocity carbon monoxide emission rates for 20 vehicles platooned and non-platooned.

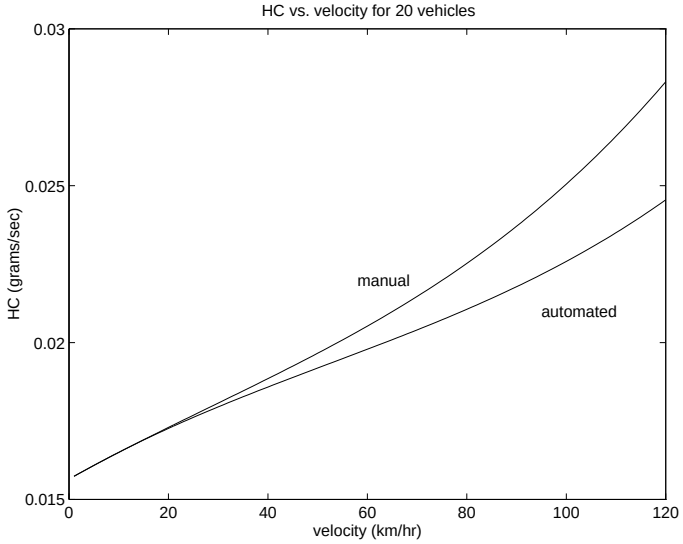

Figure 3.8. Constant velocity hydrocarbon emission rates for 20 vehicles platooned and non-platooned.

Total CO, HC, and NO_x emissions for a one kilometer lane are shown as a function of traffic flow for both the manual and automated (platooning) cases in Figures 3.11, 3.12, and 3.13 respectively. There are several key points to note in these figures:

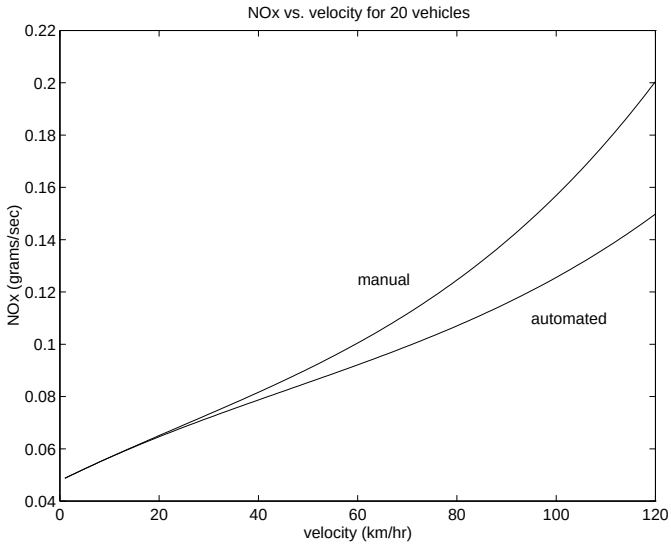

Figure 3.9. Constant velocity NOx emission rates for 20 vehicles platooned and non-platooned.

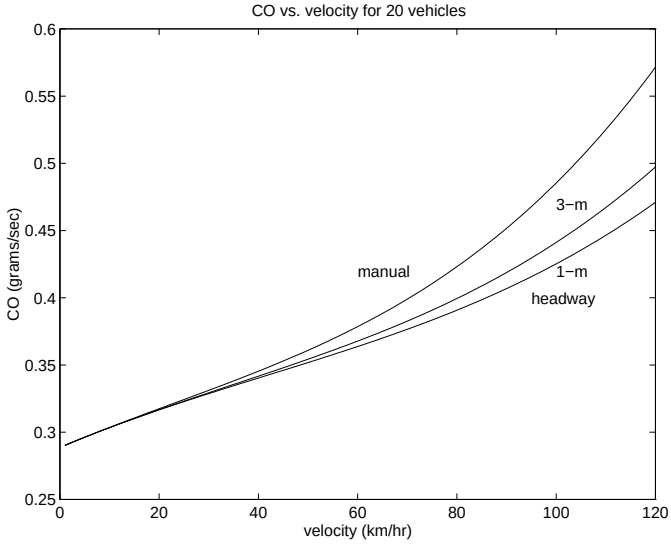

Figure 3.10. Constant velocity carbon monoxide emission rates for 20 vehicles non-platooned and platooned for the cases of 1 meter and 3 meter spacings.

1) The maximum traffic flow for a manual lane is 2053 vehicles/hour at an average vehicle speed of 48 km/hour. At the same traffic volume, the automated lane produces roughly *half* as much emissions as in the manual case, regardless of whether the platoon size is 15 or 20 vehicles:

	CO (gm/s)	HC (gm/s)	NO_x (gm/s)
manual	0.76	0.0415	0.1882
automated	0.40	0.0210	0.1190

2) Given the emissions rate for maximum manual traffic volume, roughly *twice* the traffic volume can occur in the automated lane (regardless of whether platoon size is 15 or 20 vehicles) to produce the same amount of emissions:

	flow - CO	flow - HC	flow - NO_x
manual	2053	2053	2053
automated	3899	4005	3005

3) The maximum traffic flow for an automated lane is 8286 vehicles/hour at an average speed of 103 km/hour for a constant platoon size of 20 vehicles. The associated emissions at this point is roughly *twice* that of the maximum flow rate of manual driving:

	CO (gm/s)	HC (gm/s)	NO_x (gm/s)
manual	0.76	0.0415	0.1882
automated (20)	1.75	0.0911	0.5214
automated (15)	1.64	0.0868	0.4610

It is important to point out that the emissions associated with higher traffic densities and lower average speeds for the manual case are underestimated in these curves. Remember that these emissions are calculated based on steady-state velocities, and the negative slope region of the flow-density curve is inherently unstable, leading to stop-and-go traffic. The accelerations associated with stop-and-go traffic will lead to a greater amount of emissions.

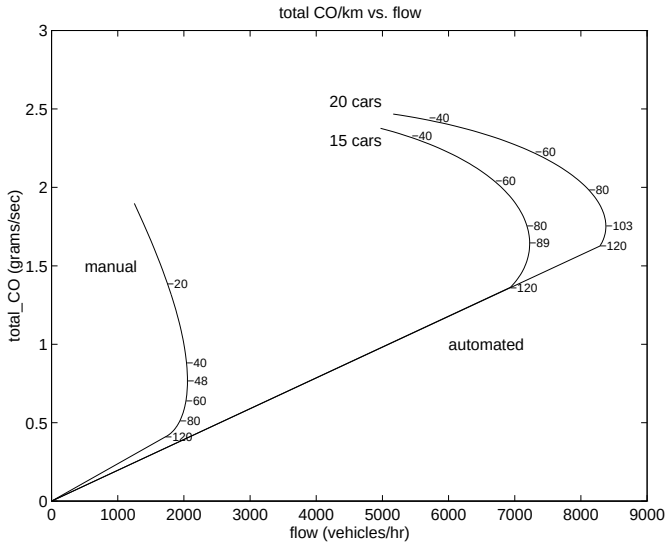

Figure 3.11. Total CO emissions versus traffic flow for manual and automated traffic, for a one kilometer lane. Velocity values (km/hr) are annotated on the curve.

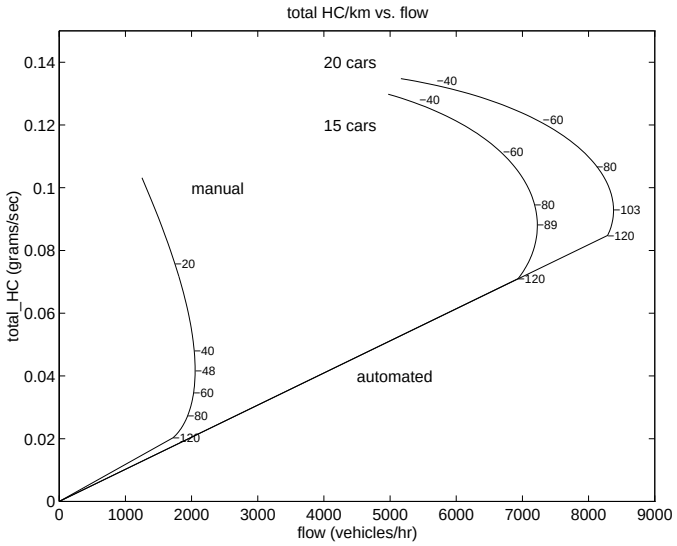

Figure 3.12. Total HC emissions versus traffic flow for manual and automated traffic, for a one kilometer lane. Velocity values (km/hr) are annotated on the curve.

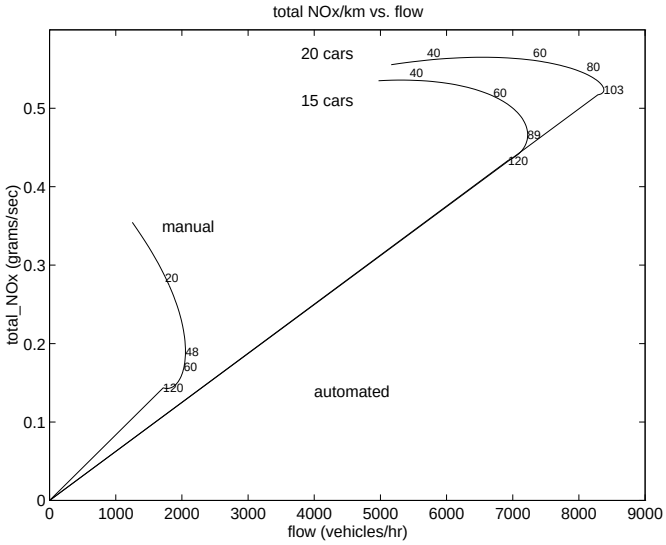

Figure 3.13. Total NO_x emissions versus traffic flow for manual and automated traffic, for a one kilometer lane. Velocity values (km/hr) are annotated on the curve.

3.6 VEHICLE EMISSIONS FOR AHS MANEUVERS

The emission rates for automated traffic calculated in the previous section were based on steady-state traffic flow with platoons traveling at constant velocities. However, this idealized traffic flow will be difficult to achieve since the entrance and egress of vehicles in the AHS will cause traffic stream disturbances, inducing variations in speed (i.e., accelerations and decelerations). At the heart of these velocity variations are several vehicle/platoon maneuvers such as a vehicle joining a platoon, one platoon merging with another, or a vehicle leaving a platoon. Using the SmartPath simulator and emissions model, we have investigated several of these maneuvers that can have a large impact on emissions production.

3.6.1 Free-Speed Accelerations

When a vehicle enters the AHS and switches to automated control, it must first accelerate in the transition lane to reach the prescribed highway velocity. If using a modern vehicle with an emissions-control strategy as described in Chapter 2, this free-speed acceleration rate can have a dramatic impact on cumulative AHS emissions. If the commanded acceleration is sufficiently high, the power demand on the vehicle's engine will be large and the vehicle will enter a state of power enrichment (see Chapter 2). During power enrichment, the air-fuel ratio is commanded rich for peak power performance, and as a result, prodigious amounts of emissions are produced. For the modeled vehicles in our simulations, CO emissions increase by two orders of magnitude when in the power enrichment state.

In the current SmartPath implementation, vehicles entering the AHS are commanded to a constant free-speed acceleration rate of 1 m/s^2. At low speeds, the power demand at this acceleration rate is small. However, at high speeds, the power demand on the vehicle's engine is already large due to the aerodynamic drag factor (which increases with the square of velocity). A 1 m/s^2 acceleration rate places further power demand on the engine, which may cause it to enter power enrichment. The vehicles modeled in the current simulation enter power enrichment at a velocity of 34 m/s (122 km/h), when accelerating at 1 m/s^2 on level ground.

3.6.2 Platoon Merge

As part of the AHS architecture implemented in SmartPath (Hsu et al. 1991), two neighboring platoons in the same lane will merge to create a longer platoon if they are less than the optimal platoon length (specified by the link layer, see (Hsu et al. 1991)). When the lead platoon falls within the detection range of the following platoon, communication is initiated between the

platoon leaders, and the merge maneuver proceeds. As with the free-speed acceleration, the acceleration rate of the merging, upstream platoon can have a significant effect on the production of vehicle emissions. If the acceleration rate is high enough, not only will the leader of the upstream platoon enter power enrichment mode, but every vehicle that belongs to the upstream platoon as well.

In the current SmartPath version, platoons perform the merge maneuver at a constant 2 m/s^2 acceleration. When traveling at a modest 20 m/s (72 km/h) and accelerating at this rate, the modeled vehicles easily enter the power enrichment state when traveling on level ground. In fact, at that acceleration rate, a leader of a platoon will enter power enrichment if it is traveling at 12 m/s (43 km/h) or greater, and a follower vehicle will undergo power enrichment at 13 m/s (46 km/h) or greater, getting a slight benefit from the aerodynamic drafting effect.

3.6.3 Platoon Split

When a member of a platoon needs to exit the AHS, a platoon split maneuver is performed. In a platoon split, the platoon is divided at the vehicle that needs to exit. The upstream segment of the platoon decelerates as a whole, then accelerates back up to the nominal highway speed, leaving a sufficiently large safety gap between the two platoons. The leader of the upstream platoon (the vehicle that needs to exit) then changes lanes, and the second vehicle in the platoon becomes the new leader. If the downstream platoon is still within sensing range of the upstream platoon, then the upstream platoon will perform a merge maneuver, rejoining the two segments.

An example split maneuver is illustrated for a three vehicle platoon as a time-distance diagram in Figure 3.14. At approximately six seconds into the simulation, the split is initiated and vehicles 2 (middle line) and 3 (bottom line) decelerate at a constant rate of -2 m/s^2 for approximately 4 seconds. The two vehicles then accelerate at 2 m/s^2 until they are back at the nominal highway velocity of 20 m/s. Vehicle 2 then changes lanes, maintaining an approximate 20 m/s velocity. Vehicle 3 decelerates while vehicle 2 is changing lanes, then begins to accelerate at 2 m/s^2 in order to rejoin vehicle 1 (top line), which has not changed its velocity throughout the maneuver. This merge acceleration lasts for approximately 9 seconds, after which vehicle 3 decelerates and joins up with vehicle 1.

The corresponding velocity, acceleration, power demand (normalized to maximum rated power), and CO emissions for vehicles 2 and 3 are shown in Figures 3.15 and 3.16 respectively. It can be seen that during the period when vehicles 2 and 3 accelerate after their initial deceleration, the power demand on the two vehicles is greater than the enrichment threshold, and the corresponding CO emission rate is far greater than that produced during constant velocities. The

power demand is also very high when vehicle 3 performs its merge maneuver with vehicle 1, and the CO emissions rate for vehicle 3 is again at its maximum.

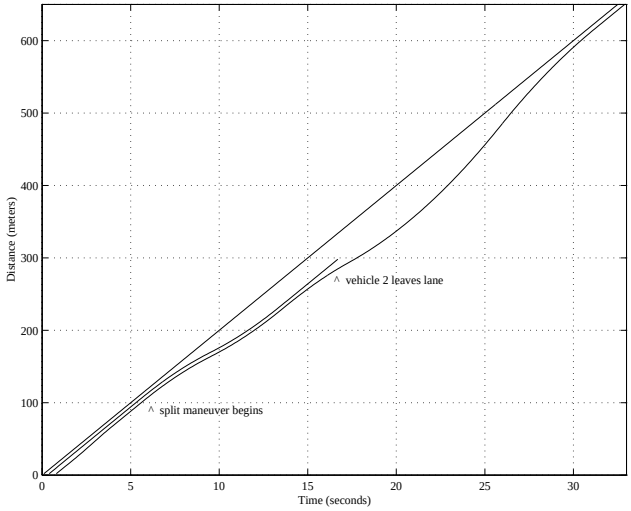

Figure 3.14. Time-distance diagram of a 3 vehicle platoon, split maneuver.

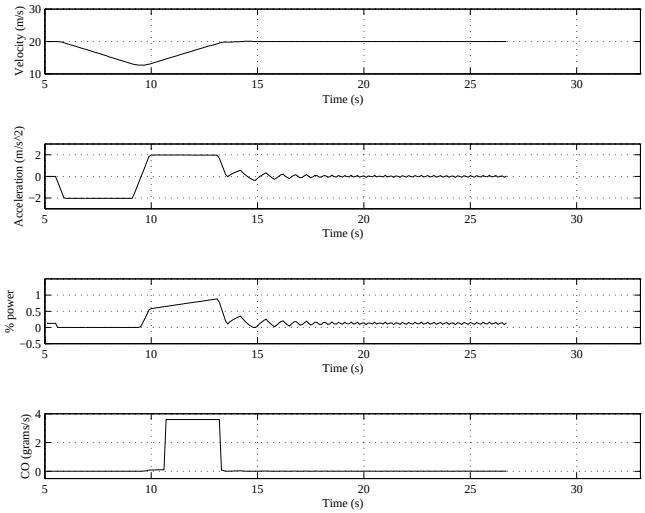

Figure 3.15. Vehicle 2 velocity, acceleration, normalized power demand, and CO emissions for maneuver.

3.6.4 Constant Power Acceleration Approach

Instead of using constant accelerations when performing these platoon maneuvers, we have modified the acceleration strategy used in the AHS simulation. In its initial design, SmartPath assigns accelerations that are held constant for different components of each maneuver. Not only is this detrimental when considering vehicle emissions, in some cases it is impossible to perform the commanded accelerations given limitations in engine power. For example, when traveling at

high speeds, a commanded acceleration of 2 m/s^2 will be impossible to perform since the power demand on the engine will exceed what it can actually produce.

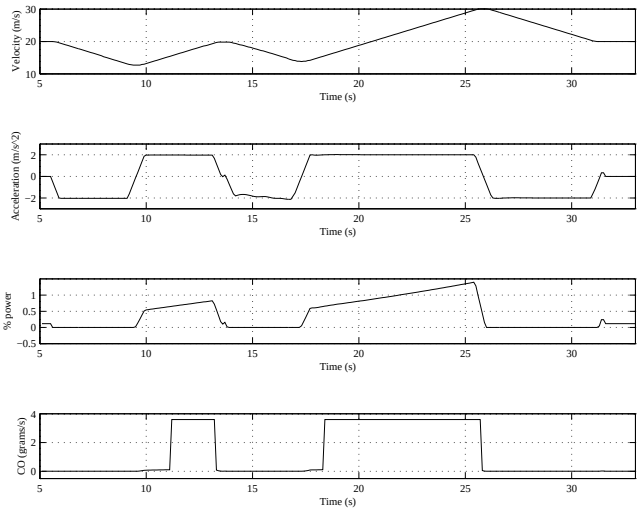

Figure 3.16. Vehicle 3 velocity, acceleration, normalized power demand, and CO emissions for maneuver.

Based on equations of vehicle dynamics, we have devised a constant power approach when vehicles accelerate in the simulation. The inertial power requirements for a vehicle (in kilowatts) are given in simplest form as:

$$P_{inertial} = \frac{M}{1000} \cdot V \cdot \left(a + g \cdot \sin\theta\right) \tag{3-11}$$

where M is the vehicle mass (kg), V is the vehicle velocity (meters/second), a is the vehicle acceleration (m/s^2), g is the gravitational constant (9.81 m/s^2), and θ is the road grade angle. The power requirements due the drag components are given in simplest form as:

$$P_{drag} = \left(M \cdot g \cdot C_r + \frac{\rho}{2} \cdot V^2 \cdot A \cdot C_a \right) \cdot \frac{V}{1000} \tag{3-12}$$

where C_r is the rolling resistance coefficient, ρ is the mass density of air (1.225 kg/m^3, depending on temperature and altitude), A is the cross sectional area (m^2), and C_a is the aerodynamic drag coefficient. Thus the total tractive power requirements placed on the vehicle (at the wheels) is given as:

$$P_{tractive} = P_{inertia} + P_{drag} \tag{3-13}$$

If the maximum power of the engine is limited such that the vehicle does not go into power enrichment mode, acceleration can be determined as:

$$Acceleration = \frac{1000 \cdot \left(P_{maximum} - P_{drag}\right)}{M \cdot V} - g \cdot \sin\theta \qquad (3\text{-}14)$$

Using this methodology, each vehicle in the simulation will achieve its highest possible acceleration performance without going into the power enrichment mode. This is substantially different than simply using constant acceleration values during the platoon maneuvers.

This acceleration methodology was applied to the same split maneuver described in the previous section. Figure 3.17 shows the time-distance diagram of the three vehicle trajectories, and Figures 3.18 and 3.19 show the velocity, acceleration, power, and CO emissions of vehicles 2 and 3. Again, the leader vehicle (vehicle 1, top line in Figure 3.17) does not change speed at all, and thus appears as a straight line. Vehicle 2 and 3 still perform the same maneuver, but because they do not acceleration as quickly as before, the maneuver itself takes longer to perform (the maneuver is finished after 32 seconds compared to 26 seconds shown in Figure 3.14). The savings in emissions, however, is significant. Cumulative CO emissions for the constant-acceleration split are 60.4 grams, while the cumulative CO emissions for the constant-power split are 5.9 grams, an order of magnitude less (10.2).

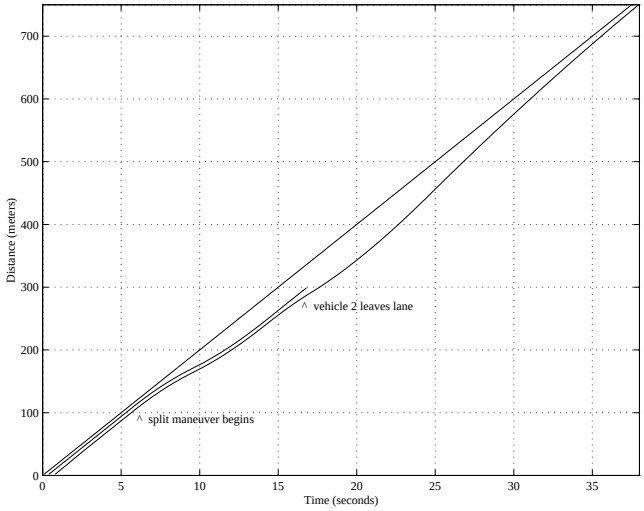

Figure 3.17. Time-distance diagram of a 3 vehicle platoon, constant-power split maneuver.

3.6.5 Modified Split Protocol

Another method for reducing cumulative AHS emissions is to modify the protocols of the various vehicle/platoon maneuvers. In the initial implementation of SmartPath, the protocols were designed primarily from a safety standpoint. However, it is possible to design the protocols

so that vehicle emissions are minimized while still maintaining a sufficiently high degree of safety.

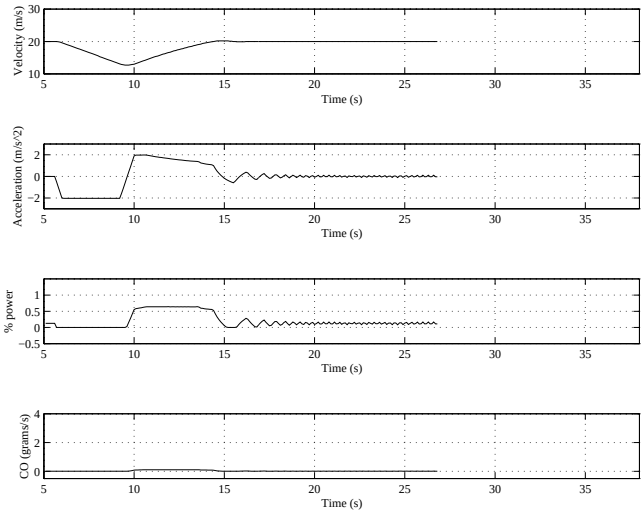

Figure 3.18. Vehicle 2 velocity, acceleration, normalized power demand, and CO emissions for maneuver.

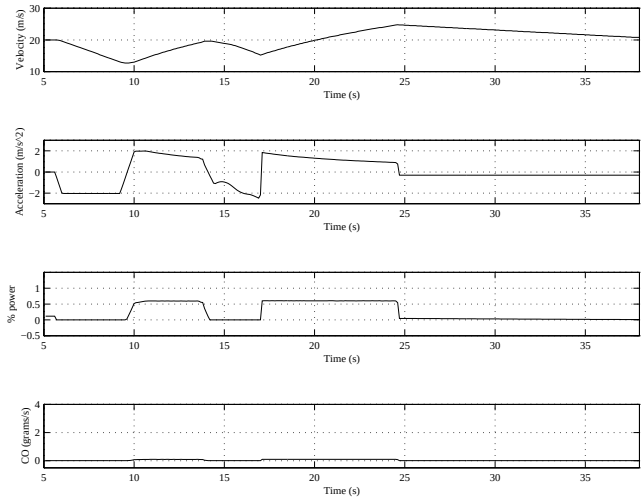

Figure 3.19. Vehicle 3 velocity, acceleration, normalized power demand, and CO emissions for maneuver.

As an example, we modified the protocol of the same split maneuver described in the previous sections. Using the original constant acceleration approach, the protocol was modified such that when the split begins, vehicle 2 simply changes lanes. Instead of having both vehicles 2 and 3 slow down and then speed back up in order to create a gap between the front of vehicle 2 and the back of vehicle 1, vehicle 2 initiates a lane change immediately while operating within the platoon. The safety of this maneuver modification should still remain high, since the spacings between vehicles remain small, and any collision will have only a small impact. After vehicle 2 changes lanes, vehicle 3 again performs a merge with vehicle 1, but in this case, the distance

between the two vehicles is shorter than before. The trajectories of the vehicles are shown in Figure 3.20. The corresponding velocities, accelerations, power, and CO emissions are shown for vehicles 2 and 3 in Figures 3.21 and 3.22, respectively.

With this maneuver modification, the maneuver is finished after 14 seconds, compared to the 26 seconds of the original scenario. Cumulative CO emissions for the modified split are 23.6 grams, compared to the 60.4 grams of the original split maneuver. Emissions could be further reduced by combining the two methods described in this and the previous section.

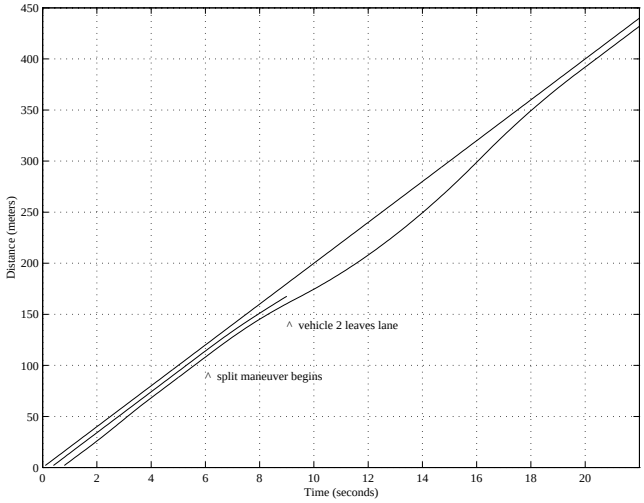

Figure 3.20. Time-distance diagram of a 3 vehicle platoon, modified split maneuver.

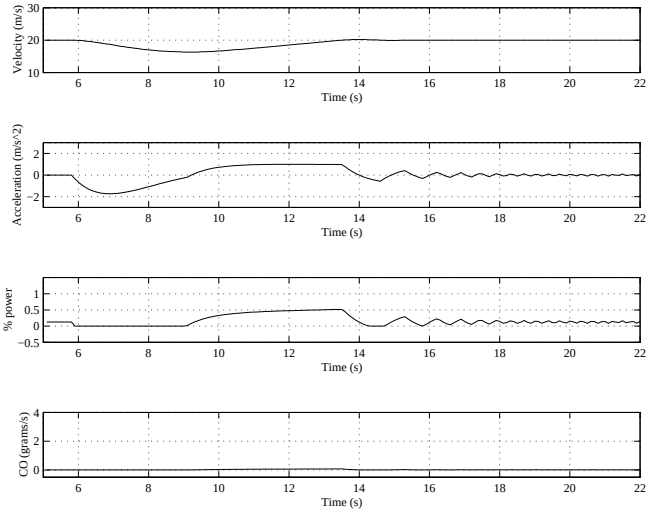

Figure 3.21. Vehicle 2 velocity, acceleration, normalized power demand, and CO emissions for maneuver.

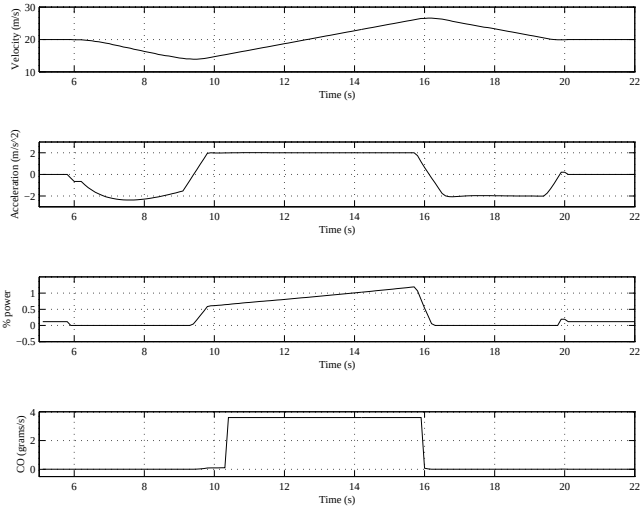

Figure 3.22. Vehicle 3 velocity, acceleration, normalized power demand, and CO emissions for maneuver.

4 Ramp Metering Emissions Analysis

4.1 INTRODUCTION

It has been suggested in recent years that ramp metering may be counter-productive from an air quality point-of-view. Many view ramp metering as a traffic control technique which shifts congestion off of the freeway and on to the surface streets, while at the same time inducing more demanding accelerations on the freeway on-ramps. In order to analyze the impact of ramp metering on air quality, we consider three primary sources of influence that ramp metering may have directly on vehicle emissions:

Freeway mainline traffic smoothing—The primary intent of ramp metering is to smooth the traffic flow on the freeway mainline and reduce overall delay for freeway travelers. By limiting the input volume to the freeway, overall freeway speeds can be increased. Further, by spacing out merging vehicles from the freeway on-ramps, the probability of acceptable gaps in the freeway traffic is much higher, causing fewer perturbations to the traffic flow. The overall traffic flow is smoother and faster, resulting in lower emissions.

Ramp, surface street congestion—When vehicles on a ramp are metered, congestion can occur on the ramp and associated surface streets under heavy traffic conditions. This congestion is characterized by slow, stop-and-go traffic conditions, leading to higher emissions produced by the vehicles waiting to get on the freeway.

Hard accelerations from the meters—When a vehicle finally reaches the ramp meter and eventually proceeds on to the freeway, it may require rapid acceleration to reach the freeway traffic speed. These accelerations may put an enormous load on the engine and can result in relatively short bursts of high emissions. Vehicle emissions generated in this case depends highly on factors such as road geometry (i.e., positive/negative ramp grade, ramp length from meter, etc.) and the average mainline traffic speed that the merging vehicle attempts to achieve.

In this preliminary analysis, we have considered each one of these direct effects separately and have conducted a number of simulation experiments to estimate the emissions impact. However, the overall effect of ramp metering on vehicle emissions is highly dependent on a number of situational factors such as the *topology of the road network* (e.g., spacing of ramps, surface street to highway interface, etc.), the *road geometry* (e.g., number and types of lanes, road grade of the highway and ramps, etc.), the *type of ramp metering used* (e.g., fixed cycle vs. traffic

responsive), the *vehicle mix* (e.g., proportion of trucks and cars, etc.), and the *overall VMT*. In this study, simulation experiments have been carried out using the FRESIM traffic model (described in Section 4.3) coupled with the modal emissions model described in Chapter 2. Within this experimental framework, only the direct effects described above were analyzed and other indirect effects (e.g., ramp metering can also significantly reduce the number of freeway incidents (i.e., traffic accidents), thus improving freeway speeds, leading to lower emissions) were ignored. It is intended that this preliminary analysis serve as a starting point for other more comprehensive studies that may or may not be specific to actual ramp metering implementations.

4.2 BACKGROUND

Ramp metering does not increase the capacity of the freeway, but rather protects it from break down by allowing only one vehicle at a time to enter the freeway. When a long string of unmetered traffic packed closely together merges from a ramp, typically there are insufficient gaps in the freeway flow to accommodate all of them. This causes vehicles to slow down and possibly switch lanes, causing disturbances to freeway traffic. By eliminating these disturbances, the overall traffic flow can be smoother and faster, resulting in lower emissions.

A review of various ramp metering studies conducted in different parts of the US (e.g., Denver, Detroit, Portland, Seattle and Los Angeles) indicates a wide range of reductions in travel times and increases in speeds on the freeways (Robinson et al. 1989). For example, in the operational system in Minneapolis-St. Paul, evaluations have shown that average freeway speeds increased from 55 to 74 km/hr (34 to 46 mile/hr, 35% improvement) (Robinson et al. 1989).

In the paper (Corcoran et al. 1989), ramp metering effects in the Denver area were described. Before and after studies at one of the five freeway demonstration project locations indicated a 58% increase in travel speed (from 53 to 84 km/hr) during the AM peak period. Subsequently, the study area was expanded to 26 locations and similar results were observed.

The study (Robinson et al. 1989) summarized the ramp metering application in several U.S. cities. For example in Portland, Oregon there was a 156% increase in average speed on the north-bound PM peak hour traffic along I-5. Between 1981 and 1987, travel times decreased by 48% due to ramp metering implementation in Seattle, Washington. Similarly, in Detroit, Michigan and Austin, Texas freeway speeds increased by 8% and 60% respectively.

In another study, Nsour et al. investigated the impacts of ramp metering on traffic flow with and without diversion. This study reiterated the findings of previous studies that indicated ramp metering improves the traffic flow on the freeway, but adversely affects the total system because

of the overflow queues behind the meters, which spill back onto the surface streets (Nsour et al. 1992).

In a two phase, five volume report, Nihan et al. have addressed the issues of forecasting freeway and ramp volumes, and lane occupancies for real-time use in ramp metering applications including data collection efforts for the Washington State Department of Transportation. A statistical pattern recognition model based on parametric and non-parametric approaches was developed to forecast traffic conditions on the freeway 1 to 3 minutes ahead of time. This study also looked at the reactive vs. proactive solutions to congestion formation due to ramp metering (Nihan et al. 1993).

There have also been several simulation model implementations to analyze the effects of ramp metering. For example, Al Kadri developed a discrete, stochastic, mesoscopic simulation model within the framework of contextual systems approach for freeway ramp metering control (Al Kadri 1991). Further, Hamad utilized the Integrated Traffic Simulation (INTRAS) model to study various strategies of metering flow onto the freeway as well as between the freeways to evaluate the benefits of such strategies (Hamad 1987).

In the paper (Chang et al. 1994), an integrated real-time ramp metering model for non-recurrent freeway congestion was described and preliminary results were presented. The model consists of an algorithm to capture the dynamic traffic state evolution which was fully integrated with INTRAS. An effective solution algorithm implemented in real-time has been proposed to determine the time-varying metering rates. The effectiveness of the model increases with the severity of accidents and the level of congestion according to the authors.

A microcomputer-based optimization scheme was developed by researchers at the Texas Transportation Institute that will assist engineers in developing efficient freeway control strategies to enhance the real-time freeway surveillance and control (Chang et al. 1994). Another study presented a number of case studies of freeway-to-freeway ramp and mainline metering in the U.S. The study suggests that a complete and thorough analysis should take place before the installation of any freeway-to-freeway or mainline metering system, including safety and environmental concerns (Jacobson et al. 1994).

The effect of response limitations on traffic-responsive metering strategies was analyzed in the paper (Banks 1994). A scheme for analyzing response errors is presented and applied to the simulated results of proposed modifications to the San Diego system. The study recognized that the most important limitation of the estimation methodology was that the difference between the

maximum and minimum metering rates tends to be small relative to normal random variation in mainline input flows at the minimum counting interval of 30 seconds.

Researchers at the University of Minnesota have developed a methodology to determine the best metering thresholds for a given section of a freeway, under normal weather conditions, using the control-emulation method and downhill simplex optimization procedure based on historical demand and current day measurements (Stephanedes et al. 1993). The optimal thresholds for each ramp in a given section of the freeway are estimated based on the system-wide traffic conditions.

Zhang et al. in a report entitled "On the Optimal Ramp Control Problem: When Does Ramp Metering Work?" formulated the ramp control problem as a dynamic optimal process to minimize the total time spent in the system which includes a freeway section and its entry / exit ramps (Zhang et al. 1995). The same author in another study entitled "An Integrated Traffic Responsive Ramp Control Strategy via Nonlinear State Feedback" proposed a nonlinear controller using a series of neural networks for non-steady state traffic conditions. The authors claim that the initial traffic simulation results presented in the report demonstrate the controller's potential effectiveness (Zhang et al. 1995).

Air quality impacts of high-occupancy-vehicle (HOV) lanes and ramp metering were discussed by Shoemaker and Sullivan in their paper entitled "HOV Lanes and Ramp Metering: Can They Work Together for Air Quality?" (Shoemaker et al. 1994). The authors claim that in an environment of worsening congestion, ramp metering has limited life (e.g., one-fourth of the ramp meters in the Los Angeles area become useless during the most congested periods of the day).

In the majority of the ramp meter literature, there is little direct analysis of the effects on vehicle emissions. Because current emission models such as CARB's EMFAC and EPA's MOBILE are based on average emissions over extended driving cycles and are insensitive to localized variations in speed and acceleration, they cannot be efficiently combined with microscale traffic simulation models that are capable of simulating ramp metering. However, by using a modal emission model such as the approach described in Chapter 2, the impact on vehicle emissions can be evaluated. In order to perform simulation experiments dealing with ramp metering and emissions, we have combined our preliminary modal emissions model with the model FRESIM, described in the next section.

4.3 FRESIM SIMULATION MODEL

FRESIM is a microscale freeway simulation model in which each vehicle is modeled as a separate entity. The behavior of each vehicle is modeled in detail through the interaction with the surrounding environment which includes the freeway geometry and other vehicles. FRESIM is an improved model over its predecessor INTRAS. FRESIM can simulate a wide range of freeway geometries which include one to five lane freeway mainlines with one to three lane ramps and interfreeway connectors, variations in grade, different radii of curvature, lane additions and lane drops anywhere on the freeway, freeway blockage incidents, and auxiliary lanes (lanes used to merge on and off freeway) (FHWA 1993; Halati et al. 1991). It provides realistic simulation of operational features such as a comprehensive lane-changing model, clock time and traffic-responsive ramp metering, comprehensive representation of the freeway surveillance system, representation of six different vehicle types including heavy vehicle truck movement, and can simulate ten different driver types ranging from timid to aggressive drivers.

4.3.1 Integration of FRESIM and Modal Emissions Models

FRESIM can also report cumulative emissions at specified intervals during the simulation run. These emission values are based on a predetermined table indexed by velocity and acceleration. Thus for each vehicle in the simulation, an emission value is calculated during each update interval by taking each vehicle's velocity and acceleration value and looking up the emissions indexed by those values. The emission values for all vehicles are integrated over the simulation reporting interval and are reported in the FRESIM output files.

Unfortunately, emission calculations based on velocity and acceleration parameters alone do not take into account other load producing factors such as road grade. For this reason, we have taken a different approach to calculating emissions using the modal emissions model described in Chapter 2. FRESIM does not directly output the trajectories of the individual vehicles in the simulation, so the source code of FRESIM was obtained and modified to output vehicle trajectory information. For each simulation update interval, trajectory information for each vehicle is produced, consisting of the vehicle's velocity, acceleration, link number, distance from the origin of the link, and lane number. The emissions for each vehicle are then calculated by piping the trajectory information directly to the modal emissions model. The model is represented as a program that accepts the trajectory information input and calculates instantaneous CO, HC, and NOx. This program also accumulates the emissions information and calculates statistical measures. Since the grade of each network link is known from the specified

geometry, a better emissions calculation is possible, rather than using the velocity/acceleration-based tables.

4.3.2 Simulation Setup

For the study of ramp metering and the associated emissions impact, various simulation experiments were performed. The road geometry for the majority of the experiments consisted of a two lane freeway segment with an on-ramp consisting of a single lane and a 152.4 meter (500 feet) merge section, shown in Figure 4.1. Initially, a vehicle free flow speed of 96.5 km/hr (60 mi/hr) is set in the simulation, and only one type of vehicle (i.e., passenger vehicle) is considered in the simulated traffic flow. FRESIM's acceleration/velocity vehicle performance table was calibrated to a 1991 Ford Taurus in order to match the emissions function represented in the post-processing model. Each lane in the mainline traffic flow was set to carry a maximum flow of 2200 vehicles per hour. For nearly all of the simulations, the run time was set at 20 minutes.

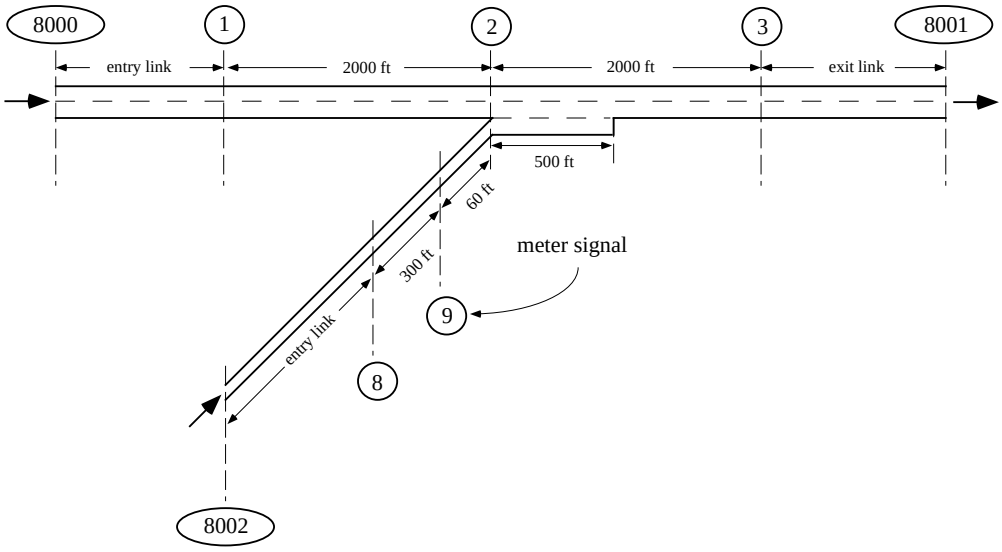

Figure 4.1. Freeway geometry for FRESIM ramp meter experiment (not to scale).

4.4 SIMULATION EXPERIMENTS

4.4.1 Mainline Traffic Flow and Emissions

In order to estimate the mainline speed increase due to ramp metering and its effect on emissions, several simulation experiments using the FRESIM model (summarized above) were performed. These simulation experiments were carried out with the following two objectives in mind:

1) to confirm the previously established relationship between ramp volumes and mainline freeway speeds in case of non-metered ramps;

2) to study the impact of varying ramp meter cycle times on mainline freeway speeds for different ramp volumes.

Based on the measured speed increase, we then predict the overall emissions benefit using results of our emissions modeling.

Mainline Speed Reduction due to High Ramp Volumes

A series of simulation runs was conducted to identify the relationship between non-metered ramp volumes and the corresponding mainline freeway speeds. Ramp volumes were varied from zero to 1200 vehicles/hour in increments of 200, while the upstream traffic volume remained at the constant 2200 vehicles per hour per lane. The corresponding mainline freeway speeds (average of speeds on links 1-2 and 2-3) were measured and plotted in Figure 4.2.

Figure 4.2 confirms the fact that as ramp volumes increase, mainline freeway speeds drop significantly. However, a close look at the plot also reveals that the drop in speeds is more dramatic for lower ramp volumes (up to approximately 600 vehicles/hour-lane) when compared to higher volumes. The drop in the mainline freeway speeds is nearly 40% for ramp volumes of 600 vehicles/hour-lane from the 97 km/hr free speed. There is only a 24% drop between ramp volumes of 600 to 1200 vehicles/hour-lane. Overall, the freeway speeds fell approximately 54% from their free speed of 97 km/hr for a ramp volume of 1200 vehicles/hour-lane. More testing should be done using different ramp/freeway geometries consisting of a larger number of lanes and different volumes on the freeway.

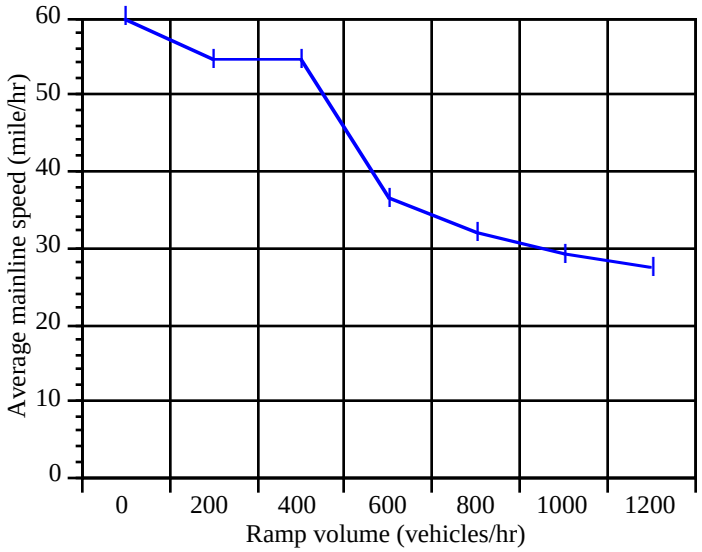

Figure 4.2. Average mainline freeway speed versus traffic volume on a non-metered ramp.

Mainline Speed Increase from Ramp Metering

As mentioned previously, freeway ramp control systems are used to control the flow of vehicles onto the freeway and thereby maintain freeway operations at an acceptable level of service. There are basically two types of ramp metering available: fixed-time and traffic-responsive. Fixed-time control is obtained by presetting the metering rates in accordance with time of day based on historical data such as volume from the mainline and the ramps. Traffic-responsive control is obtained by using real-time volume, speed, and density data collected from vehicle detectors on the ramps and mainline.

Four different types of metering strategies can be implemented in FRESIM. They are 1) clock time ramp metering; 2) demand/capacity metering; 3) speed control metering, and 4) gap acceptance merge control metering. Card type 37 is used to code ramp metering in FRESIM. Depending upon the number coded (1, 2, 3, or 4) in the second entry (column 8) of this card, one of the four control strategies can be implemented. If '1' is coded in column 8, metering headway in seconds for clock time metering is specified in the fourth entry (columns 13-16). In case of demand/capacity metering (specified by coding '2' in the second entry), capacity of the freeway in vehicles per hour is entered in the fifth field (columns 17-20). The user must also specify the detectors on the link that will provide input to the metering algorithm using the metering detector specification card (card type 38) and the surveillance card (card type 28). If speed control metering strategy is selected by coding '3' in entry 2, then the first speed threshold is entered in entry 6 (columns 21-24). If the speed measured by the detector is below the speed threshold specified in this entry, the metering signal is set to the metering rate specified in entry 7 (columns 25-28). Gap acceptance merge control metering can be selected by coding '4' in entry 2. When this strategy is selected, the minimum acceptable gap, in tenths of a second, is specified in entry 12 (columns 45-48). Ramp vehicles are released by the control signal to merge smoothly in gaps in this type of ramp control. Gaps are expressed in units of time and detected in the outside freeway lane. However, in our current simulation, only the first strategy i.e., clock time ramp metering, is implemented for testing various scenarios.

Simulation experiments were carried out using the same freeway/ramp geometry shown in Figure 4.1. Again, upstream traffic volume remained at the constant 2200 vehicles per hour per lane and mainline traffic speeds were measured. Using the clock time ramp metering control strategy in FRESIM, different cycle lengths were tested at various ramp volumes. Figure 4.3 illustrates the relationship between various cycle times and average mainline freeway speeds for one particular ramp volume, i.e., 1400 vehicles/hour. Ramp meter cycle times were varied from 1 second to 8 seconds as shown in the plot. A close look at the plot reveals that mainline freeway speeds

increased significantly from 25.4 mi/hr (40.8 km/hr) for zero second cycle length (i.e., no ramp metering) up to 52.27 mi/hr (84.1 km/hr) for a six second cycle length (more than doubled). For cycle lengths greater than 6 seconds, the speed increase was less dramatic (52.27 mi/hr (84.1 km/hr) at 6 seconds to 54.35 mi/hr (87.5 km/hr) at 8 seconds).

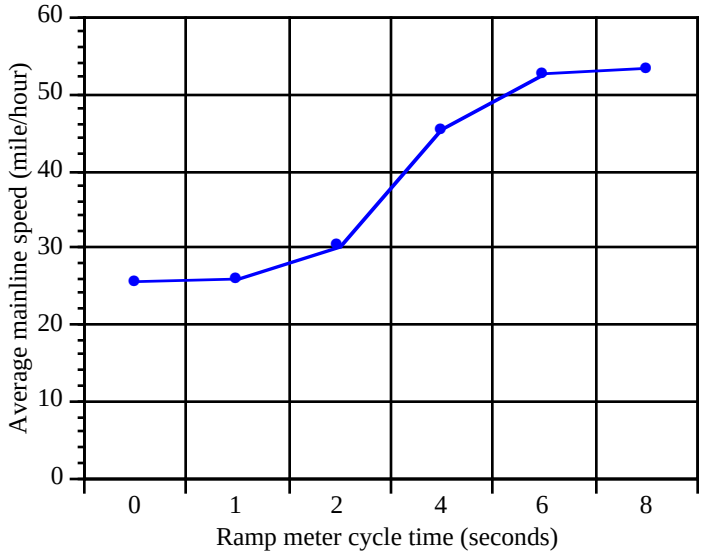

Figure 4.3. Average mainline freeway speed versus ramp meter cycle time for 1400 veh/hr ramp volume.

Based on the modal emissions model calibrated for the Ford Taurus, we have also acquired emissions as a function of meter cycle time. Figure 4.4 shows total link emissions for carbon monoxide. Similarly, Figures 4.5 and 4.6 illustrate the dependence of hydrocarbons and oxides of nitrogen on meter cycle time. These emission values are given as grams per second per mile on the freeway link.

It can be seen that the emissions go up slightly for ramp meter cycle times of one and two seconds. This is due to the fact that ramp metering at this rate does not limit the traffic volume on the ramp (a one second interval corresponds to a max flow rate of 3600 vehicles/hour-lane, two seconds corresponds to 1800 vehicles/hour-lane; these values are above the 1400 assigned volume). However, by spacing out the vehicles entering the mainline flow, the traffic turbulence is less, and the average vehicle speed is higher. In the model FRESIM, the amount of emissions is at a maximum around the average speeds of 30 to 45 mi/hr (48 to 72 km/hr), due to larger variations in vehicle velocity profiles (i.e., stop-and-go traffic). Thus, by first improving average traffic speeds slightly, emissions will reach a peak value, before falling off at higher average speeds.

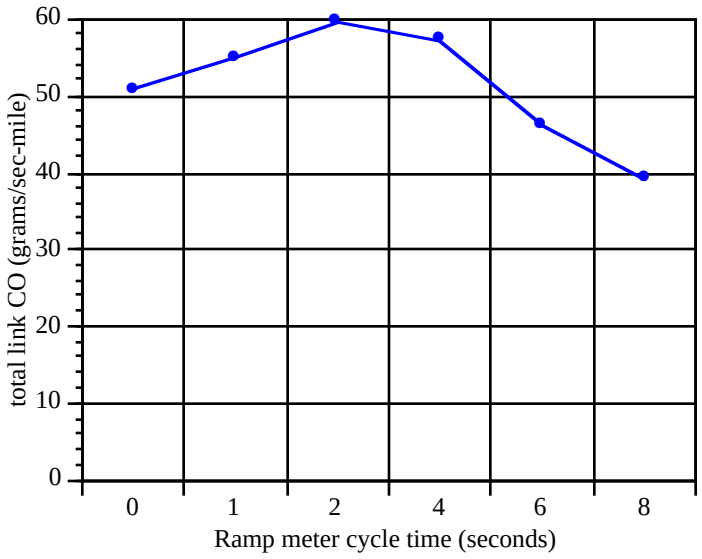

Figure 4.4. CO emissions rate per mile versus ramp meter cycle time.

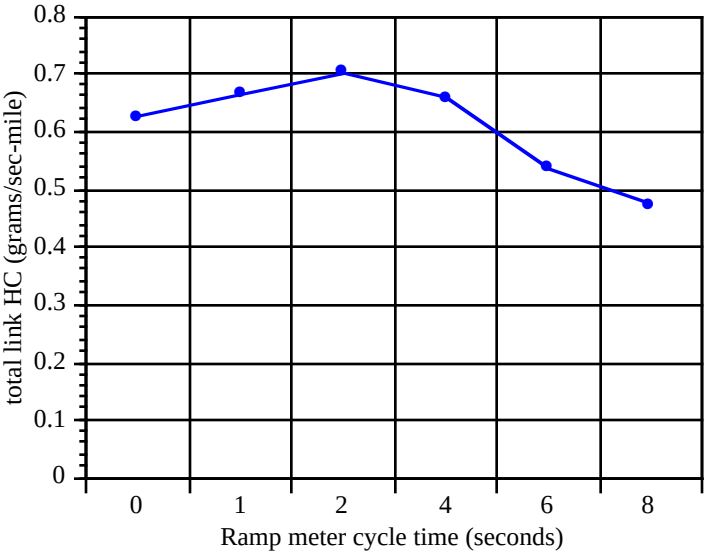

Figure 4.5. HC emissions rate per mile versus ramp meter cycle time.

4.4.2 Ramp Queuing and Emissions

While managing traffic congestion, ramp metering shifts the congestion off the freeway mainline, placing it on the freeway entrance ramps and associated surface streets. Ramp metering gives priority to mainline traffic at the expense of those entering the freeway. This often leads to significant backups behind the meters as well as on local surface streets if meters are not properly timed. In general, most of the ramp metering systems are implemented only during peak traffic periods.

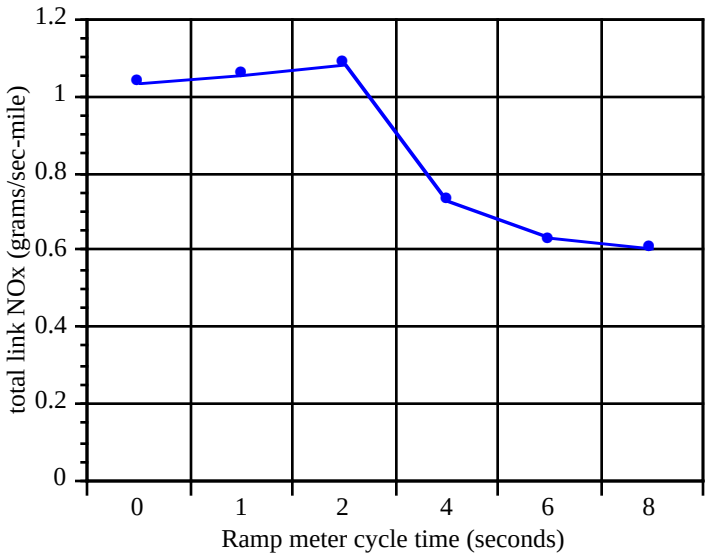

Figure 4.6. NO_x emissions rate per mile versus ramp meter cycle time.

In order to evaluate vehicle emissions caused by this congestion shift, we have performed a set of simulation experiments that analyzes vehicle queuing on freeway ramps. In this preliminary evaluation, we analyzed only the congestion that forms on the freeway on-ramp itself, ignoring the congestion that spills onto the surface streets.

The simulation is carried out using a simulation program capable of modeling vehicles individually, described in (Barth et al. 1993). The microscale simulation model is very similar to the platoon simulator described in detail in Chapter 3, which models individual vehicle dynamics. The primary difference between the two is that instead of generating platoons and modeling automated vehicle control algorithms, vehicles are generated individually and manual car-following logic is employed.

We considered the same road geometry as shown in Figure 4.1. The length of the ramp is 500 ft (152 meters) and near the entrance to the mainline freeway, there is a ramp meter with variable cycle times. We are mainly concerned with the amount of emissions and wait time associated with the ramp meter cycle times. It is assumed that for each green interval of the meter, only one vehicle can proceed (green time is approximately one second). The meter cycle time is then measured as the total duration between green times (i.e., red time + green time).

In all of the simulation experiments, the entire length of the on-ramp is loaded with vehicles. Vehicles are generated at the beginning of the ramp at the maximum generation rate that the on-ramp can handle, with the initial vehicle velocity matched to the average speed of the queue. Various experiments have been carried out with different meter cycle times. The density of

vehicles, given in number of vehicles per foot, is shown as a function of cycle time in Figure 4.7. It is apparent that as the cycle time increases, so does the density. A polynomial fit of the order three was made to the measured data and is also shown in the figure. The error bars associated with the data points correspond to the standard deviation in measurements for each cycle time.

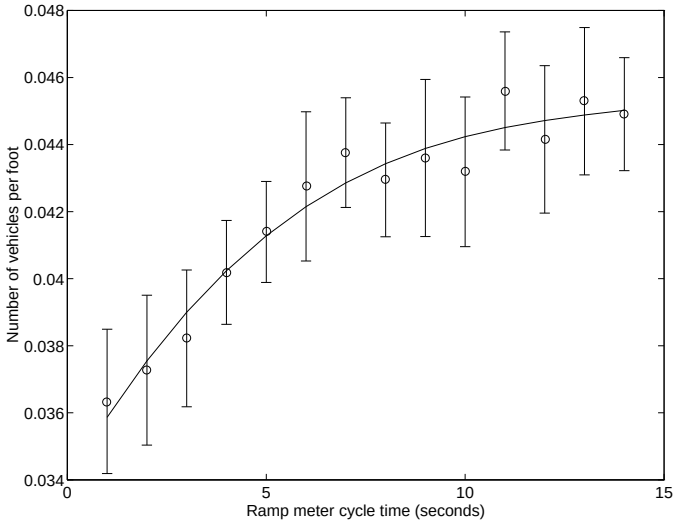

Figure 4.7. Vehicle density versus ramp meter cycle time.

Similarly, the relationship between average queue velocity and ramp meter cycle time is shown in Figure 4.8. Since longer cycle times generate more vehicles on the on-ramp, the average velocity of the entire queue is decreased. As before, the error bars associated with the data points correspond to the standard deviation in measurements for each cycle time, and a polynomial of order three is also shown in the graph.

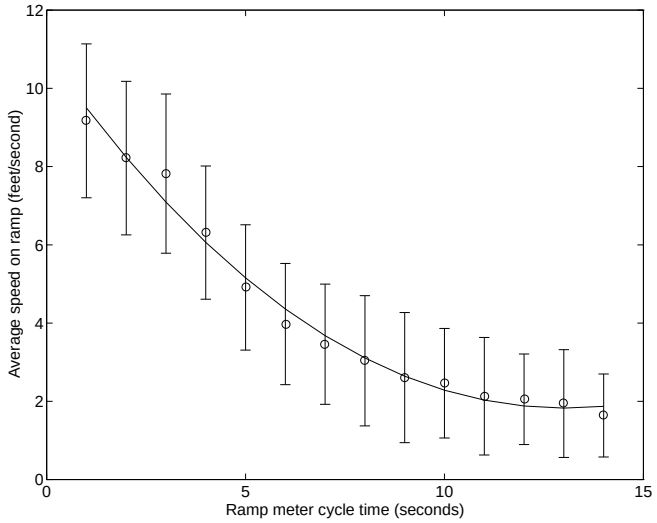

Figure 4.8. Average vehicle speed on ramp versus ramp meter cycle time.

Using the modal emissions model with the ramp queuing simulations, we are able to predict CO, HC, and NO_x emissions for different steady-state ramp cycle times. These results are shown in Figure 4.9. It is apparent that with shorter meter cycle times, emissions are generally greater due to higher fluctuations in speed (i.e., greater number and larger magnitudes of accelerations, decelerations). With a longer red interval time, the number of vehicles on the ramp is high and the vehicles on the ramp are very passive due to longer stop times.

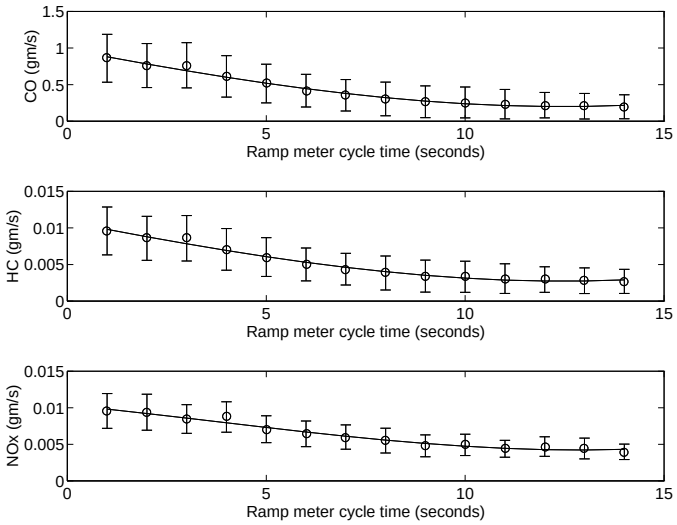

Figure 4.9. Emissions versus ramp meter cycle time.

Finally, the time an individual vehicle has to spend on the ramp increases when the red time is longer. This is shown in Figure 4.10, where data was taken for several meter cycle times. As before, a polynomial fit is also shown and the error bars correspond to the standard deviation in the multiple samples around each data point. At higher wait times, the standard deviation of the times also increases.

4.4.3 Ramp Accelerations and Emissions

The third, and possibly most overlooked impact ramp metering may have on vehicle emissions is the inducement of hard accelerations from the ramp meter to the freeway merge points. Because ramp meters effectively shorten the distance a vehicle has to accelerate up to freeway speeds, greater loads are placed on the vehicle engine, resulting in higher emissions. As described in Chapter 2, under heavy load conditions, a modern closed-loop emission controlled vehicle will enter a “power enrichment” mode under high engine load conditions. When in the power enrichment mode, the air-fuel ratio is commanded rich in order to protect the catalytic converter from excessive heat and to obtain a greater boost in power. During this enrichment mode, vehicle

emissions are significantly higher (two to three orders of magnitude) (Meyer et al. 1992; Cadle et al. 1993; Kelly et al. 1993).

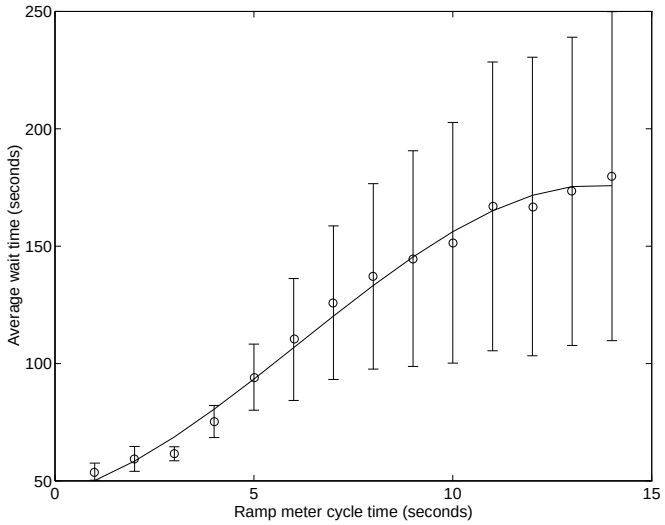

Figure 4.10. Average wait time versus ramp meter cycle time.

We have developed a simulation model that predicts velocity and acceleration profiles for vehicles accelerating between constrained speeds and distances, when engine power is kept constant. This model has been combined with the modal emissions model described in Chapter 2, which takes into account the phenomenon of power enrichment. With such a model, it is possible to predict emissions produced during various cases of ramp accelerations.

Given initial starting and final speeds, road grade, and distance to accelerate, the model iterates over several constant engine power levels to determine whether the vehicle can obtain the final velocity in the prescribed distance. The main assumption of this method is that the engine power level remains constant throughout the entire acceleration. This assumption is roughly equivalent to having a driver determine the required throttle position at the start of the acceleration (knowing the distance and grade), and keeping the throttle position constant throughout the entire acceleration. For each power level, the model updates the acceleration of the vehicle every second using equations of vehicle dynamics. Also updated are the vehicle's velocity and position. If the vehicle reaches the end of the prescribed distance and is not at the required speed, a higher engine power constant is chosen, and the process repeats until a successful acceleration is achieved. The emissions are then calculated for that engine power level for the duration of the acceleration.

This simulation model has been used to evaluate a small sample of freeway on-ramps in Southern California and it was found that some ramps are so short and steep that they produce

upwards of 200 times as much CO emissions as that produced at freeflow freeway speeds, based on the same power demand modal emissions model used before (Barth et al. 1993).

Using this acceleration strategy, typical velocity and acceleration curves are plotted versus time in Figures 4.11 and 4.12. These curves correspond to the zero grade case for an acceleration from 10 to 55 mi/hr (16 to 88 km/hr). Note that the instantaneous acceleration of the vehicle steadily decreases when the engine power demand is kept constant.

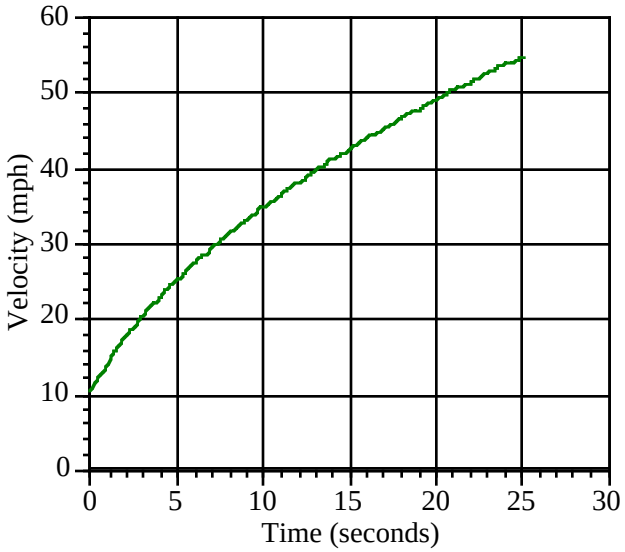

Figure 4.11. Velocity vs. time for zero grade, accelerating from 10 to 55 mi/hr (16 to 88 km/hr).

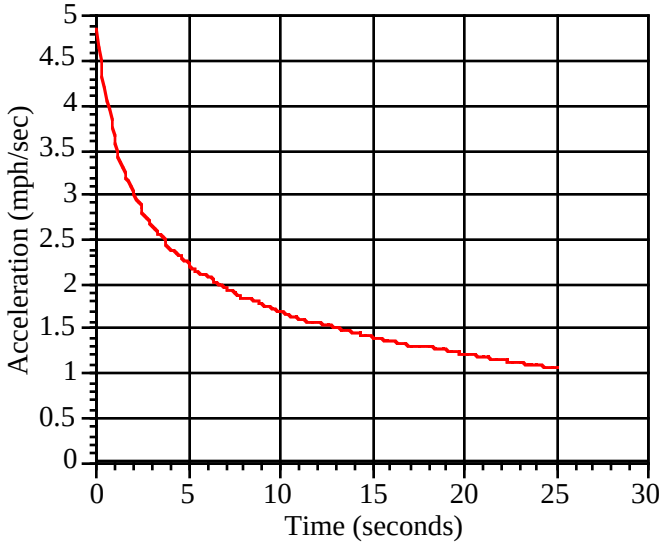

Figure 4.12. Acceleration vs. time for zero grade, accelerating from 10 to 55 mi/hr (16 to 88 km/hr).

Effect of Ramp Meter Cycle Time

Using the same freeway on-ramp geometry illustrated in Figure 4.1, the ramp acceleration model was used to study the effect of ramp meter cycle times. The initial starting speed was set to 10 mi/hr (16 km/hr) and the final speed was determined from the simulated average speed of the mainline flow determined in Section 4.4.1. For the non-metered case, a cycle time of zero seconds was used, and the length of the ramp extended from node 8 in Figure 4.1 and ended at the end of the merging lane. For the metered case, simulations were run with a ramp meter cycle time of 1 to 8 seconds, and the length of the ramp extended from the meter (node 9 in Figure 4.1) to the end of the merging lane. When comparing the metered and non-metered case, it is important to consider this effect of available ramp length on vehicle accelerations.

Figure 4.13 shows typical CO emission rates for the ramp described in Figure 4.1. There is clearly a gradual increase in the rate of emissions as the ramp meter cycle time increases. Additionally, Figure 4.13 shows a very sharp increase for a ramp meter cycle time of eight seconds. Both the gradual and sharp increase in the emission rates are related to three factors: ramp length, freeway speeds, and the open-loop operation of the vehicle's emission control system.

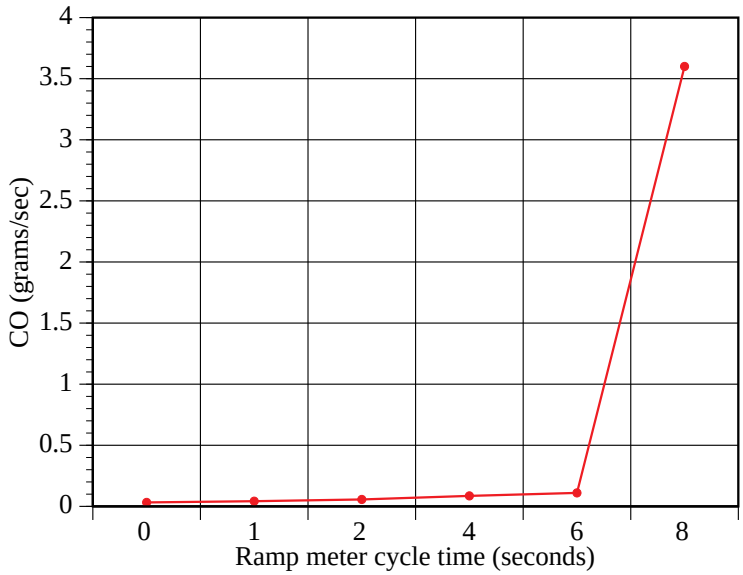

Figure 4.13. CO emissions for different ramp meter cycle times.

Shorter ramp lengths lead to harder accelerations if a vehicle wishes to reach the same cruising speed once it enters freeway traffic. Considering length as the only factor, one should see a constant emission rate for equal length ramps (1-8 second cycle times) that is higher than the

longer ramp case (no meter, 0 cycle time). However, when the average freeway cruising speed is taken into account, there is a gradual increase in emissions for ramps of the same length. This is due to the fact that lower ramp meter cycle times produce lower average mainline freeway speeds (see Figure 4.3). In other words, vehicles do not have to accelerate to a very high freeway speed for lower ramp meter cycle times, which results in lower emission rates.

The third factor that comes into play is the power enrichment effect described in Chapter 2. A vehicle enters the power enrichment mode of operation when it undergoes a hard acceleration on a short ramp, traveling from an initial low speed to a relatively high mainline freeway cruising speed. This is what occurs for a modeled vehicle when the ramp meter cycle time is set to 8 seconds (see Figure 4.13).

Effect of Ramp Length

To better illustrate the effect of varying ramp lengths on the emission rates, simulation experiments were carried out using several different ramp lengths. This was accomplished by varying the length of the merging lane section of the ramp between 250 and 2000 feet (76 and 610 meters). Figure 4.14 shows the effect on CO emissions, while Figures 4.15 and 4.16 show the effect on HC and NOx. The same shape of curve as seen in Figure 4.13 is seen in all three figures. Shorter ramp lengths result in higher emissions and the vehicle enters the power enrichment mode at lower ramp meter cycle times. When in the power enrichment mode, the maximum acceleration level is achieved by the vehicle. Beyond this level the vehicle is unable to reach the mainline freeway cruising speed before it reaches the end of the ramp.

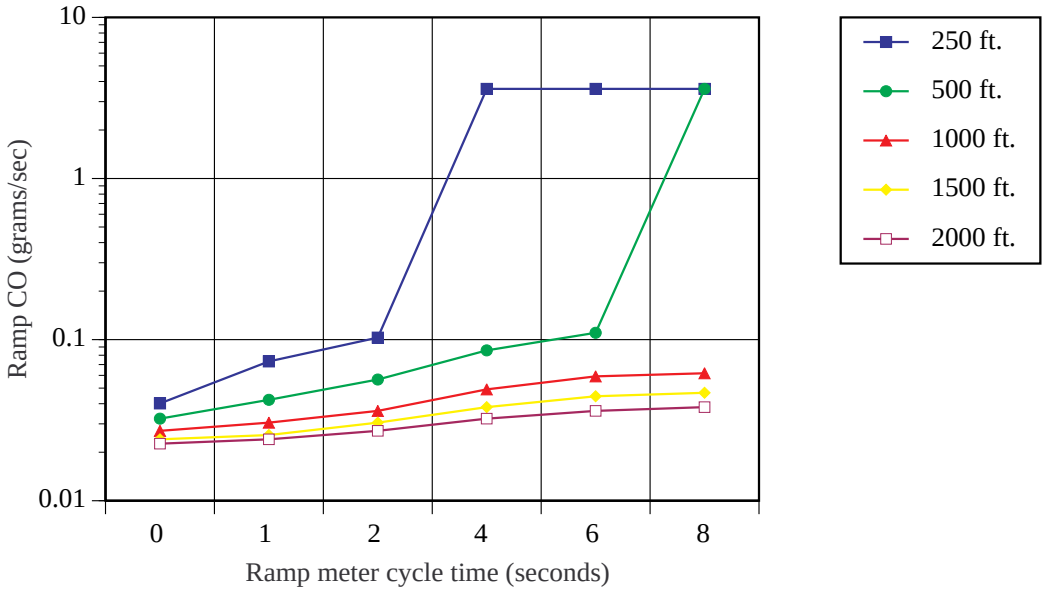

Figure 4.14. CO emissions for different ramp meter cycle times with increasing ramp length.

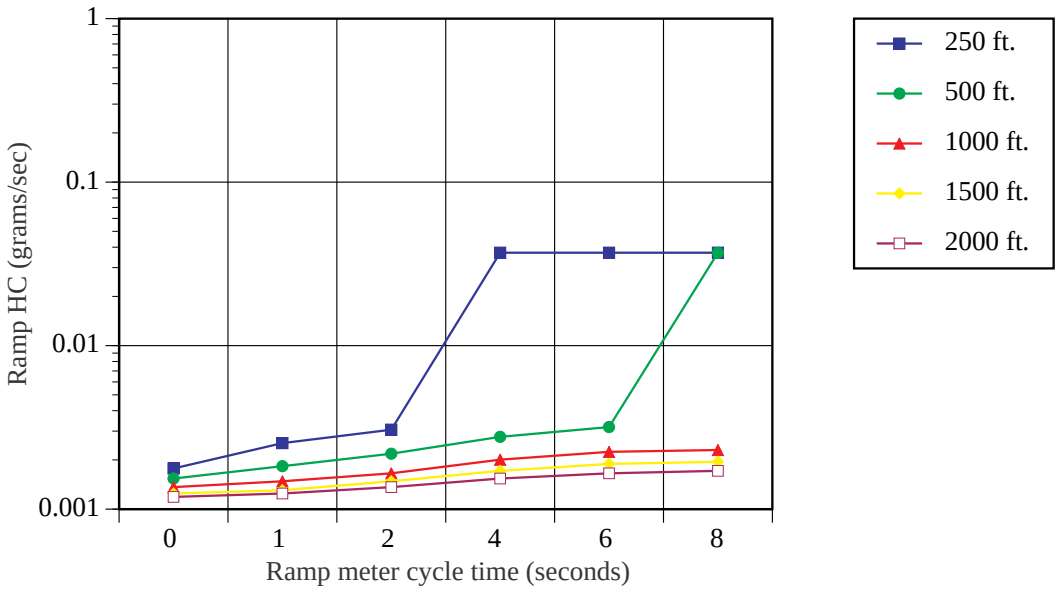

Figure 4.15. HC emissions for different ramp meter cycle times with increasing ramp length.

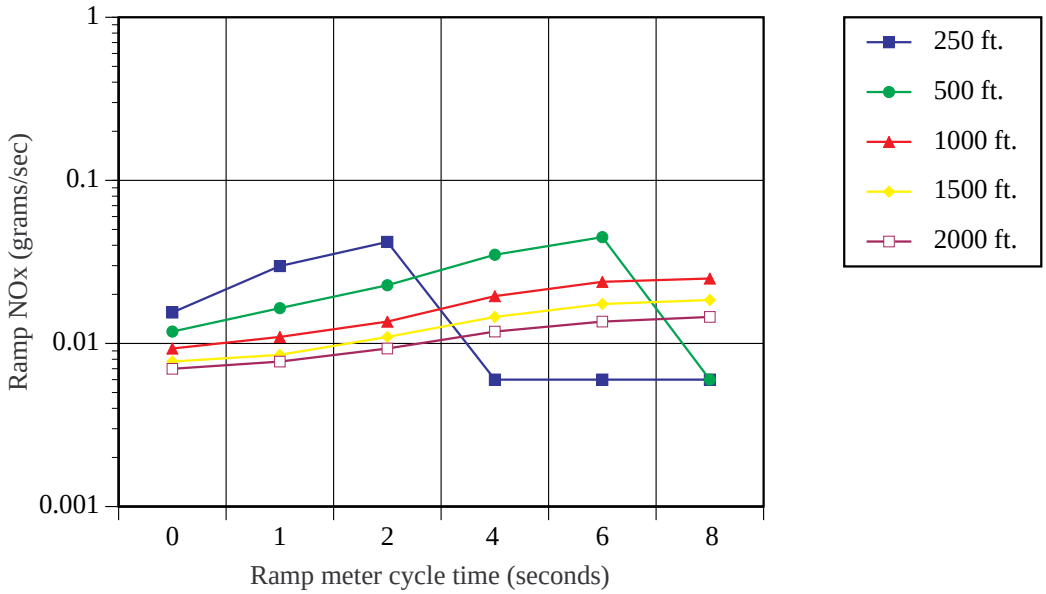

Figure 4.16. NOx emissions for different ramp meter cycle times with increasing ramp length.

Effect of Ramp Grade

In the previous simulation experiments, it was assumed that the freeway ramp was completely flat, i.e., had road grade of 0%. Increased grade has much the same effect on emission rates that shorter available ramp lengths do. Simulation experiments were carried out for varying ramp grades, ranging from 0% to 8% grade (an 8% grade is the maximum grade allowable according to the Caltrans Highway Design Manual, 5th. ed., p. 200-24.). CO results are shown in Figure 4.17, HC results in Figure 4.18, and NOx results in Figure 4.19. These results are very similar to

the graphs of varying ramp length. It should be noted that vehicles are more likely to go into power enrichment mode at higher grades and often are not able to reach the desired cruising speed before reaching the end of the ramp.

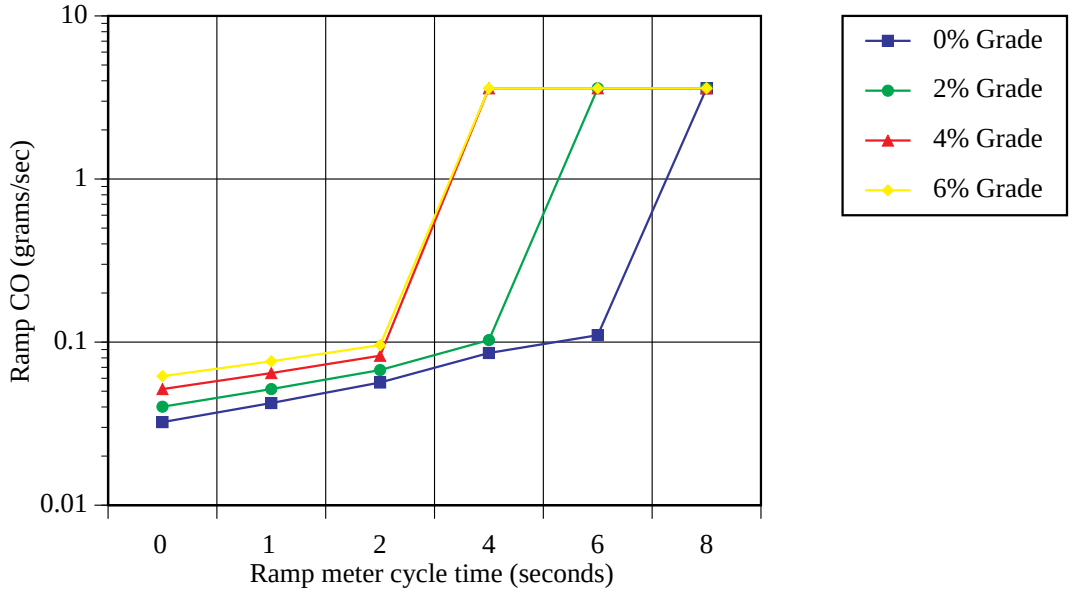

Figure 4.17. CO emissions for different ramp meter cycle times with increasing grade.

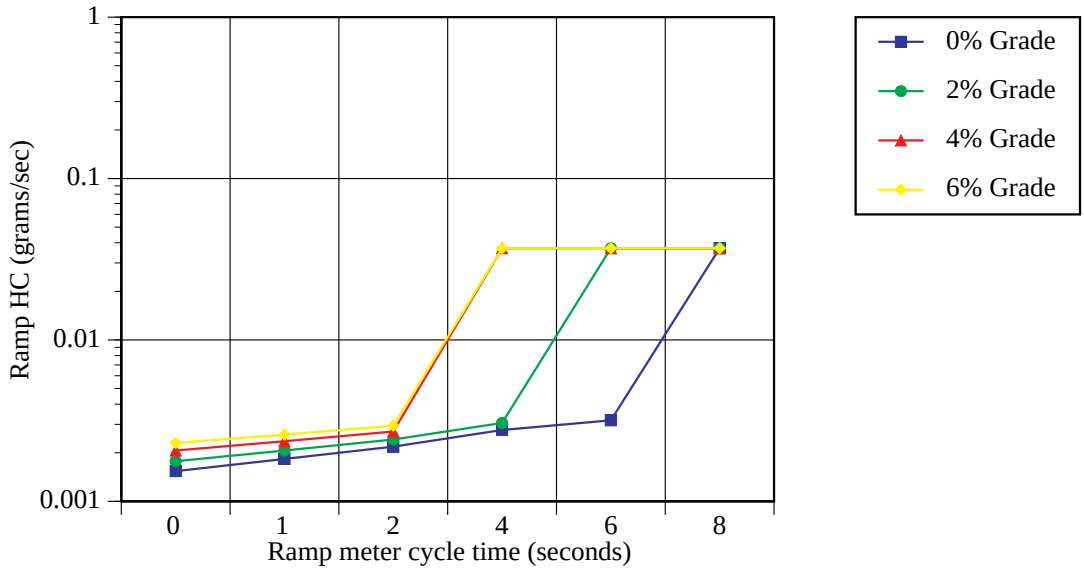

Figure 4.18. HC emissions for different ramp meter cycle times with increasing grade.

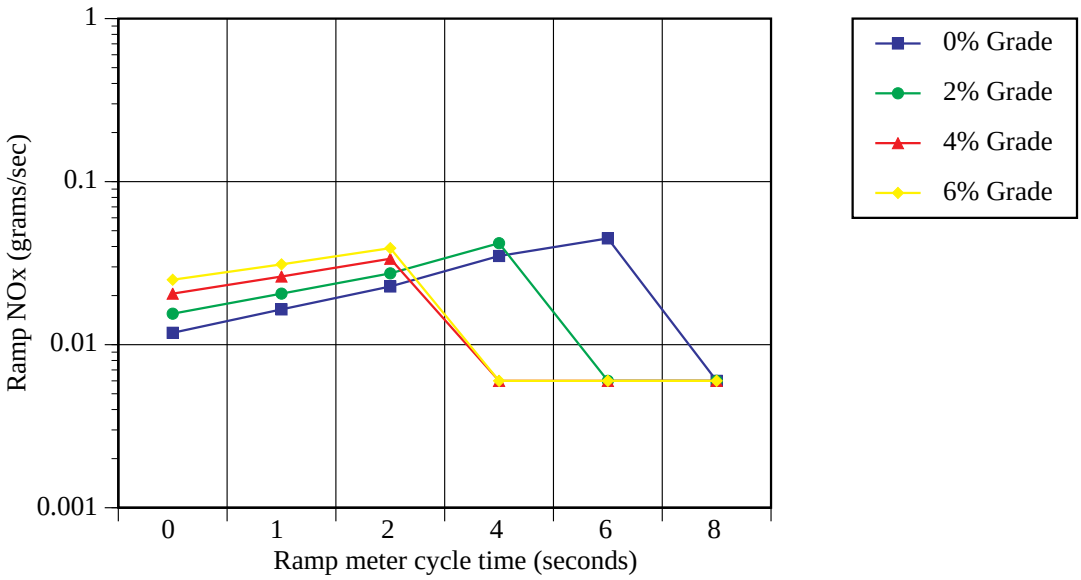

Figure 4.19. NOx emissions for different ramp meter cycle times with increasing grade.

4.5 TOTAL EMISSIONS ASSESSMENT

Thus far in the analysis, the three areas of emissions generation associated with ramp metering—mainline traffic smoothing, ramp queuing, and hard ramp accelerations—have been evaluated independently. In order to estimate the net emissions impact based on these ramp meter simulation experiments, it is necessary to integrate all of the results appropriately.

It is important to consider the following assumptions when reviewing the results:

- The results are only valid for the specific ramp metering scenario that is illustrated in Figure 4.1. Changes in key factors such as network topology and roadway geometry can have a drastic effect on the results.

- In the simulation, the ramp queue length was assumed to be 500 ft. (152 meters) and it was assumed that the queue would not affect surface street congestion.

- When calculating emission rates, the ramp length was considered to be 860 ft. (262 meters) for the non-metered case, and 560 ft. (171 meters) for the metered case. This is based on the fact that the ramp meter is placed near the end of the ramp rather than near the start of the ramp.

- The total freeway mainline emissions were calculated for a one mile section of freeway.

- It was assumed that the vehicles would operate at a constant rate of power (the minimum required to reach the desired freeway speed) when accelerating up the ramp.

- The total emission rates calculated are grams/second versus the ramp meter cycle times. The non-metered case is represented by a zero second cycle time.

When the three constituent parts are integrated, the results plotted in Figure 4.20 are obtained. Figure 4.20 shows total CO, HC, and NOx rates for different ramp meter cycle times. Note that the curves shown in Figure 4.20 are very similar to the CO, HC, and NOx curves in Figures 4.4, 4.5 and 4.6. The curves in those figures represented emissions for one mile of the mainline freeway. The similarity with the curves in Figure 4.23 indicates that freeway emissions contribute most of the emissions related to the ramp metering (mainly due to the high number of vehicles on the freeway).

The high contribution of freeway emissions to the total level of emissions produced can be seen more clearly in Figure 4.21, where the three constituent areas of emissions are plotted along with the total (CO is taken as representative of HC and NOx). The total CO curve follows the freeway CO curve very closely, only differing significantly at a ramp meter cycle time of eight seconds. The queue related CO contributes very little to the total CO, while the difference between the freeway CO and the total CO at a ramp meter cycle time of eight seconds is caused by the sharp increase in CO due to hard ramp accelerations.

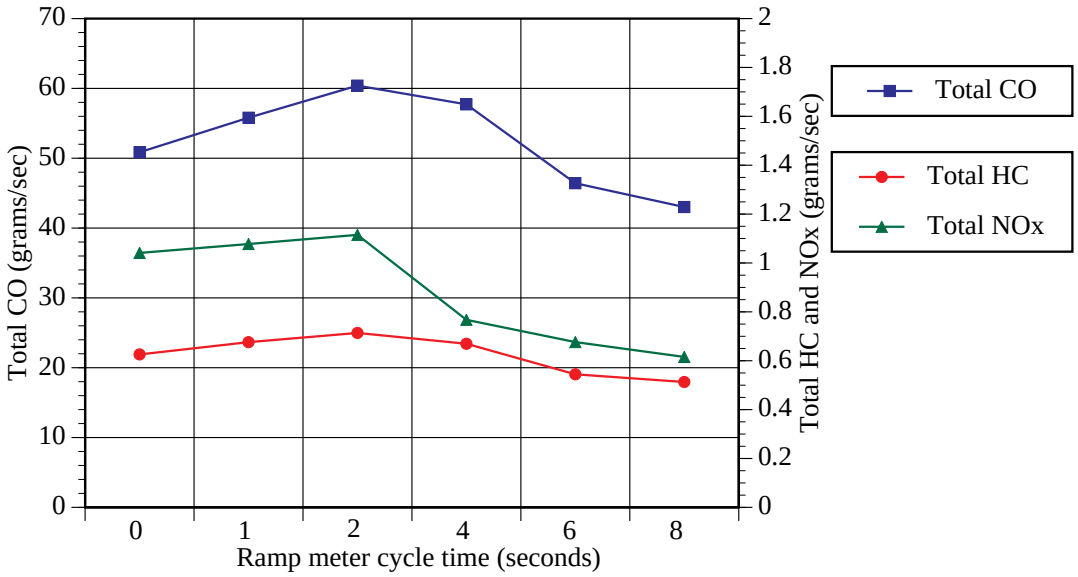

Figure 4.20. Total CO, HC and NOx emissions related to ramp metering for various ramp meter cycle times.

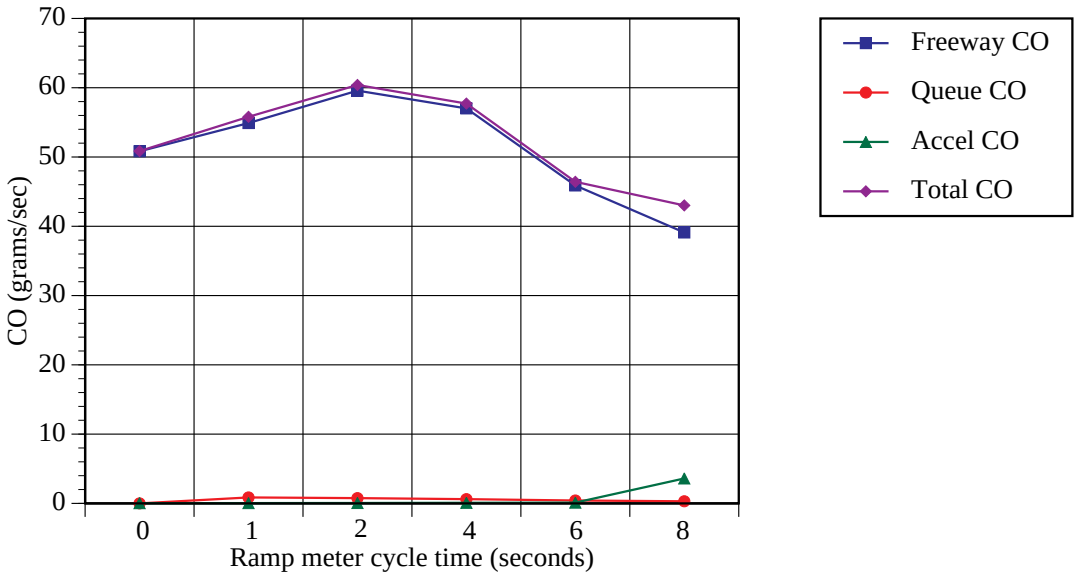

Figure 4.21. CO emissions for various ramp meter cycle times (freeway, queuing, and acceleration related CO emissions as well as total CO emissions).

To better illustrate the effect of the hard ramp accelerations on total emissions, the CO, HC and NOx emissions were normalized to one mile (because the freeway emissions were calculated for one mile of freeway). The normalized total emissions are shown in Figure 4.22.

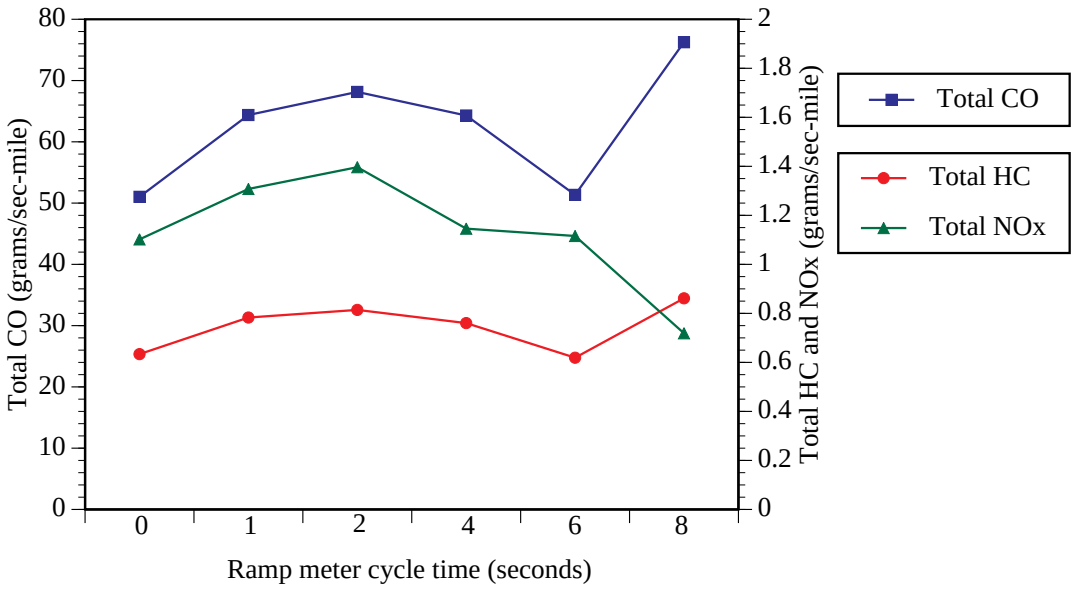

Figure 4.22. Total emissions for various ramp meter cycle times (normalized to one mile of freeway emissions).

The change in total emissions at a ramp meter cycle time of eight seconds (which was noted previously in Figure 4.21) is now very clear in Figure 4.22 for all three pollutants. Figure 4.23

shows the normalized CO constituent emissions plotted with the total normalized CO emissions. Figures 4.24 and 4.25 show the results for HC and NOx.

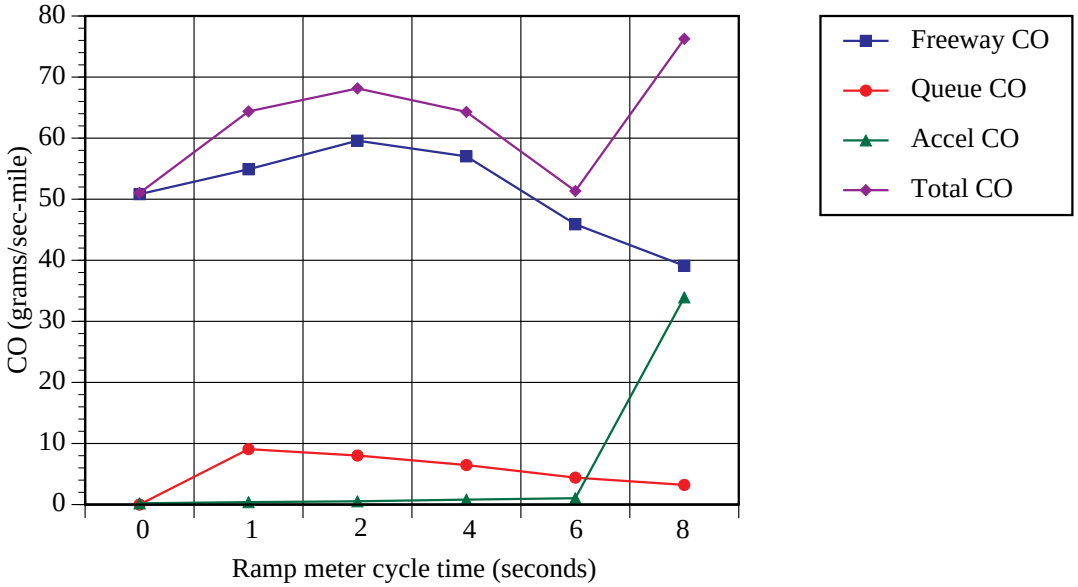

Figure 4.23. Total and constituent CO emissions for various ramp meter cycle times (normalized to one mile of freeway emissions).

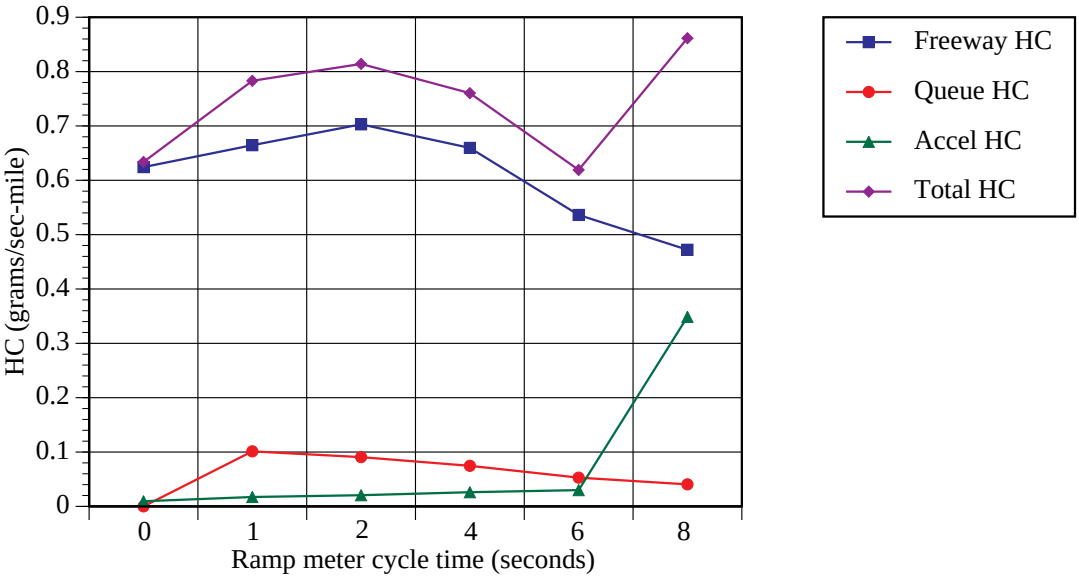

Figure 4.24. Total and constituent HC emissions for various ramp meter cycle times (normalized to one mile of freeway emissions).

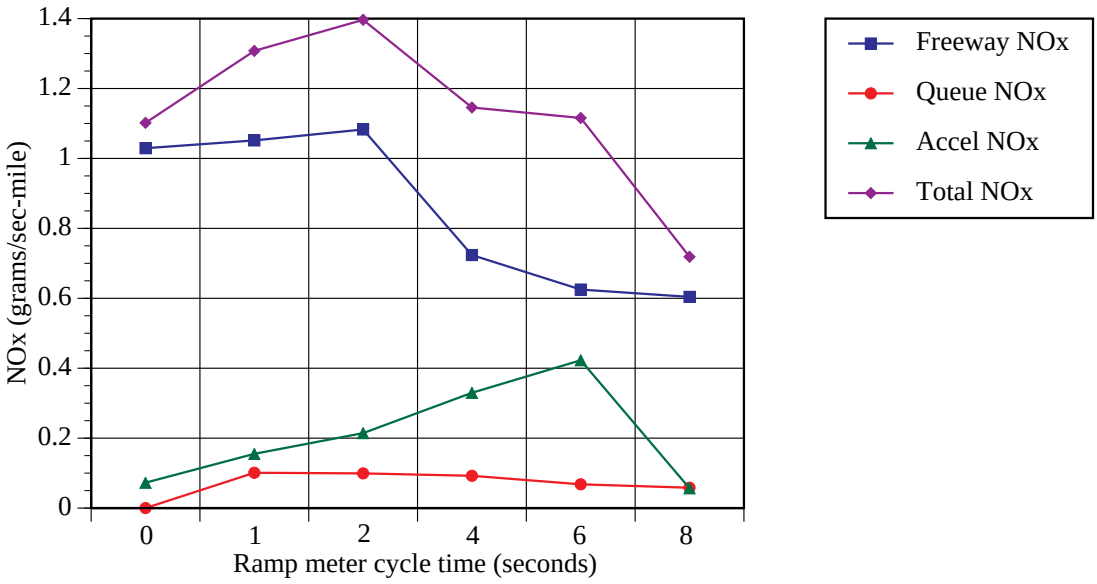

Figure 4.25. Total and constituent NOx emissions for various ramp meter cycle times (normalized to one mile of freeway emissions).

By looking at Figures 4.23, 4.24, and 4.25, one can see that total emissions are almost entirely related to the freeway emissions when the meter is not operating (zero second cycle time). This is because, in this scenario, the freeway traffic is highly congested and moving slowly. Vehicles accelerating up the ramp have the whole length of the ramp available to them and they do not have to reach very high speed because of the high level of congestion on the freeway, so their emissions are relatively negligible. There are, of course, no queue emissions at a zero second cycle time since there is no queue when the meter is not running.

At higher ramp meter cycle times (one to six seconds), the total emissions can be mostly attributed to freeway emissions, with a smaller yet noticeable contribution from the vehicles waiting in the ramp meter queue. It is in this region that the interaction among vehicles on the freeway causes the freeway emissions to reach their peak. The ramp meter queue emissions decrease with increasing cycle times, so this is also the region where queue emissions will have the most effect.

Once the ramp meter cycle time has reached eight seconds, freeway traffic has been relieved of much of its congestion and cruising speeds are approaching 60 miles per hour. While the freeway-related emissions fall because of less interaction among the vehicles, the higher speeds force the vehicles on the ramp to accelerate much harder to get up to freeway cruising speed. Often, this results in vehicles going into power enrichment mode which causes the sharp increase

in ramp acceleration-related emissions. The total emissions at this ramp meter cycle time will then also increase sharply.

Again, it is important to note that these results apply only to the one simple scenario analyzed in this study and should not necessarily be generalized to all ramp metering scenarios. The key results of this analysis are the comparisons that can be made between the cases of non-metered and metered, with different meter cycle times.

In all of the simulations carried out in this analysis, the constant power demand assumption will generate accelerations that may not truly characterize actual on-ramp accelerations. In order to determine actual velocity and acceleration profiles on ramps, the California Air Resources Board and Caltrans have sponsored a study of freeway on-ramp accelerations, performed by researchers at California State Polytechnical University, San Luis Obispo (Sullivan et al. 1993). This study has created a data set describing vehicle speeds and accelerations along a selected sample of freeway on-ramps having a variety of physical and operational characteristics. Speed and acceleration data were obtained for four different Caltrans districts and the sample was split between ramps with and without ramp metering. In addition to the acceleration and velocity data, mainline traffic conditions were also recorded. The velocity and acceleration profiles were recorded for approximately 100 different vehicles on each ramp. The measurements were made using a video camera which observed the starting point of the ramp (or meter location) and the final merge point on the freeway.

A key difference between these recorded velocities/accelerations and those that are predicted by our simulation model is that there is a considerable time lag (3-5 seconds) before peak acceleration is achieved. This implies that in general, drivers ease the throttle forward over a few seconds rather than immediately stomp down on the pedal. It is apparent that after peak acceleration is achieved, the acceleration decays as speed increases, as is predicted by the simulation model. However, based on the recorded velocities/accelerations, drivers tend to "correct" their acceleration near the end of the ramp in order to enter traffic. This phenomenon is not modeled in the simulation experiments carried out here.

5 Conclusions and Future Work

The continued research and development of ITS-related simulation models combined with modal emission models will allow us to improve our understanding of ITS vehicle activity and associated emissions. Although this line of research had only addressed the direct effects of ITS on vehicle emissions, it is important to consider the full environmental costs which include both direct and indirect effects (e.g., induced traffic demand). In addition, to further assessment using simulation modeling, field studies should be used to validate the model predictions. The paper by Little et al. describes potential field studies for ITS evaluation (Little et al. 1994).

5.1 MODAL EMISSIONS MODELING

As stated in Chapter 2 of this report, current vehicle emission models are not well suited for ITS evaluation. This is primarily due to the inherent vehicle emissions and operation data-averaging that takes place in the methodology. A more appropriate method is to use a modal type of emissions model that can be applied to traffic scenarios that are more microscale in nature.

We have outlined a modal emissions modeling approach and have implemented it for a single type of vehicle. This modal emissions model was then used in the AHS and ramp metering analysis in this research project. However, for any ITS traffic scenario, the vehicle population will likely be quite varied. To more accurately predict total emissions, emission rates for different vehicle classes must be incorporated.

CE-CERT is currently performing research to develop a more comprehensive modal emissions model that will be able to estimate emissions for a wide range of vehicles. This modeling project is being sponsored by the National Cooperative Highway Research Program (NCHRP) and consists of extensive testing of over 300 vehicles. The resulting modal emissions modeling set will accurately reflect speed, acceleration, engine load, and start conditions on emissions under a variety of driving characteristics and vehicle technologies. As this modal emissions modeling set matures, it can be readily applied for ITS evaluation.

Even though the preliminary results in this report are based on a single vehicle, trends can be seen and important conclusions can be made regarding the utility of linking modal emissions with dynamic vehicle activity.

5.2 AHS VEHICLE EMISSIONS

Based on microscale simulation models and modal emissions data for a modern, closed-loop emission controlled vehicle, steady-state (i.e., constant velocity) emission rates have been estimated for both manual and automated lanes. An automated lane using platooning can improve the traffic flow by a factor of four, and at maximum flow values, the total emissions (grams per second per kilometer) increase is by a factor of two (for the modeled Ford Taurus). If only half of the automated lane capacity is used, the traffic flow improves by a factor of two, and the associated emission rates are roughly the same as the full-capacity manual case. If the automated lane carries the same traffic volume as in the manual case, the emissions are reduced by a factor of two. These results are due to reduced engine power demand on vehicles that are platooning and on higher vehicle densities achieved in an automated scenario.

Further, preliminary analysis has been carried out to evaluate vehicle emissions associated directly with the AHS maneuvers of free-speed accelerations, platoon merging, and platoon splits. The current version of SmartPath uses a constant acceleration strategy in these maneuvers. This can be problematic at high speeds since a constant acceleration constraint can cause a modern emission-controlled vehicle to enter a power enrichment state, in which very high emissions are produced. We have devised a constant-power approach which limits the accelerations of automated vehicles, eliminating power enrichment states, and greatly reducing emissions. Emissions can also be reduced by developing “emission-friendly” protocols, that do not require high power episodes while still maintaining system safety. Also, by keeping the size of platoons as large as possible, traffic density and highway capacity will both increase, and the number of vehicles benefiting from the aerodynamic drafting effect increases.

This analysis assumed a constant platoon size of 20 vehicles, however, platoons will vary in length due to vehicles dynamically entering and leaving platoons as they travel from their specific origins to destinations. Shorter length platoons will lead to lower automated lane capacities and higher average vehicle emissions.

In order to minimize emissions in an AHS, several points should be observed:

- The size of platoons should be kept as large as possible; this increases the density of traffic and increases the highway capacity, and the number of vehicles benefiting from the aerodynamic drafting effect increases.

- During AHS maneuvers, vehicles should be commanded so that they operate at power levels below the threshold where they enter a power enrichment state. By eliminating power enrichment events, significantly lower emissions result.

- The number of maneuvers in general should be kept to a minimum, which will keep the traffic flow smoother, resulting in less accelerations and decelerations that lead to higher emissions.

Further research must be carried out to better characterize vehicle emissions associated with stop-and-go traffic in the unstable traffic flow-density regions. If congestion is to be avoided, the traffic should be kept in the positive slope region of the flow-density curve (see Figure 3.4). When in the positive slope region, interaction between vehicles in traffic is minimal, leading to smoother traffic flow. It can be seen that the extent of the positive slope region is much greater for the automated lane when compared to the manual lane. For the automated case, the network and link layer controllers in the AHS will attempt to keep traffic in the stable operating regime at all times.

Another area that can be explored in the future is an analysis of the problems associated with the end-points of automation, i.e., the dumping of high flow rates onto off-ramps, arterials, and collectors. In effect, automation causes peak period compression, meaning that higher flow rates occur throughout the system. In some cases this could cause congestion on off-ramps, arterials, and collectors at automation egress points. The emissions associated with these cases should also be examined.

In addition, macroscale modeling techniques need to be developed for estimating system-level emissions of an AHS. Instead of modeling every vehicle at high time resolutions, aggregate traffic parameters for an AHS can be used as input to a macroscale emissions model. Examples of traffic parameters indexed over different AHS roadway sections may be vehicle density, entrance/exit density, and ratio of average traffic speed over assigned free speed. This aggregate model would then allow the accurate estimation of cumulative tailpipe emissions in system-level applications.

Again, it is important to point out that the emission rates used in this analysis were for a single vehicle. For current manual driving, the vehicle population is quite varied, and to more accurately predict total emissions, emission rates for different vehicle classes must be incorporated. For an automated scenario, however, the vehicle population will be somewhat more restricted. Vehicles that have automated platoon technology will tend to be newer passenger vehicles with closed-loop emission control systems, similar to the vehicle modeled

here. It may be that by the time AHS technology is in place in our transportation systems, vehicle emission control technology will have improved to the point where the potential problems outlined in this report do not apply.

5.3 RAMP METERING EMISSIONS

Vehicle emissions associated with ramp metering have been analyzed, with an emphasis on three sources of influence: 1) freeway traffic smoothing, 2) ramp and surface street congestion, and 3) hard accelerations from the meters. In this preliminary research, simulation experiments have been carried out using the FRESIM traffic model coupled with the modal emissions model described in Chapter 2.

The overall effect of ramp metering on vehicle emissions is highly dependent on a number of localized factors such as the *topology of the road network* (e.g., spacing of ramps, surface street to highway interface, etc.), the *road geometry* (e.g., number and types of lanes, road grade of the highway and ramps, etc.), the *type of ramp metering used* (e.g., fixed cycle vs. traffic responsive), the *vehicle mix* (e.g., proportion of trucks and cars, etc.), and the *overall VMT*. In this research, only generic scenarios of ramp metering were analyzed, and caution is urged in applying these results to specific instances of ramp metering. The purpose of this preliminary study is to identify the specific ramp metering influences on vehicle emissions and to gauge their overall impact.

As expected, simulation experiments have shown that the use of ramp metering increases the overall traffic speed on the mainline by restricting the ramp volume and by minimizing the disturbances caused by merging vehicles. As the ramp meter cycle time increases, the traffic volume from the ramp decreases and the freeway speeds increase, resulting in a total emissions decrease due to lower traffic density and smoother flow.

Queues of vehicles on the on-ramps and their emissions have been studied using a simulation model. It was shown that the density of vehicles increases for longer ramp cycle times, and the average vehicle speed on the ramps decreases. However, it was shown that emissions tend to be higher for shorter ramp meter cycle times, primarily due to an increased stop-and-go effect.

We have also developed a simulation model that predicts velocity and acceleration profiles for vehicles accelerating under constrained speeds and distances, using constant engine power. This was applied to freeway on-ramps, in particular, accelerating from a ramp meter to the merge point on the freeway. If the distance is short (and if the grade is steep), the engine power required may cause the vehicle to go into the power enrichment mode, causing high emissions.

When all three sources of ramp metering emissions (i.e., freeway mainline, ramp queuing, and hard accelerations) are integrated together (again for the generic scenarios in the experimentation), the freeway mainline is the dominant emissions source, simply because of the larger number of vehicles associated with it. The amount of emissions caused by ramp queuing is small in comparison, and only when the distance to get up to speed from the meter to the merge point is short and steep, is the effect of hard accelerations an emissions factor. When developed as a function of ramp meter cycle time, the net change of emissions is small. For the case of no metering, the mainline traffic moves slower with moderately high emissions, and the acceleration required to get up to speed is small (as are the corresponding emissions) since there is a longer distance to accelerate and the final traffic speed is relatively low. For the case of metering with long cycle times, the mainline moves faster and has relatively lower emissions (due to smoother traffic flow), but the accelerations to get from the meter to the higher mainline speeds are often hard enough to drive vehicles into a power enrichment state. These hard acceleration emissions offset the benefits achieved from smoother traffic flow.

Future work includes doing an analysis of an actual freeway corridor, using modal emission functions for a diverse vehicle population, and taking into account the three effects described above. Also, the congestion shift onto surface streets sometimes caused by ramp metering was not included in this analysis—this should be investigated in more detail.

6 References

AHS Precursor Workshop. 1994. Automated Highway Systems Precursor Systems Analyses Interim Results Workshop. McLean, Virginia. FHWA.

Al Kadri, M. Y. 1991. Freeway control via ramp metering: development of a basic building block for an on-ramp, discrete, stochastic, mesoscopic, simulation model within a contextual systems approach. Ph.D. Dissertation. Portland State University.

An, F. and M. Ross. 1993. A Model of Fuel Economy and Driving Patterns. SAE Technical Paper number 930328.

Arnott, R. and K. Small. 1994. The Economics of Traffic Congestion. American Scientist Vol. 82: 446 - 455.

Banks, J. H. 1994. Effect of Response Limitations on Traffic-Responsive Ramp Metering. Transportation Research Record of the Transportation Research Board 1394: 17-25.

Barth, M. and J. Norbeck. 1993. The Development of an Integrated Transportation/Emissions Model to Predict Mobile Source Emissions. Center for Environmental Research and Technology, UC Riverside, Research Report #93-TS-002F.

Barth, M. and J. Norbeck. 1994. Transportation Modeling for the Environment, Interim Report. California PATH Program, Research Report #UCB-ITS-PRR-94-27.

Barth, M., R. Tadi, et al. 1995. The Development of an Integrated Transportation/Emissions Model for Estimating Emission Inventories. 1995 American Society of Civil Engineers Annual Conference. San Diego, CA, October, 1995.

Barth, M. J. 1995. Predicting Vehicle Emissions for Automated Highway Systems in ITS. 88th Annual Meeting of the Air & Waste Management Association. San Antonio, TX, June 1995.

Butler, J. 1992. Instrumenting a Ford Aerostar Van with a Fourier-Transform Infra-Red Spectrometer. CRC-APRAC Second Annual On-Road Vehicle Emissions Workshop. Los Angeles, CA.

Cadle, S. H., M. Carlock, et al. 1991. CRC-APRAC Vehicle Emissions Modeling Workshop Summary. Journal of Air and Waste Management Association Vol. 41: 817-820.

Cadle, S. H., R. A. Gorse, et al. 1993. Real-World Vehicle Emissions: A Summary of the Third Annual CRC-APRAC On-Road Vehicle Emissions Workshop. Journal of Air and Waste Management Vol. 43: 1084 - 1090.

CARB. 1991. Presented material at the Seminar on Transportation Modeling for Emissions Analysis: Theory and Practice. Sacramento, CA, March, 1991.

Carlock, M. 1993. Overview of On-Road Emissions Inventory Models. Proceedings of Transportation Modeling: Tips and Trip-Ups. San Mateo, CA, March, 1993.

Chang, G.-L., J. Wu, et al. 1994. Integrated Real-Time Ramp Metering Control for Non-Recurrent Congestion: Modeling and Strategy Development. Proceedings of the IVHS America 1994 Annual Meeting. Atlanta, Georgia, 1994.

Chang, G.-L., J. Wu, et al. 1994. Integrated Real-Time Ramp Metering Model for Non-Recurrent Congestion: Framework and Preliminary Results. Transportation Research Record of the Transportation Research Board 1446: 56-65.

Congress, N. 1994. Automated Highway System - An Idea Whose Time has Come. Public Roads Vol. 58 (1).

Corcoran, L. J. and G. A. Hickman. 1989. Freeway Ramp Metering Effects in Denver. ITE 59th Annual Meeting. San Diego, CA, 513-517.

CRC-APRAC-91. 1991. Presented material at the 2nd Annual CRC-APRAC On-Road Vehicle Emissions Workshop. Los Angeles, CA, March 1991.

CRC-APRAC-92. 1992. Presented material at the 3rd Annual CRC-APRAC On-Road Vehicle Emissions Workshop. San Diego, CA, April, 1992.

CRC-APRAC-94. 1994. Presented material at the 4th Annual CRC-APRAC On-Road Vehicle Emissions Workshop. San Diego, CA, May, 1994.

CRC-APRAC-95. 1995. Presented material at the 5th CRC-APRAC On-Road Vehicle Emissions Workshop. San Diego, CA, May, 1995.

Eisinger, D. 1993. Preview of MOBILE. Proceedings of Transportation Modeling: Tips and Trip-Ups. San Mateo, CA, March, 1993.

ITE. 1992. Traffic Engineering Handbook. Englewood Cliffs, New Jersey. Prentice Hall, Inc.

Eskafi, F. and D. Khorramabadi. 1993. SmartPath User's Manual. Department of Electrical Engineering and Computer Sciences, University of California, Berkeley, 1993.

Eskafi, F., D. Khorramabadi, et al. 1992. SmartPath: an Automated Highway System Simulator. ITS-PATH, UCB-ITS-PTM-92-3.

FHWA. 1986. TRANSYT-7F: Traffic Network Study Tool (Version 7F). Washington, DC. U.S. Department of Transportation.

FHWA. 1989. TRAF-NETSIM User's Manual. US Department of Transportation, Washington, DC.

FHWA. 1993. FRESIM User Guide. Federal Highway Administration, Office of Research and Development, 1993.

FTP. 1989. Code of Federal Regulations. Title 40. Parts 86-99 (portion of CFR which contains the Federal Test Procedure), Office of the Federal Register.

Gillespie, T. D. 1992. Fundamentals of Vehicle Dynamics. Warrendale, PA. Society for Automotive Engineers, Inc.

Guensler, R., S. Washington, et al. 1994. Modeling IVHS Emission Impacts; Volume I: Background Issues and Modeling Capabilities. California PATH Program, Research report.

Halati, A., J. Torres, et al. 1991. FRESIM - Freeway Simulation Model. Transportation Research Board 70th Annual Meeting. Washington, DC, paper # 910202.

Hamad, A.-R. 1987. Evaluation of Ramp Metering Strategies at Local On-Ramps and Freeway-to-Freeway Interchanges Using Computer Simulation. Ph.D. Dissertation. Michigan State University.

Hennessey, J. T. and T. Horan. 1994. Executive Summary of Conference. National Conference on Intelligent Transportation Systems and the Environment. Arlington, VA, June, 1994.

Hongola, B., J. Tsao, et al. 1993. SmartPath Simulator - Version MOU62. ITS-PATH, UCB-ITS-PWP-93-8.

Hsu, A., F. Eskafi, et al. 1991. The Design of Platoon Maneuver Protocols for IVHS. California PATH Program, ITS, University of California, UCB-ITS-PRR-91-6.

Ioannou, P. A., C. C. Chien, et al. 1992. Autonomous Intelligent Cruise Control. Surface Transportation and the Information Age, Proceedings of the IVHS America 1992 Annual Meeting. Newport Beach, California, 97 - 112.

ITE. 1990. IVHS special issue. ITE Journal Volume 60 (11).

Jacobson, E. L. and J. Landsman. 1994. Case Studies of U.S. Freeway-to-Freeway Ramp and Mainline Metering and Suggested Policies for Washington State. Transportation Research Record of the Transportation Research Board 1446: 48-55.

Karaaslan, U., P. Varaiya, et al. 1990. Two proposals to improve freeway traffic flow. California PATH Program, ITS, University of California, UCB-ITS-PRR-90-6.

Kelly, N. A. and P. J. Groblicki. 1993. Real-World Emissions from a Modern Production Vehicle Driven in Los Angeles. Journal of the Air & Waste Management Association 43: 1351-1357.

Little, C. and J. Wooster. 1994. IVHS and Environmental Impacts: Implications of the Operational Tests. National Conference on Intelligent Transportation Systems and the Environment. Arlington, VA, 315-338.

Maldonado, H. 1991. Methodology to Calculate Emission Factors for On-Road Motor Vehicles. California Air Resources Board, Technical Report.

Maldonado, H. 1992. Supplement to Methodology to Calculate Emission Factors for On-Road Motor Vehicles July 1991. California Air Resources Board, Technical Report.

Markey, J. 1993. Federal Test Procedure Review Project: Technical Report. Certification Division, Office of Mobile Sources, US EPA, EPA 420-R-93-007.

May, A. D. 1990. Traffic Flow Fundamentals. Englewood Cliffs, New Jersey. Prentice-Hall.

McGurrin, M. and P. Wang. 1991. An Object-Oriented Traffic Simulation with IVHS Applications. 2nd SAE Vehicle Navigation and Information Systems Conference. Dearborn, MI, 551-561.

Meyer, Mohaddes, et al. 1994. Incorporation of the Benefits of IVHS Technology into Regional Travel Demand Models. Meyer, Mohaddes Associates, 1994.

Meyer, M., D. LeBlanc, et al. 1992. A Study of Enrichment Activities in the Atlanta Road Network. Proceedings of an International Specialty Conference on Emission Inventory Issues. Durham, NC, 1992.

Nihan, N. L. and M. D. Babla. 1993. Application of Pattern Recognition to Forecast Congested Conditions on the Freeway for Use in Ramp Metering. Washington State Transportation Center, Federal Highway Administration, WA-RD-288.2, TNW-93-05.2.

Nsour, S. A., S. L. Cohen, et al. 1992. Investigation of the Impacts of Ramp Metering on the Traffic Flow With and Without Diversion. Transportation Research Record of the Transportation Research Board 1365: 116-124.

Ostria, S., M. Lawrence, et al. 1994. Capacity-Induced Increases in the Quantity of Travel with Special Reference to IVHS. National Policy Conference on Intelligent Transportation Systems and the Environment. Arlington, VA, June 1994.

Ostria, S. J. 1995. ITS-Induced Increases in the Quality of Travel with Special Reference to Emission Impacts. 88th Annual Meeting of the Air & Waste Management Association. San Antonio, TX, June 1995.

Pielou, E. C. 1977. Mathematical Ecology. New York. John Wiley & Sons, Inc.

Pipes, L. A. 1953. An Operational Analysis of Traffic Dynamics. Journal of Applied Physics 24(3): 274-287.

Rao, B. S. Y. and P. Varaiya. 1994. Potential Benefits of Roadside Intelligence for Flow Control in an IVHS. Transportation Research Board, 73rd Annual Meeting. Washington, DC, January, 1994.

Richardson, B. 1994. Socioeconomic Issues and Intelligent Transportation Systems. National Conference on Intelligent Transportation Systems and the Environment. Arlington, Virginia, 67 - 80.

Robinson, J. and M. Doctor. 1989. Ramp Metering: Does It Really Work? ITE 59th Annual Meeting. San Diego, CA, 503-508.

Rockwell. 1992. Potential Payoffs from IVHS: A Framework for Analysis. California PATH Program, University of California, UCB-ITS-PRR-92-7.

Ross, M. and F. An. 1993. The Use of Fuel by Spark Ignition Engines. Society of Automobile Engineering Technical Paper 930329.

Saxton, L. 1993. Automated Control-Cornerstone of Future Highway Systems. IVHS Review Summer 1993: 1-16.

SCAQMD. 1993. presented material at the National IVHS and Air Quality Workshop. Diamond Bar, California, 1993.

Sheikholeslam, S. E. 1991. Control of a Class of Interconnected Nonlinear Dynamic Systems: The Platoon Problem. Ph.D. Dissertation. University of California, Berkeley.

Shladover, S. E., C. A. Desoer, et al. 1991. Automated Vehicle Control Developments in the PATH Program. IEEE Transactions on Vehicular Technology 40(1): 114 - 130.

Shoemaker, B. R. and E. C. Sullivan. 1994. HOV Lanes and Ramp Metering: Can They Work Together for Air Quality. Transportation Research Record of the Transportation Research Board 1446: 33-37.

St. Denis, M. and A. M. Winer. 1993. Prediction of On-Road Emissions and Comparison of Modeled On-Road Emissions to Federal Test Procedure. A&WMA The Emission Inventory: Perception and Reality. Pasadena, California, 495 - 505.

Stephanedes, Y. J., E. Kwon, et al. 1993. Development and Application of On-Line, Integrated Control Strategies for Optimal Metering, Incident Management and Driver Guidance in Freeway Networks. University of Minnesota, Minnesota Department of Transportation, MN/RC-94/13.

Stevens, W. B. 1994. The use of System Characteristics to Define Concepts for Automated Highway Systems (AHS). Transportation Research Board, 73rd Annual Meeting, paper number 940990. Washington, DC, 1994.

Sullivan, E. C., N. Devadoss, et al. 1993. Vehicle Speeds and Accelerations Along On-Ramps: Inputs to Determine the Emissions Effects of Ramp Metering. Transportation Research Group, Applied Research and Development Facility, California Polytechnic State University, San Luis Obispo.

Tierney, E. J. 1991. I/M Network Type: Effects on Emission Reductions, Cost, and Convenience. US EPA, EPA-AA-TSS-IM-89-2.

TRB. 1985. Highway Capacity Manual, Special Report 209. Washington, DC. TRB.

US DOT. 1995. National Program Plan for Intelligent Transportation Systems (ITS). ITS America, May, 1995.

US EPA. 1993. Review of Federal Test Procedure Modifications Status Report. Office of Mobile Sources, Office of Air & Radiation, US Environmental Protection Agency.

US EPA. 1995A. Final Technical Report on Aggressive Driving Behavior for the Revised Federal Test Procedure Notice of Proposed Rule Making. Office of Air and Radiation, Office of Mobile Sources, Certification Division, US Environmental Protection Agency.

US EPA. 1995B. Regulatory Impact Analysis, Federal Test Procedure Revisions. Office of Mobile Sources, Office of Air and Radiation, US Environmental Protection Agency.

US EPA. 1995C. Support Document to the Proposed Regulations for Revisions to the Federal Test Procedure: Detailed Discussion and Analysis. US EPA, Office of Air and Radiation.

Van Aerde, M. 1992. INTEGRATION: A Model for Simulation Integrated Traffic Networks, User's Guide for Model Version 1.4 d. Transportation Systems Research Group, Department of Civil Engineering, Queens University.

Varaiya, P. and S. Shladover. 1991. Sketch of an IVHS Systems Architecture. California PATH Program, ITS, University of California, UCB-ITS-PRR-91-3.

Vaughn, K. and D. Murphy. 1995. Air Quality Impacts of IVHS. ITS America Annual Conference. Washington, D.C., 1195-1201.

Warner, C. 1985. Spatial Transportation Modeling. Beverly Hills. Sage Publications.

Washington, S., R. Guensler, et al. 1993. Air Quality Impacts of Intelligent Vehicle Highway Systems. Transportation Planning and Air Quality II. New York, NY, American Society of Civil Engineers.

Washington, S. P. 1995. Carbon Monoxide Impacts of Electronic Tolling Operations: Two Conflicting Assessments of a Promising Intelligent Transportation Technology. 88th Annual Meeting of the Air & Waste Management Association. San Antonio, TX, June 1995.

Winer, A. and M. S. Denis. 1993. On-Board Vehicle Emissions Measurements. Environmental Science and Engineering Program, UC Los Angeles, Research report.

Zabat, M., S. Frascaroli, et al. 1994. Drag Measurements on 2, 3, & 4 Car Platoons. SAE Technical Paper 940421.

Zabat, M., N. S. Stabile, et al. 1995. Estimates of Fuel Savings from Platooning. ITS America Annual Conference. Washington, D.C., 1202-1208.

Zhang, H. and S. G. Ritchie. 1995. An Integrated Traffic Responsive Ramp Control Strategy via Nonlinear State Feedback. Institute of Transportation Studies, University of California, Irvine, UCI-ITS-WP-95-2.

Zhang, H., S. G. Ritchie, et al. 1995. On the Optimal Ramp Control Problem: When Does Ramp Metering Work. Institute of Transportation Studies, University of California, Irvine, UCI-ITS-WP-95-4.

Zhang, W.-B., S. Shladover, et al. 1994. A Functional Definition of Automated Highway Systems. California PATH Program, ITS, University of California, UCB-ITS-PRR-94-9.